

Dato: 31.01.1986

Rapport/Notat Nr. FO 8605

	<h1>HAVFORSKNINGSINSTITUTTET</h1>		
	Nordnesparken 2,	Postboks 1870,	5011 Bergen.

**Rapportens Tittel:**

ECOLOGICAL INVESTIGATIONS IN THE BARENTS SEA, AUGUST 1985

Report from PRO MARE-cruise no.5.

Forfatter/Saksbehandler: Harald Loeng (editor)	Avdeling:
Oppdragsgiver ref: NFFR, NAVF, MD	Prosjekt Nr:
	Ansvarlig:

**Sammendrag:**

Between 29 July and 19 August 1985, the R/V "G.O.Sars" carried out investigations in the northern Barents Sea. The cruise was organized by the Institute of Marine Research (IMR). The main purpose was to carry out investigations on the physical and biological environment and the feeding conditions of capelin, an IMR project under PRO MARE.

Several scientist working on other PRO MARE projects participated on this cruise in a coordinated study program.

This report presents the first results of the different projects.

**Stikkord:**

- Field observations
- .....
- Ecology
- .....
- Barents Sea
- .....
- PRO MARE
- .....

**Sendt til:**

- .....
- .....
- .....
- .....
- .....



## PREFACE

The cruise with R/V "G.O. Sars" to the Barents Sea in August 1985 represented a continuation of studies at the Institute of Marine Research (IMR) on the feeding conditions of capelin. The cruise was organized by IMR's project "Feeding conditions of capelin" within the framework of the Norwegian Research Program on Marine Arctic Ecology (PRO MARE). Several other PRO MARE projects, covering the fields of microbiology, nitrogen dynamics, microzooplankton and sedimentation, participated on the cruise in a coordinated study program. In addition, two visiting scientists from USA joined in the cruise.

The scientific program centered on two main topics. The first concerned the vertical structure of physical, chemical and biological properties within the water column. The second was a special study of the capelin distribution on the northern front during its seasonal feeding migration.

The present report consists of separate contributions from the various participating projects. The results are preliminary and an integrated and comprehensive data analysis has not yet been attempted.

The PRO MARE program is sponsored by the Norwegian Fisheries Research Council (NFFR), the Norwegian Council for Science and Humanities (NAVF) and the Ministry of Environment (MD).

Bergen, 31 January 1986

Hein Rune Skjoldal  
Chairman, PRO MARE

## CONTENT

	Page
H. Loeng, A. Hassel, F. Rey and H.R. Skjoldal: Physical and biological oceanography and capelin front study	5
S. Kristiansen and T. Farbrot: Nitrogen cycling in the Barents Sea, July-August 1985	61
C.D. Hewes: Nanoplankton biomass in the Barents Sea	63
W.S. Chamberlin: Bio-optical properties of the Barents Sea during summer	69
T.F. Thingstad, Ø. Enger and E.F. Skjoldal: Microbial heterotrophic activity	75
T. Dale: Microplankton in the Barents Sea in August 1985.	103
P. Wassmann: Sedimentation of organic material in the Barents Sea	121

PHYSICAL AND BIOLOGICAL OCEANOGRAPHY AND CAPELIN FRONT STUDY

By

H. LOENG, A. HASSEL, F. REY and H.R. SKJOLDAL

Institute of Marine Research  
P.O. Box 1870,  
N-5011 Nordnes, Norway

INTRODUCTION

The physical conditions in the northern Barents Sea in autumn are characterized by marked vertical stratification due to low salinity melt water. The great stability of the water column strongly influences the vertical organization and functional properties of the pelagic ecosystem. Of particular importance in this respect is the separation of material flow in the food web dependant on production based on regenerated and vertically admixed nutrients, respectively.

A series of selected stations positioned in water masses with different physical conditions were occupied during the cruise. On these "large stations" an extensive program was carried out to provide a fairly detailed description of the vertical structure of chemical and biological properties. Our observations included hydrography, nutrients, in situ chlorophyll fluorescence, phytoplankton biomass, species composition and primary production, and zooplankton biomass, species composition and nutrient excretion.

A special study of capelin on its seasonal northwards feeding migration was carried out. A characteristic feature of the capelin distribution at this time of the year is a fairly

narrow band with high abundance of capelin. This "capelin front" has, in previous years, been observed to migrate northward at a speed of 3-6 nautical miles per day. We surveyed the capelin front in the area between  $28^{\circ}$  and  $35^{\circ}$ E. In this survey we were assisted by R/V "Håkon Mosby" (University of Bergen) which was carrying out another PRO MARE cruise. An extensive series of MOCNESS profiles of zooplankton abundance and composition was obtained with stations positioned in front of (i.e. north of), in, and behind the capelin front. The study area was revisited about one week later with a second survey of capelin and zooplankton sampling carried out.

Gelatinous zooplankton (i.e. ctenophores and medusae) can play an important ecological role as predators on herbivorous zooplankton and thereby compete for food with pelagic fishes. The existing information on gelatinous zooplankton in the Barents Sea is sparse. During this cruise we emphasized obtaining quantitative data on gelatinous zooplankton. Since many of them disintegrate upon preservation, all MOCNESS samples were analysed alive on board the ship. Ctenophores and medusae were sorted out, identified, and their numerical abundance and wet weight biomass were determined.

Magnar Hagebø, Roger Kvalsund, Fernando Mora, Lena Omli and Ågot Sætveit participated as assistants on the cruise. In addition, Hagebø and Omli were responsible for nutrients and zooplankton samples analyses.

#### SAMPLING AND METHODS

Survey routes and stations are shown in Fig. 1. A complete list of stations and sampling are given in Appendix A (page 57).

The distance between stations along the courselines varied from 5 to 15 nautical miles. Standard hydrographic sampling was carried out with a Neil Brown Mk III CTD sonde mounted together with a General Oceanic Rosette Sampler equipped with 2.5 l Niskin bottles. Sampling depths of the water column were selected by consideration of both the physical structure as

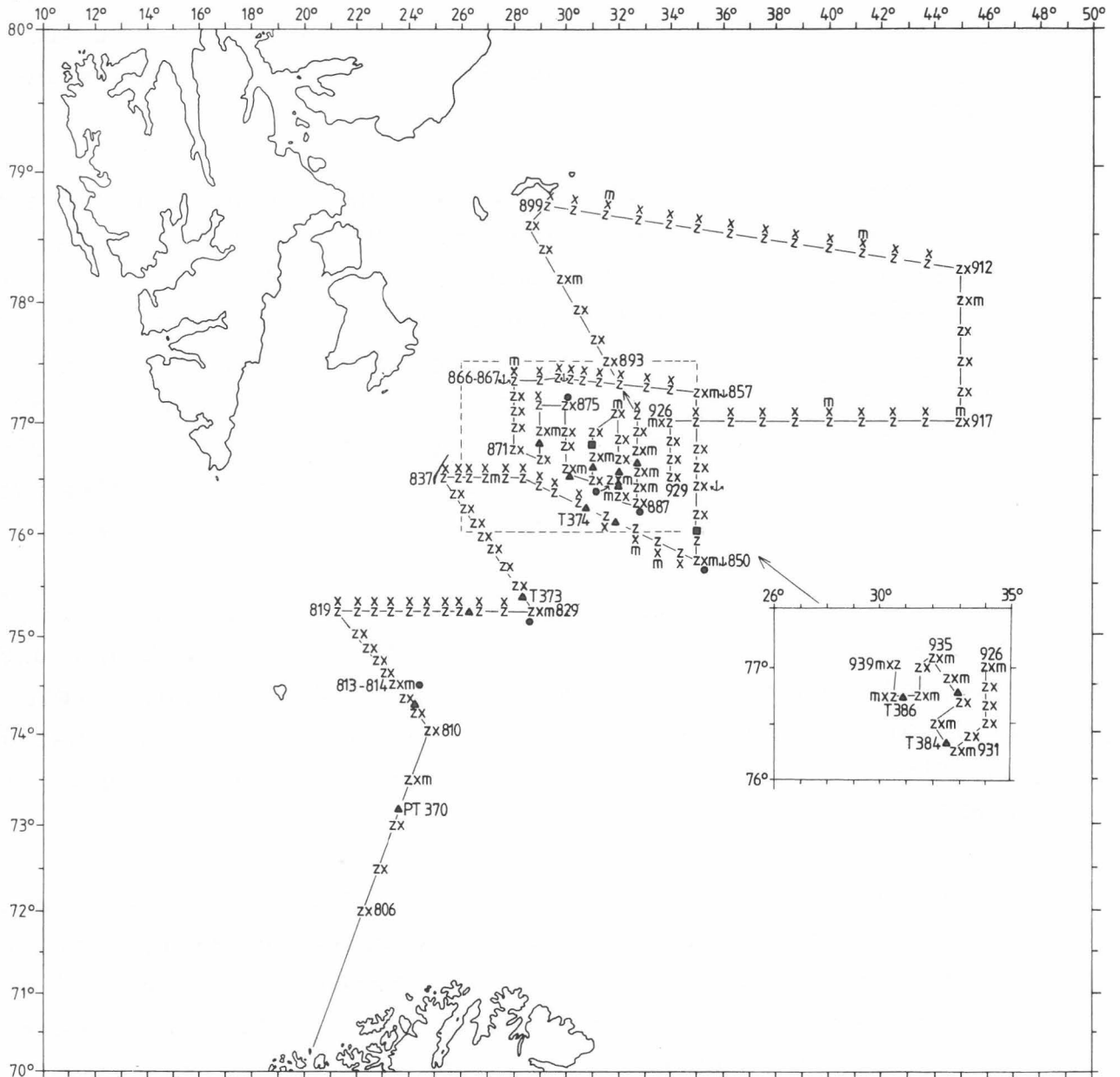


Fig. 1. Survey routes and stations for R/V "G.O. Sars" in the period 1-19 August 1985. Z - CTD, X - water samples and Juday net, m - MOCNESS, ⚓ - current meters, ● - sedimentation trap, △ - pelagic trawl, □ - bottom trawl. The numbers show the station numbers, T-numbers are trawl station number.

determined by the CTD profile, and biological structure through a profile of the chlorophyll in vivo fluorescence obtained with an in situ fluorometer (Q-Instruments, Denmark). Emphasis was placed upon obtaining representative water samples from the upper mixed layer above, at, and immediately below the major in situ chlorophyll fluorescence maximum as well as from deeper water.

At all stations water samples were taken for analysis of nutrients (all depths), phytoplankton pigments (down to 100-125 meters) and phytoplankton species composition (a few selected depths).

At selected stations, additional samples were obtained at a few depths with 30 l Niskin bottles. These water samples were prefiltered through a 250  $\mu\text{m}$  mesh Nynetex plankton net. Subsamples were obtained for the analysis of POC/PON, POP, P*S*i, Chl. a, phytoplankton species composition, and photosynthesis v/s light relationships. Subsamples were also used for additional analyses and experiments by other participating scientists. At these selected stations additional samples were taken at all depths for the analysis of ammonia and oxygen.

The samples for nutrient analysis ( $\text{NO}_2^-$ ,  $\text{NO}_3^-$ ,  $\text{PO}_4^{3-}$ ,  $\text{SiO}_4^{4-}$ ) were kept cold at  $+1^\circ\text{C}$  in the dark for a few hours until analyzed with an autoanalyzer using standard methods (FØYN et al., 1981). Ammonia analysis was carried out manually using a modified indophenol method. Oxygen analysis was made using the Winkler method.

Samples for pigment analysis ( $290 \pm 3$  ml) were filtered through 0.45  $\mu\text{m}$  membrane filters and subsequently stored frozen. Within a few days, the pigments were extracted in the dark with 90% acetone for at least 18 hours at  $1-2^\circ\text{C}$ . After centrifugation, the fluorescence of the extract was measured both before and after acidification with 5% v/v hydrochloric acid, using a Turner III filter fluorometer. The fluorometer was calibrated against pure chlorophyll (Sigma). Estimation of chlorophyll a and phaeopigment concentrations were made using the equations of LORENZEN (1966).

Photosynthesis v/s light experiments were carried out by inoculating 100 ml water samples with approx. 4  $\mu\text{Ci}$   $\text{Na}_2\text{H}^{14}\text{CO}_3$  and incubating them in a laboratory incubator with fluorescent light. Ten different light intensities were available ( $0-300 \mu\text{E}\cdot\text{m}^{-2}\cdot\text{sec}^{-1}$ ) with light attenuated by neutral density filters. The incubator was maintained at a subsurface water temperature.



Incubation time was about 4 hours. Following incubation the samples were immediately filtered through 0.4  $\mu\text{m}$  membrane filters and these were placed in liquid scintillation vials. The filters were then fumed with HCl for 10 minutes and 7 ml Optifluor scintillation cocktail was added. Radioactivity was measured using a Packard liquid scintillation spectrometer. Calculation for the P v/s L curve was made using the equation of PLATT et al. (1980).

Incident solar radiation was measured continuously during the cruise with a Lambda quantum sensor (cosine type). At a few stations, underwater solar radiation was directly measured with a Lambda scalar quantum sensor.

Samples for composition of phytoplankton species are being examined with the inverted microscope method.

Samples for POC/PON, POP and P*S*i are still not analyzed.

Juday net, MOCNESS trawl and pump were used to collect zooplankton. A small 36 cm diameter Juday-net with opening area 0.1 m<sup>2</sup> and mesh size 250  $\mu\text{m}$  was hauled vertically from the near bottom to the surface at all stations to obtain a measure of the total biomass in the water column. A 50% subsample was strained through a 850  $\mu\text{m}$  gauze to separate large and small forms of plankton (>850  $\mu\text{m}$ -fraction and 250-850  $\mu\text{m}$ -fraction). The two fractions were stored frozen until determination of dry weight was made. The other half of the catch was preserved in 4% formaldehyde for species identification and quantification.

MOCNESS-01 (Multiple Opening and Closing Net and Environmental Sensing System) is a remote controlled plankton trawl with nine nets. The opening area is 1 m<sup>2</sup>, and the mesh size used was 333  $\mu\text{m}$ . The gear was lowered to a depth of approximately 20 m above the ocean bottom where the first net was released at a speed of about 2 knots. Successive horizontal hauls were obtained at selected depths. The closing/opening of the nets was performed between the main depths. Thus most of the catching took place within rather limited depths ( $\pm$  5 m). The

last net was sampled when the gear was visible from the ship. This corresponded to approximately 5 m depth. Time, flow counts, angle of net-frame, and depth were recorded automatically with a Commodore computer. From this the amount of filtered water was calculated to be about 200 to 400 m<sup>3</sup> for each net. After removing gelatinous macroplankton (ctenophores and medusa, except siphonophores) for identification and measurements in a fresh condition, the samples were divided with a plankton divider. One half was filtered and frozen for later determination of dry weight. The other half was preserved in formaline. A preliminary taxonomic identification was obtained on board by deciding which plankton categories were the most dominant with respect to biomass. This work was based on a visual and superficial examination of the preserved plankton in bottles.

An immersible plankton pump (HUFSA) was used at 12 stations to get a detailed picture of the plankton distribution in the upper 50-80 meters. The pump is based on a Flygt 4400-410 2kW mixer mounted in a bent tube with 42 cm diameter on a platform. A plankton net with mesh size 250  $\mu$ m was attached to the upper end of the tube. The plankton pump is based on the same concept as the Flygt mixer described in SOLEMDAL and ELLERTSEN (1984), but with smaller dimensions and capacity. The theoretical flow is 8.4 m<sup>3</sup>/min. The actual filtering capacity has not yet been measured, but an identical pump equipped with a 180  $\mu$ m mesh net was found to filter 4.23 m<sup>3</sup>/min, or about half the capacity of the theoretical undisturbed flow (KURT TANDE, pers. comm.). However, results are here given as mg dry weight/minute pumping time. Pumping time was 3 minutes at each depth. In most cases pumping depths were selected in relation to the chlorophyll maximum, with 5-10 m intervals. The samples were divided for dry weight and for preservation.

The distribution of capelin was observed by operating digital echo integrators. Echo intensities were integrated continuously, and mean values per nautical mile were recorded for each 5 nautical mile. Trawl stations were carried out both for identification purposes and in order to obtain observations of

length, weight, maturity stage, stomach filling degree and age of capelin. Some capelin were also preserved by freezing for later identification of stomach content in relation to food resources.

## RESULTS

Only a part of the data collected during the cruise are worked up until now. In this report, the horizontal and vertical distribution of temperature and salinity are briefly described together with the distribution of chlorophyll a and nutrients. In addition, some selected stations (which were common for most of the participating scientists) are described in more detail. The zooplankton results are concentrated to the description of its vertical distribution and species composition.

### Horizontal distribution of hydrography and chlorophyll a

The horizontal distribution of temperature and salinity at 50 m are shown in Fig. 2. This depth is below the pycnocline, and the water masses are therefore not influenced either by melt water or by temperature heating from the atmosphere. Consequently, Fig. 2 indicates the areas which were occupied by Arctic and Atlantic water masses, and also shows the position of the oceanic Polar front.

Water with temperature below  $0^{\circ}\text{C}$  and with salinity from 34.4 to  $34.6^{\circ}/\text{oo}$  is usually characterized as Arctic water (LOENG 1985), while water of Atlantic origin in this area has salinity above  $34.9^{\circ}/\text{oo}$ . Water with salinity between 34.6 and  $34.9^{\circ}/\text{oo}$  is a mixture between these two main water masses.

The position of the southgoing Bear Island Current is easily seen between the two sharp fronts in the temperature distribution along the eastern slope of the Svalbard Bank, from Hopen south to Bear Island. The core had a temperature below  $-1^{\circ}\text{C}$ . The western front was against a permanent eddy above the most shallow part of the bank area, while the eastern front was against the Atlantic water which is flowing northwards.

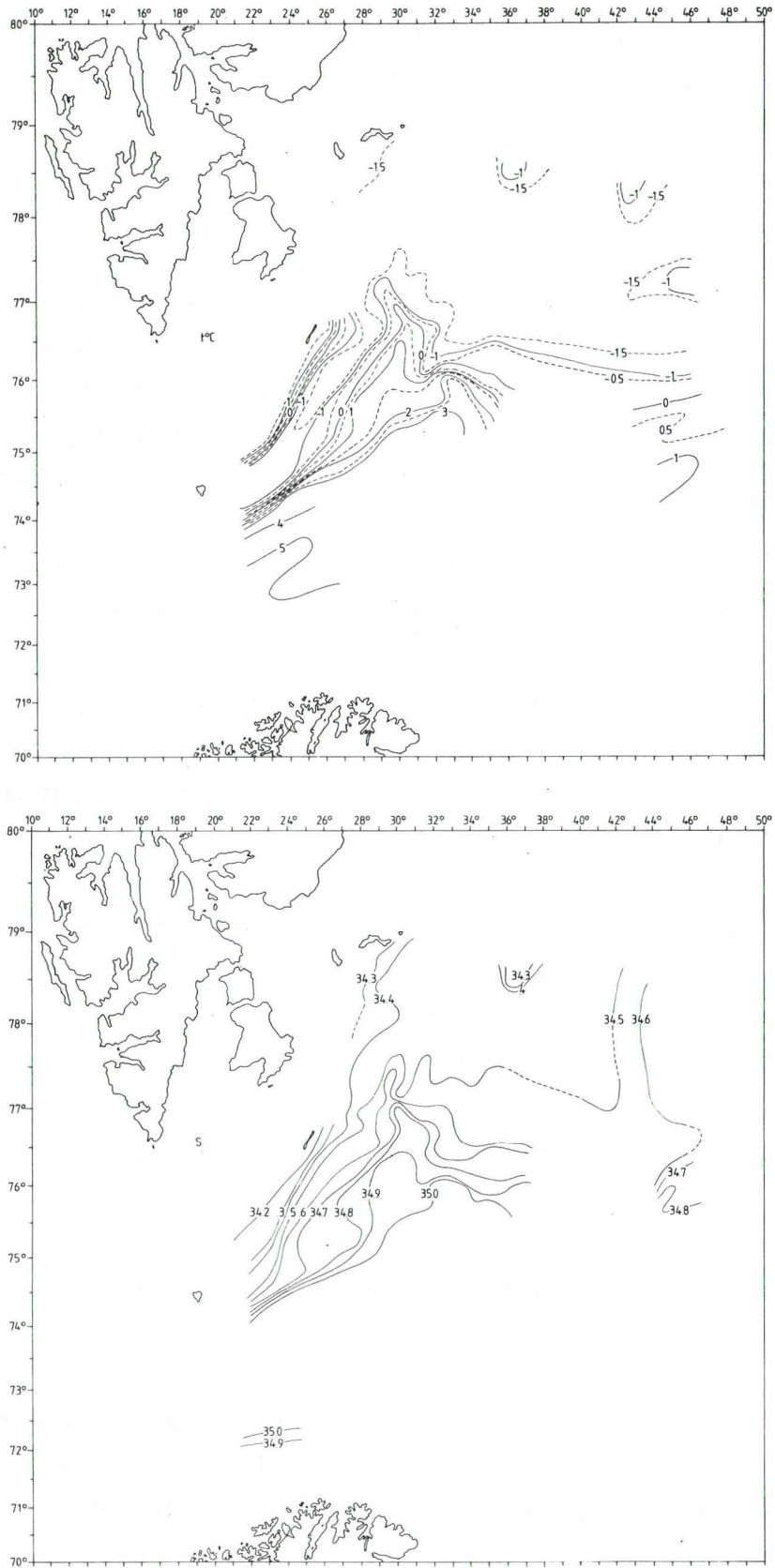


Fig. 2. Temperature (upper) and salinity (lower) at 50 m in August 1985. Based on data from R/V "G.O. Sars" and R/V "Håkon Mosby".

Relatively few stations were taken in the northern and eastern part of the investigated area, so the position of isolines in these areas were more uncertain. However, it seems clear that Arctic water covered most of the area north of  $76^{\circ}\text{N}$ .

In order to give an estimate of the phytoplankton biomass distribution in the whole investigated area, we have calculated an average chlorophyll a concentration for the upper 50 meters at every station. The distribution of these average concentrations is shown in Fig. 3. In the southern part of the area there was a distinct zone with average concentrations lower than  $0.5 \text{ mg}\cdot\text{m}^{-3}$ . This zone coincided with the Polar front region between the Arctic water on the shallow Svalbard Bank and the Atlantic water inflow to the Barents Sea. In both latter areas average chlorophyll a was larger than  $1 \text{ mg}\cdot\text{m}^{-3}$  but its vertical distribution was quite different. Meanwhile, at the stations above the bank, chlorophyll a was more or less homogeneously distributed with depth down to the bottom, in the

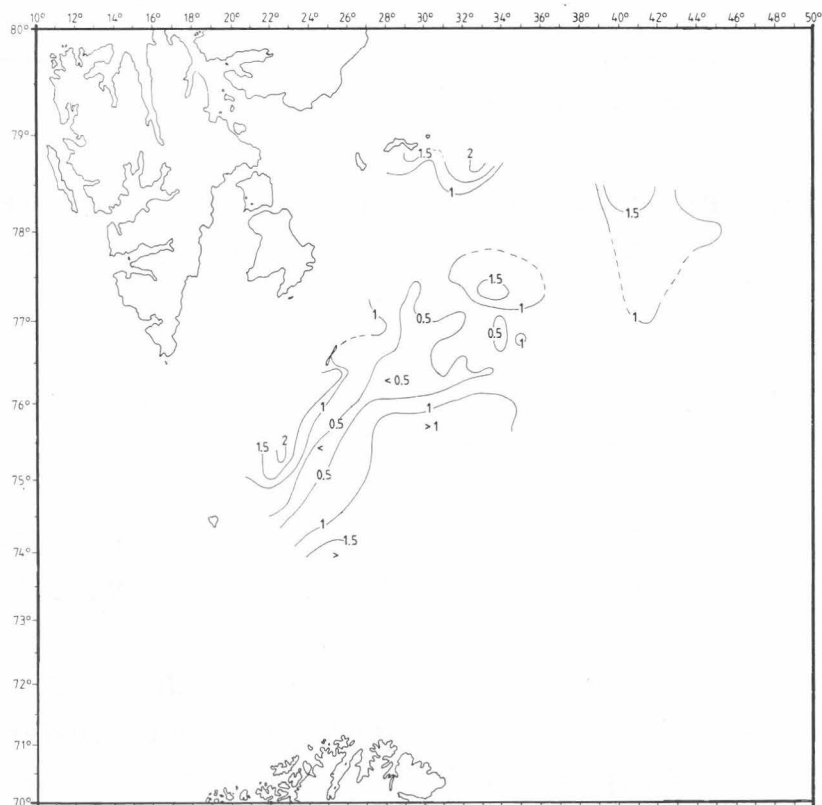


Fig. 3. Average chlorophyll a concentrations ( $\text{mg}\cdot\text{m}^{-3}$ ) in the upper 50 m of the water column.

other area chlorophyll a showed a clearly distinct subsurface maximum below the pycnocline, and the surface concentrations usually were lower than  $0.3 \text{ mg}\cdot\text{m}^{-3}$ . In the northern part of the investigated area average chlorophyll a concentrations were usually larger than  $1 \text{ mg}\cdot\text{m}^{-3}$ . At almost all stations a marked subsurface chlorophyll a maximum was found below the pycnocline. The chlorophyll a concentration at the maximum increased northwards, reaching its highest value ( $>8 \text{ mg}\cdot\text{m}^{-3}$ ) at the station where average chlorophyll a was larger than  $2 \text{ mg}\cdot\text{m}^{-3}$ . In the whole area an average of 78% of the chlorophyll a was found in the size range less than  $10 \mu\text{m}$ .

Nutrients, with the exception of phosphate, were completely exhausted in the upper layer.

#### Vertical distribution

The description of the physical conditions and the distribution of nutrients and chlorophyll a has been concentrated to four sections. These are named A, B, C and D.

Section A: from Hopen eastwards to the Central Bank (st. 837-850, Fig. 1).

Section B: from the Central Bank north to the Great Bank (st. 850-857) and then west to the Svalbard Bank (to st. 866, Fig. 1).

Section C: from Kong Karls Land eastwards to  $45^{\circ}\text{E}$  (st. 899-912 on Fig. 1).

Section D: along  $45^{\circ}\text{E}$  from  $78^{\circ}15'\text{N}$  south to  $74^{\circ}00'\text{N}$  ("G.O. Sars" st. 912-917 and "Håkon Mosby" st. 125-139).

A common feature for all sections were the well mixed surface layer (10-20 m deep), separated from the underlying water masses with a sharp transition layer. In the areas which had been ice covered during the previous winter, the surface layer consisted of melt water with salinity below  $34.0^{\circ}/\text{oo}$  and

a relatively high temperature which varied with the latitude. In areas with no ice during winter, the transition layer was less sharp and had been developed mainly due to warming from the atmosphere.

The nutrient distribution at the four sections was characterized by the complete exhaustion of nitrate and silicate and the low concentrations of phosphate in the upper 20 to 30 meter depth. In this layer chlorophyll a showed very low concentrations ( $0.2-0.5 \text{ mg}\cdot\text{m}^{-3}$ ) and most of it was found in the size fraction less than  $10 \mu\text{m}$ . These findings indicate that the upper layer had reached an oligotrophic state. Below the oligotrophic layer nutrients increased sharply with depth giving form to a very marked nutricline. A conspicuous chlorophyll a maximum, varying in magnitude, was found associated to the nutricline. Below the subsurface maximum, chlorophyll a decreased rapidly to concentrations usually below  $0.1 \text{ mg}\cdot\text{m}^{-3}$ . On the other hand, nutrient concentrations increased gradually with depth.

#### Section A

-----  
The eastern slope of the Svalbard Bank was covered by four sections (Fig. 1) in order to map the position of the Bear Island Current. Section A is the most northern of these sections, and the vertical distribution of temperature, salinity and  $\sigma_t$  are shown in Fig. 4. The distribution of water masses was practically the same in the other three sections.

The position of the Bear Island Current is most easily seen in the temperature section. The core of the current is defined by  $t < -1^\circ\text{C}$ , but water with  $t < 0^\circ\text{C}$  also belongs to the current system. In all four sections on the bank, the current was situated below the pycnocline, and restricted to area with bottom depth between approximately 75-150 m. In January 1985, the Bear Island current in the same area was situated in the upper 75 m of the water column (HASSEL, LOENG and SKJOLDAL 1986).

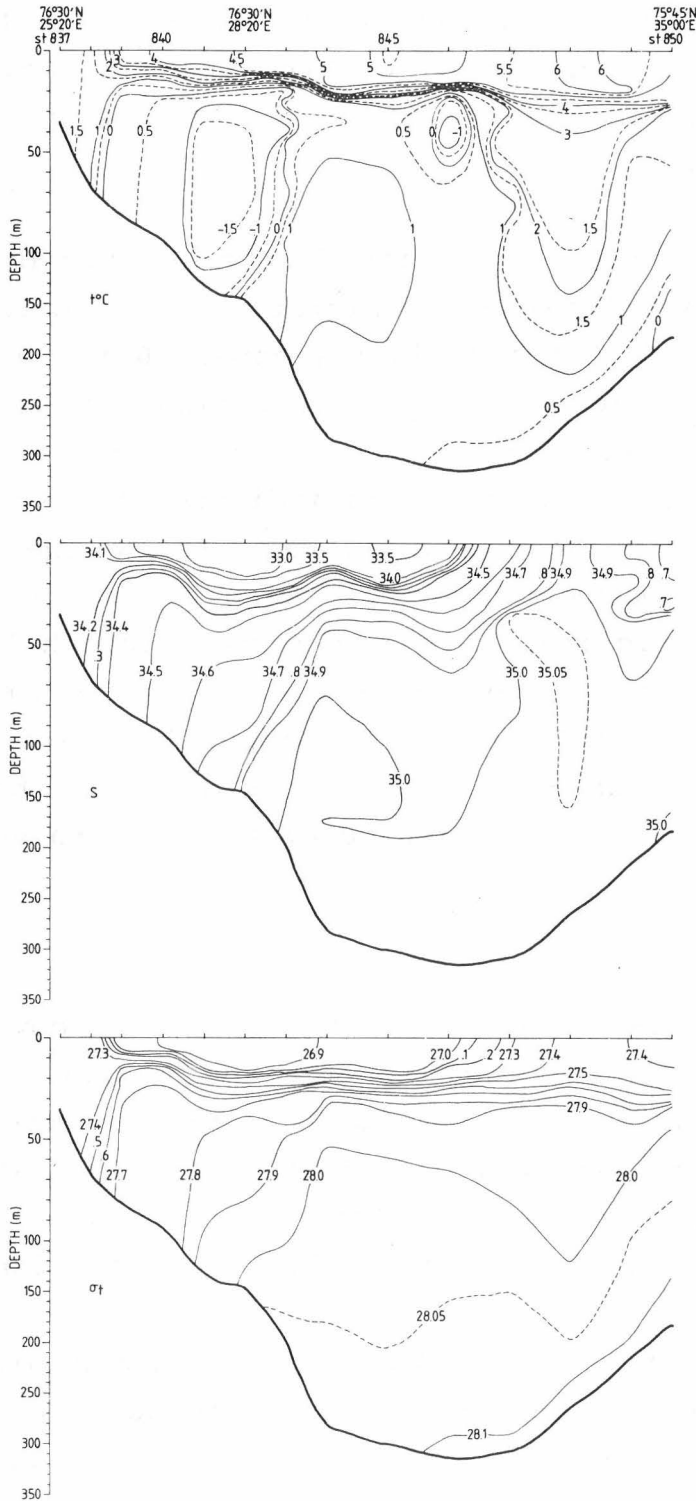


Fig. 4. Distribution of temperature, salinity and  $\sigma_t$  in section A.

The Atlantic water ( $S > 35.0^{\circ}/\text{oo}$ ) was flowing northwards in the deeper area between the Svalbard Bank and the Central Bank. The core ( $S > 35.05^{\circ}/\text{oo}$ ) was found in the eastern part of the section. The temperature section indicates a division of the



Atlantic current, one branch flowing northwards along the Svalbard Bank ( $t > 1^{\circ}\text{C}$ ) and the other branch ( $t > 1^{\circ}\text{C}$ ) close to the Central Bank.

The temperature section shows a small area with low temperature ( $t < 0^{\circ}\text{C}$ ) at st. 846. This is a part of the intermediate Arctic water, situated above the Great Bank.

The vertical distributions of phosphate, nitrate, silicate and chlorophyll a are shown in Fig. 5. One special feature at this section was the complete vertical mixing of the water column observed at the bank area near the Hopen Island. Also in this area, the highest surface values of silicate and chlorophyll a concentration were found. The front between Arctic water and the Atlantic water was also easily identified by the marked vertical gradient of nutrients (specially nitrate) that reached the bottom. At the deeper layers, the main inflow of Atlantic water can also be identified by their high nutrient concentrations (phosphate  $>0.8 \mu\text{m}$ ; nitrate  $>12 \mu\text{m}$  and silicate  $>6 \mu\text{m}$ ).

The subsurface chlorophyll a maximum was clearly evident only in the eastern part of the section, in the area dominated by Atlantic water.

#### Section B

-----

There were three main features in this section which need some comments (Fig. 6). Firstly, the flow of Atlantic water eastwards between the Central Bank and the Great Bank. The temperature was here just above  $0.5^{\circ}\text{C}$  and the salinity was above  $34.9^{\circ}/\text{oo}$ . The water with  $\sigma_t > 28.1$  close to the bottom is bottom water formed on the Central Bank during the last winter.

The second main feature is the intermediate layer of cold Arctic water on the Great Bank and the Svalbard Bank. The temperature was below  $-1^{\circ}\text{C}$  in most of the water column, and the position of the deepest  $-1^{\circ}$ -isotherm indicate the approximate depth of winter convection in this area. The two cores with  $t < -1.5^{\circ}\text{C}$  indicate the position of two different current system.

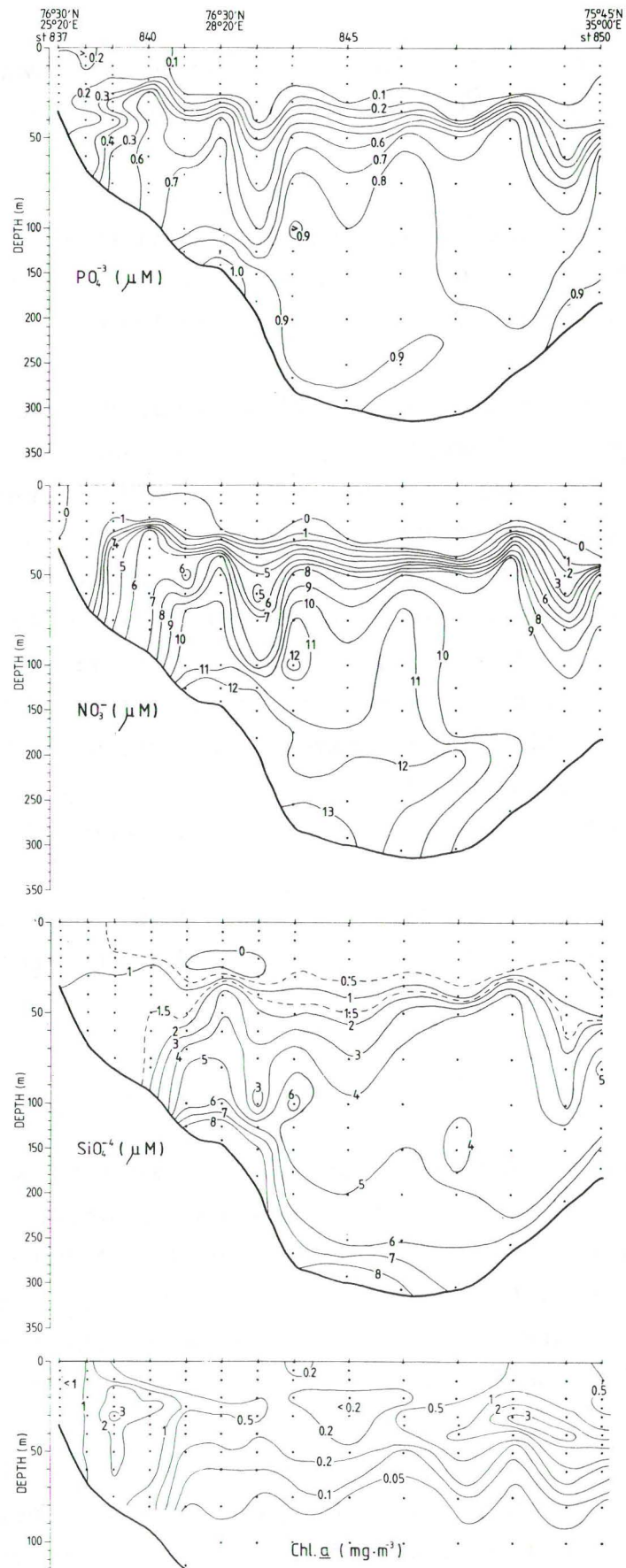


Fig. 5. Distribution of phosphate, nitrate, silicate and chlorophyll a in section A.

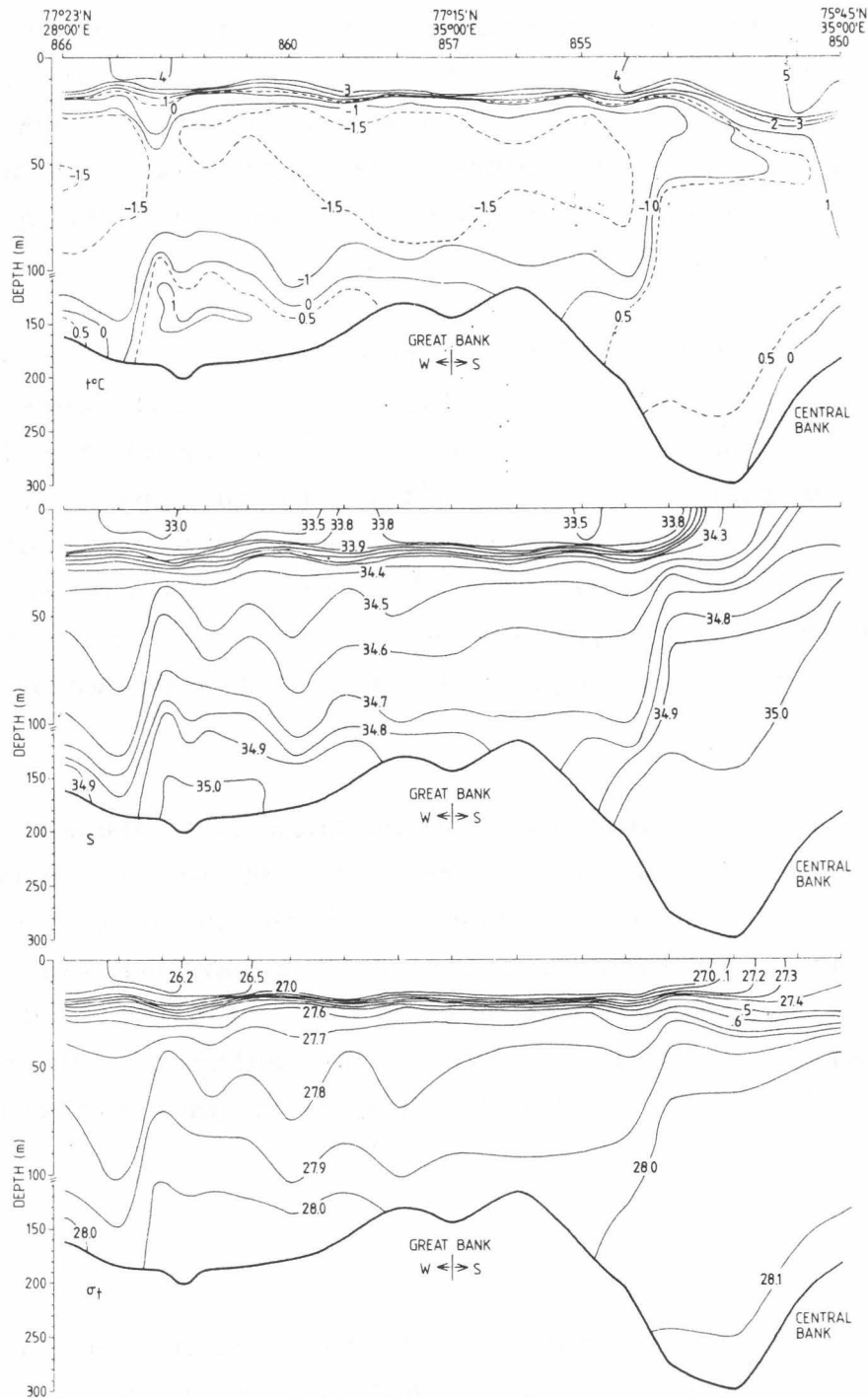


Fig. 6. Distribution of temperature, salinity and  $\sigma_t$  in section B.

The core above the Great Bank belongs to the Persey Current coming from northeast, while the core in the western part of the section probably is a part of the East Spitsbergen Current. Further south these water masses together form the Bear Island Current.

The third and last phenomena which can be observed in this section is the Atlantic water flowing northwards close to the bottom between the Svalbard Bank and the Great Bank (st. 859 - 864 on Fig. 6). The current is most easily traced by its salinity which is higher than  $34.9^{\circ}/\text{oo}$ , or even greater than  $35.0^{\circ}/\text{oo}$  near the bottom.

The vertical distributions of phosphate, nitrate, silicate and chlorophyll a are shown in Fig. 7. A gradual deepening of the nutricline from north to south was clearly observed. This is mainly the result of a transition in the physical conditions (deepness and sharpness) when moving from Arctic waters in the north to Atlantic waters in the south. In the deeper layers the Atlantic water laying just above the Great Bank had a higher nutrient content than the Atlantic water near the Central Bank.

The subsurface chlorophyll a maximum was present along the entire section and lay deeper in the water column in the southern part compared to that found in the north and above the Great Bank. The largest chlorophyll a maximum was found above the Great Bank in waters colder than  $-1.5^{\circ}\text{C}$ . A deepening of this maximum, associated with a deepening of the nutricline, can possibly be attributed to sinking of phytoplankton.

#### Section C

-----

Fig. 8 shows the distribution of temperature, salinity and  $\sigma_t$  in a section from Kong Karls Land east-southeastwards to  $45^{\circ}\text{E}$ . The section crossed the shallowest part of the Great Bank (st. 905-906), and on each side of the bank there were deeper basins. The distribution of all parameters clearly indicated a vortex above the top of the bank area. The transition layer was also less sharp in this area compared to other stations along the section.

In each of the two basins, there was an intermediate layer of Arctic water characterized by  $t < -1^{\circ}\text{C}$  and  $34.3 < S < 34.6$ . As

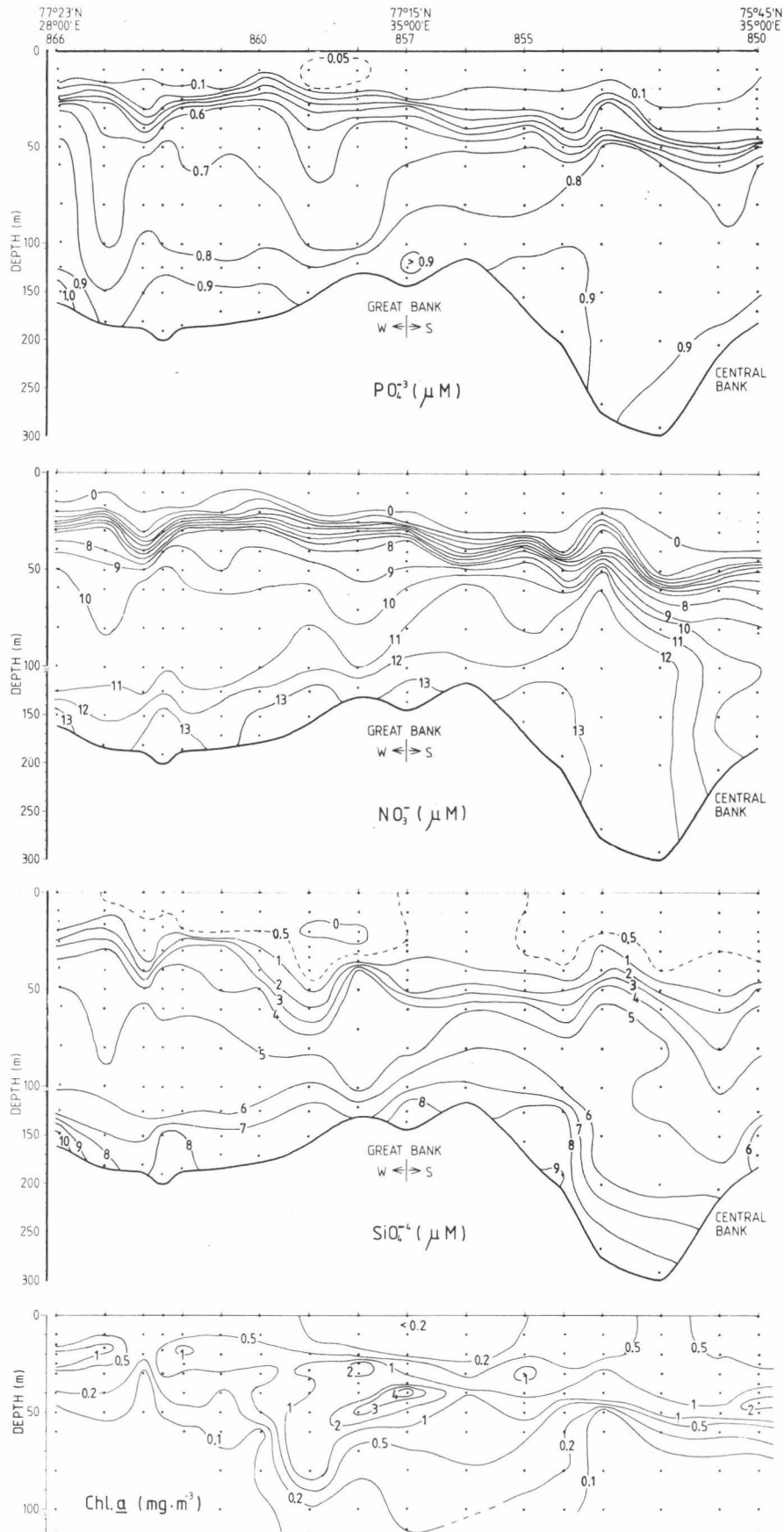


Fig. 7. Distribution of phosphate, nitrate, silicate and chlorophyll a in section B.

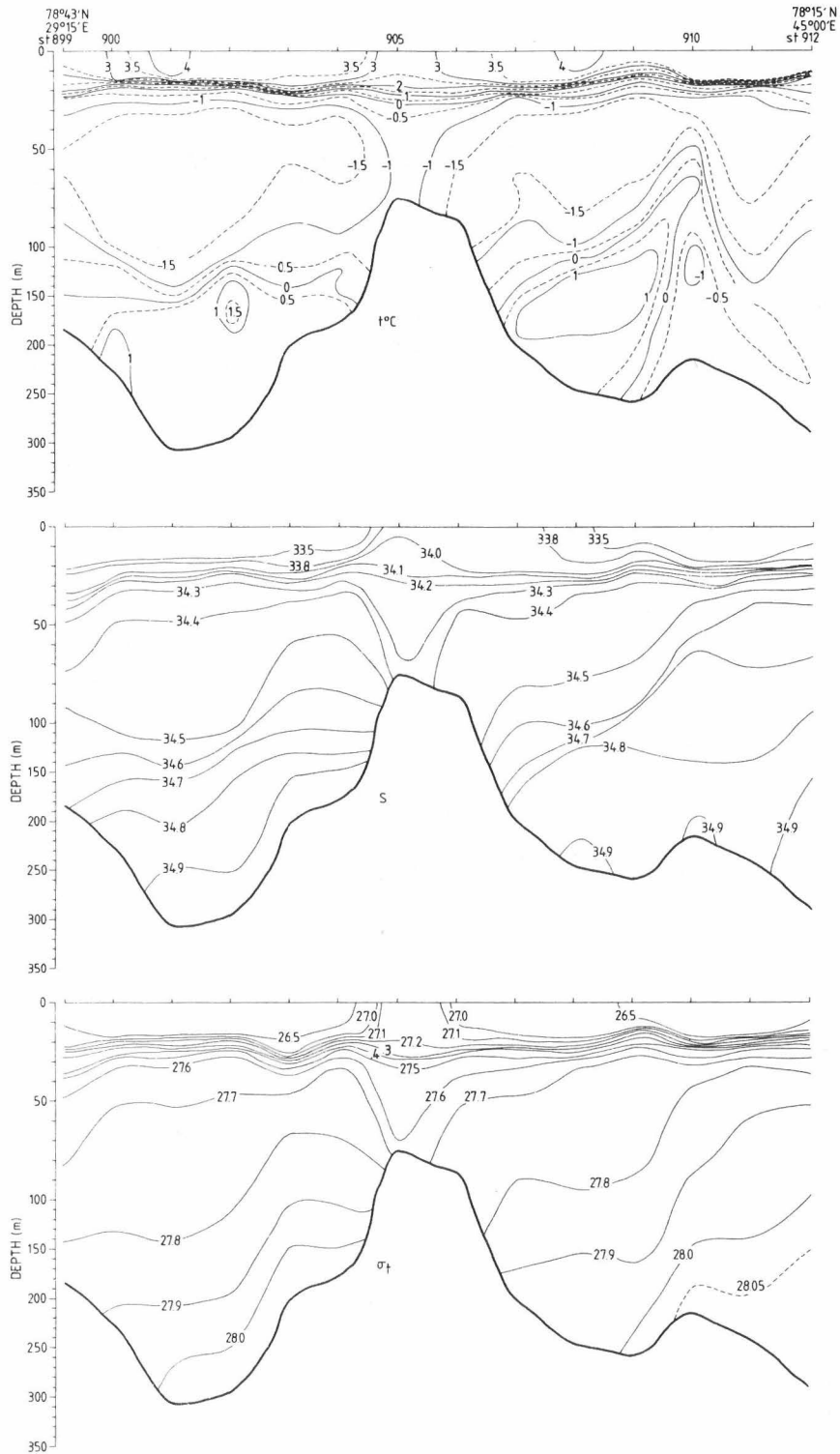


Fig. 8. Distribution of temperature, salinity and  $\sigma_t$  in section C.

depicted most clearly in the western basin there was an increase both in temperature and in salinity, close to the bottom of the water column. The water with temperatures higher than

0°C is of Atlantic origin. It has most probably come from the south (see section B, the area between the Svalbard Bank and the Great Bank). However, this water may also have been flowing into the Barents Sea from the north. This should be subjected to closer investigation.

In the eastern basin, there seemed to be a northgoing current, linked to the eastern slope of the bank. Due to the relatively low salinity ( $S < 34.9^{\circ}/\text{oo}$ ) the water is most probably a mixture of Atlantic and Arctic water. However, the knowledge of both the distribution of water masses and the circulation in this part of the ocean is too little, in which to draw any conclusions about watermasses in this area.

The vertical distributions of phosphate, nitrate, silicate and chlorophyll a are shown in Fig. 9. The nutricline lay at the same depth along the whole section. An exception to this was the area above the shallow part of the Great Bank where the presence of an eddy forced the lower part of the nutricline to bent down towards the bottom. In deeper water the nutrient-rich Atlantic water and mixed water were easily observed at both sides of the bank.

The chlorophyll depth profile had two maxima in the regions both east and west of the Great Bank. These were also the areas where the highest chlorophyll a maxima were found.

#### Section D

-----  
The stations in the northern part of the section (Fig. 10) were taken from R/V "G.O.Sars", while the stations between 76°45'N and 74°00'N were occupied by R/V "Håkon Mosby". The Institute of Geophysics, University in Bergen, has kindly provided us with the hydrographical data from this vessel.

There was a difference in the hydrographic regime north and south of station 130 (Fig. 10). The northern part of the section had a typical intermediate layer of cold water. In contrast with the other sections, the temperature increased

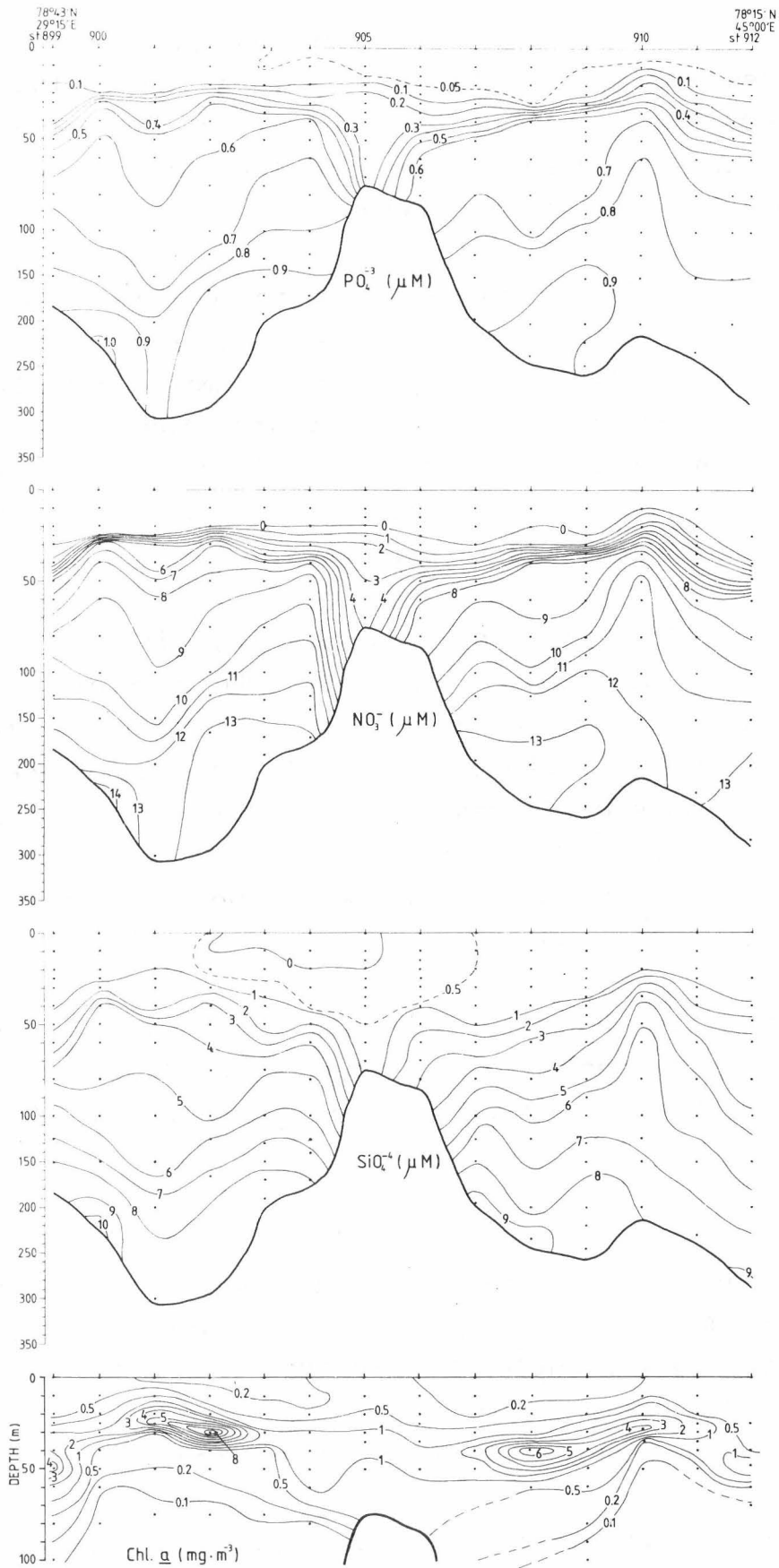


Fig. 9. Distribution of phosphate, nitrate, silicate and chlorophyll a in section C.



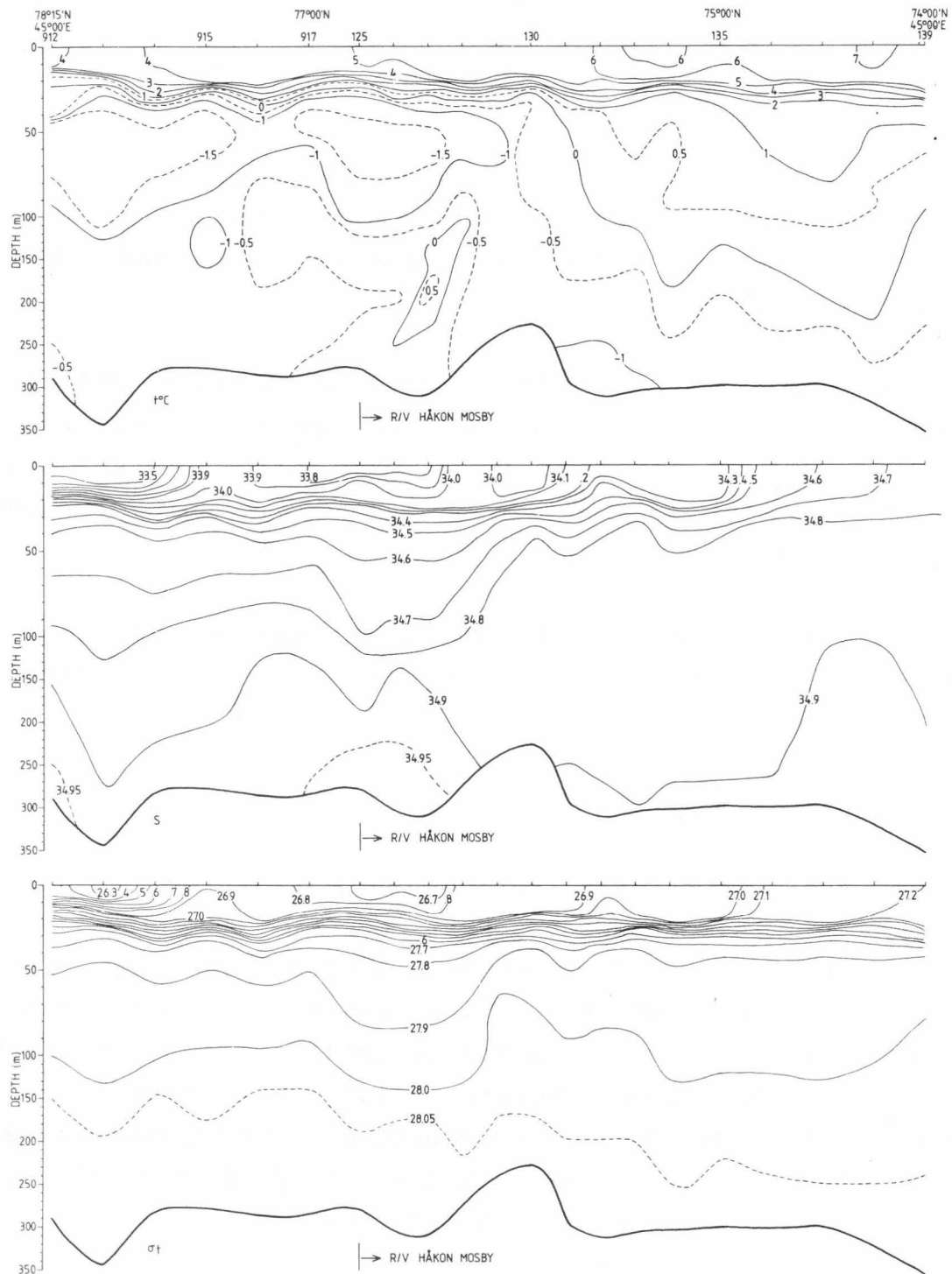


Fig. 10. Distribution of temperature, salinity and  $\sigma_t$  in section D.

very little towards the bottom. In a small area we found salinity above  $34.95^{\circ}/\text{oo}$ , which may be the last part of the Atlantic water flowing westwards between the Central Bank and the Great Bank (see section B).

In the southern part of the section, the salinity was between  $34.8$  and  $34.9^{\circ}/\text{oo}$  in most of the water column, and the tempera-

ture varied from  $-1^{\circ}$  to  $1^{\circ}\text{C}$ . This is a typical mixture of Atlantic and Arctic water.

If the data from the surface layer are examined, it is noted that both salinity and temperature had a steady increase from north to south, and the sharpness of the transition layer decreased.

The vertical distributions of phosphate, nitrate, silicate and chlorophyll a are shown in Fig. 11. The nutricline was found more or less at the same depth from north to south and the nutrient content of the deeper layers was quite homogeneous along the section.

Although the subsurface chlorophyll a maximum was found along the whole section, it was very weak, reaching concentrations scarcely above  $1 \text{ mg}\cdot\text{m}^{-3}$ .

#### The selected stations

During the cruise ten stations were selected for detailed sampling both with respect to the amount of sampling levels and the biological parameters to be measured. The purpose was to get information about the vertical biological stratification in a fairly well stratified physical environment as typified for the Barents Sea during summer. Efforts were made in order to assure that these stations represented those hydrographical and biological conditions as usually found during the summer season. The station positions are shown in Fig. 1.

#### General description

-----

We have grouped the stations in three main categories according to their hydrography:

- A. Stations having a shallow upper layer of meltwater with salinities usually lower than  $33.7^{\circ}/\text{oo}$  on top of Arctic water ( $S < 34.8^{\circ}/\text{oo}$  and  $t < 0^{\circ}\text{C}$ ) which dominated the rest of the water column (to the bottom) (Fig. 12, st. 813, 857, 867, 898 and 909).

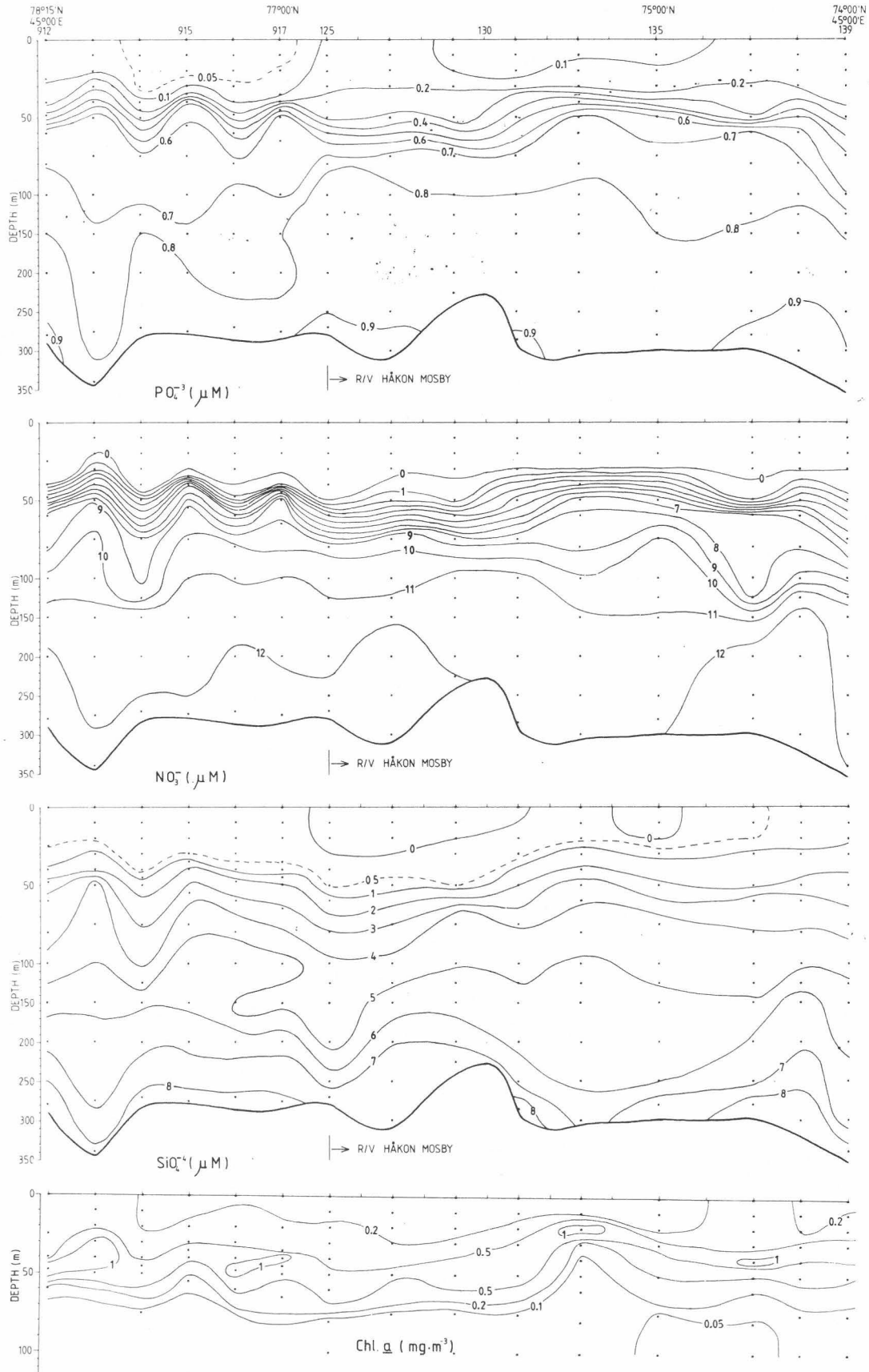


Fig. 11. Distribution of phosphate, nitrate, silicate and chlorophyll a in section D.

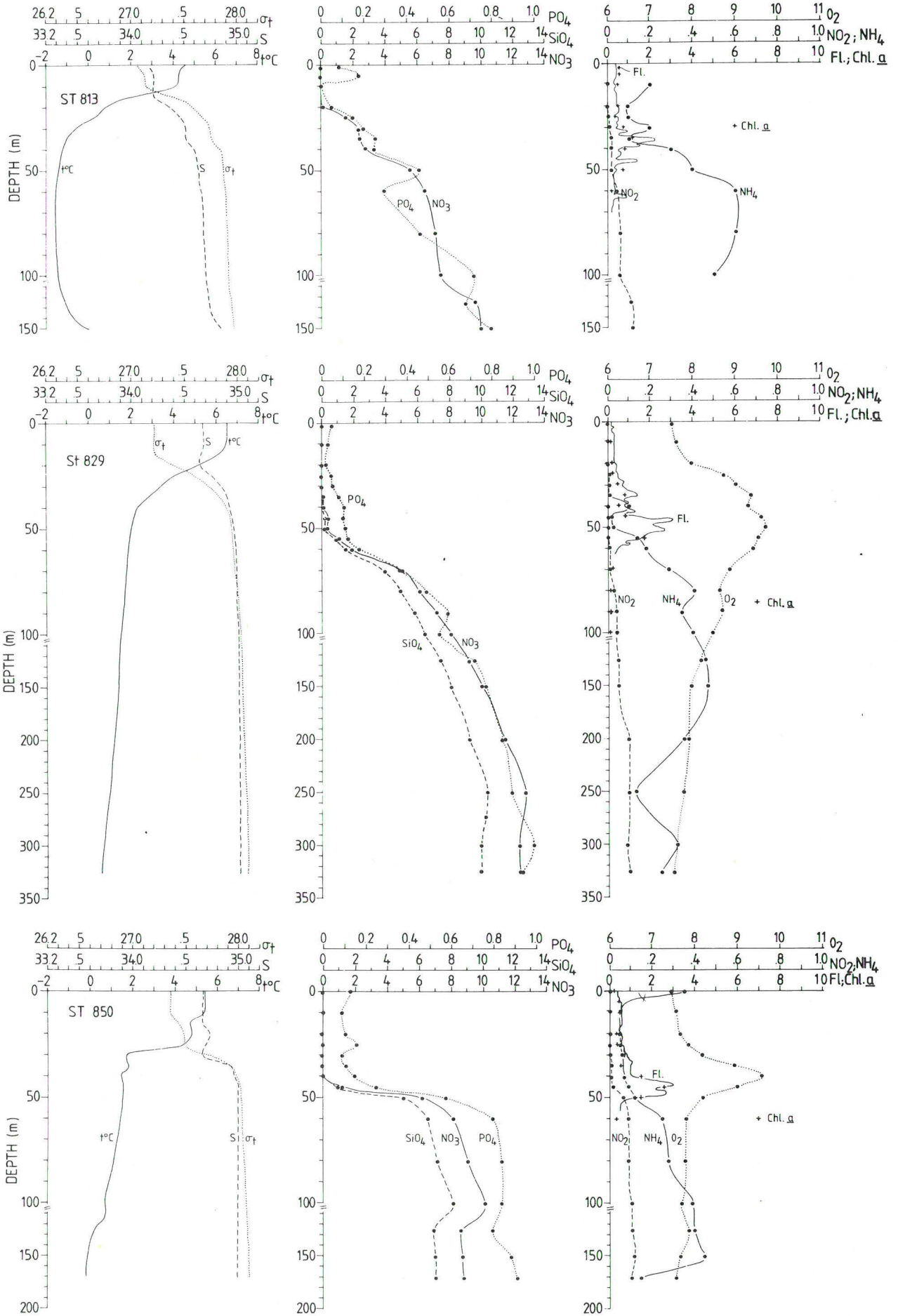


Fig 12 . Vertical profiles of temperature, salinity and  $\sigma_t$  (left), phosphate, nitrate and silicate ( $\mu\text{M}$ ) (middle), and oxygen ( $\text{ml}\cdot\text{l}^{-1}$ ), nitrite, ammonia ( $\mu\text{M}$ ), Chl. *in vivo* fluorescence and Chl *a* ( $\text{mg}\cdot\text{m}^{-3}$ ) (right) at some selected stations.

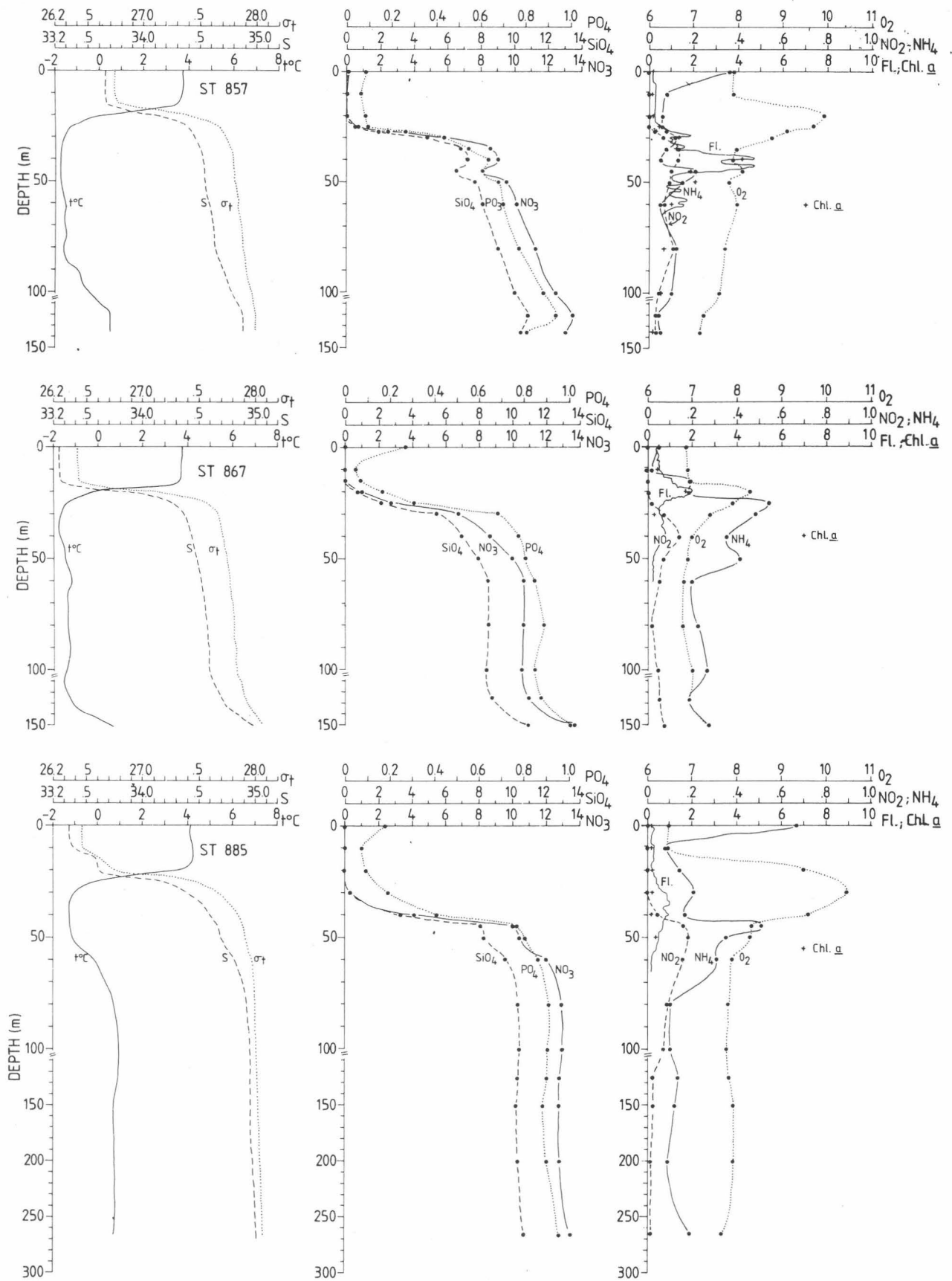


Fig. 12. continued.

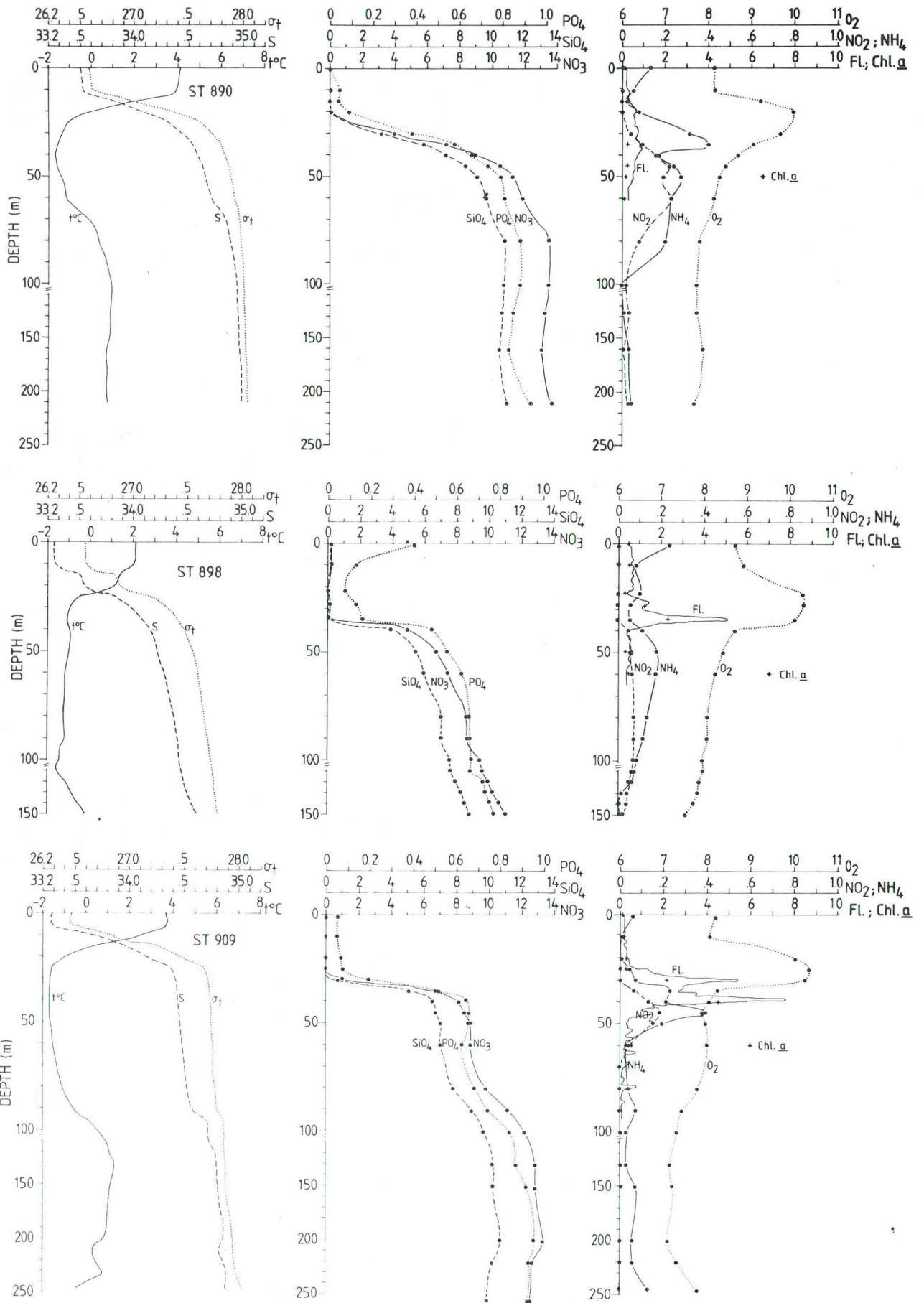


Fig. 12. continued.

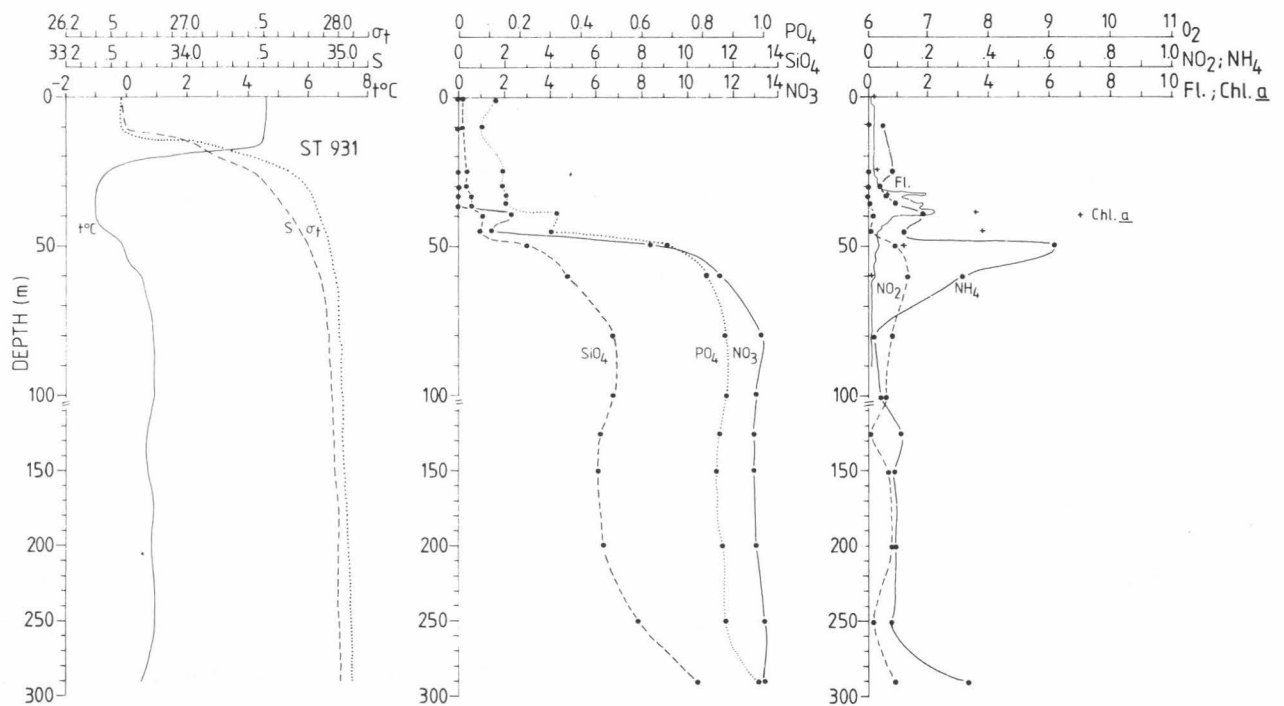


Fig. 12 continued.

- B. Stations with a shallow upper layer of meltwater ( $S < 33.7^{\circ}/\text{oo}$ ) lying over an intermediate layer (20-60 m) of Arctic water with  $t < -1.5^{\circ}\text{C}$ . Below 60 m the water column was dominated by water of Atlantic origin characterized by  $S > 34.9^{\circ}/\text{oo}$  and  $t > 0^{\circ}\text{C}$  (Fig. 12, st. 885, 890 and 931).
- C. Stations with surface layer of mixed water, ( $S > 34.5^{\circ}/\text{oo}$  and  $t > 4^{\circ}\text{C}$ ) that lay above Atlantic water having  $S > 34.9^{\circ}/\text{oo}$  and  $0^{\circ} < t < 2^{\circ}\text{C}$  (Fig. 12, st. 829 and 850).

The vertical distributions for some chemical and biological parameters at these stations are also shown in Fig. 12, and their characteristics are summarized in Table 1.

Below we have focused on some main features from these stations.

Table 1. Physical, biological and chemical parameters from the selected stations. Barents Sea, August 1985.

Group	Station Number	Hydrography				Pycnocline Depth (m)	Pycnocline t (°C)	Nutricline Depth (m)	Nutricline NO <sub>3</sub> <sup>-</sup> (µM·m <sup>-1</sup> )	CHL A MAX.		Ammonia MAX		Oxygen MAX		Satur. (%)		
		Upper Layer t°C	Subsurface S <sup>o</sup> /oo	Subsurface t°C	Bottom S <sup>o</sup> /oo					Depth (m)	Conc. (mg·m <sup>-3</sup> )	Depth (m)	Conc. (µM)	Depth (m)	Conc. (ml·l <sup>-1</sup> )			
	813	4.3	34.2	-1.6	34.6	-1.0	34.7	10-30	0.03	20-50	0.18	35	2.2	30	0.2	-	-	-
	857	3.5	33.6	-1.7	34.6	-0.5	34.8	15-25	0.08	25-35	0.80	40	4.6	45	0.2	20	9.91	122
A	867	3.8	33.2	-1.5	34.5	-1.0	34.7	15-25	0.09	15-30	0.43	20	2.0	25	0.5	20	8.27	121
	898	2.1	33.3	-1.1	34.2	-1.0	34.5	10-25	0.04	35-40	1.00	35	5.0	50	0.2	25	10.29	126
	909	3.7	33.3	-1.7	34.5	1.0	34.8	5-25	0.06	25-40	0.57	39	7.0	45	0.4	25	10.36	123
	885	4.1	33.5	-1.3	34.6	0.8	35.0	20-30	0.09	30-45	0.65	35	1.0	45	0.5	30	8.34	121
B	890	4.1	33.5	-1.7	34.6	0.8	35.0	10-25	0.07	20-45	0.70	37	0.9	35	0.4	20	9.95	124
	931	4.6	33.6	-1.0	34.6	0.5	35.0	10-25	0.07	35-50	0.60	38	2.0	50	0.6	-	-	-
C	829	6.5	34.7	2.0	34.9	0.5	35.0	15-40	0.03	50-70	0.24	50	3.0	40	0.1	50	9.53	125
	850	4.5	34.7	1.5	35.0	0.0	35.0	25-35	0.04	40-50	0.62	45	3.0	-	-	40	9.58	124

- The pycnocline extended from an average of  $13.5 \pm 5.8$  m to  $28.5 \pm 5.3$  m. Those stations with surface layer of mixed water (group C) had a pycnocline which extended slightly deeper than the other stations (group A and B). The pycnocline was, with few exceptions, almost twice as strong at the stations in group A and B than for the stations in group C.
- The nitrate nutricline consequently lay deeper than the pycnocline by an average of  $29.5 \pm 10.7$  m to  $45.5 \pm 10.9$  m. In most cases the nutricline started at the bottom of the pycnocline. Its average strength was  $0.58 \pm 0.25 \mu\text{M} \cdot \text{m}^{-1}$  and was slightly more shallow and stronger at the station groups A and B. The nutricline for phosphate and silicate followed more or less the same trend as for nitrate.
- The main chlorophyll a subsurface maximum lay at an average of  $34.7 \pm 7.8$  m, just at the middle of the average nitrate nutricline. It was found deeper at the stations dominated by Atlantic waters, but the larger concentrations were found at the most northern stations. This indicates that the phytoplankton bloom had not taken place very long before. As expected, chlorophyll a attained the lowest concentration at the stations of group B since



these were typical of the ice-edge area during spring where the phytoplankton bloom had first taken place in the Barents Sea.

- For several stations the ammonia concentration increased with depth. One or two somewhat distinct ammonia maxima were also observed near the main chlorophyll maximum. These maxima could have been due to the combined effect of heterotrophic (ammonia production) and autotrophic (ammonia consumption) activities since in most cases the ammonia minimum between its two maxima, corresponded with the chlorophyll a maximum.
- At all stations a marked subsurface oxygen maximum was found just above or at the top of the nutricline. Independent of the hydrographic characteristics of the water masses, the saturation of oxygen at its maximum was about 120-125%.

#### Photosynthesis v/s light experiments

-----

At all the selected stations, photosynthesis v/s light experiments (P/L) were carried out for several sampled depths using the radiocarbon method. A summary of the optimized parameters of the P/L curve (normalized against chlorophyll a) together with some derived parameter is shown in Table 2. In order to see how these parameters varied with depth, average and standard deviation were calculated for different depth strata (Table 3).  $P_{max}$ , the height of the plateau of the P/L curve (also known as assimilation number) decreased with depth.  $P_{max}$  is thought to depend on dark reactions of photosynthesis as well as to be temperature dependent. It may be assumed that this decrease of  $P_{max}$  with depth was mostly influenced by temperature which also decreased with depth. However, this might not always be the reason, because  $P_{max}^B$  (based on a carbon to carbon basis) can show another trend. An alternate explanation is that  $P_{max}$  changes because of variations in the chl a/C ratio with depth as will be demonstrated later.  $\alpha$ , the

Table 2. Phytoplankton biomass (Chl a) and photosynthetic parameters for stations in the Barents Sea in August 1985.

St.n <sup>r</sup>	Dyp	Klor.a	PBs	Pmax	Alfa	Beta*10E4	Im	Ik	Is	Ib
813	10	0.40	1.78	1.76	0.0626	1.0	182.7	28.0	28.4	17762.
813	25	0.31	1.54	1.32	0.0593	20.8	87.8	22.3	25.9	739.
813	35	1.07	1.75	1.58	0.0659	14.0	102.7	23.9	26.5	1246.
829	30	0.50	2.17	2.14	0.0515	1.0	263.1	41.5	42.1	21681.
829	50	0.58	1.26	1.24	0.0794	1.0	105.6	15.7	15.8	12555.
850	10	0.47	1.28	1.26	0.0467	1.0	169.1	27.1	27.5	12834.
850	35	0.85	1.60	1.30	0.0591	31.2	80.9	21.9	27.0	512.
850	45	1.49	1.05	0.91	0.0448	13.7	82.4	20.4	23.4	764.
857	10	0.18	4.08	2.37	0.0527	105.9	138.5	45.0	77.5	385.
857	30	0.94	1.51	1.17	0.0341	24.1	120.7	34.2	44.4	628.
857	40	4.42	0.67	0.61	0.0538	9.3	50.5	11.4	12.4	719.
857	60	0.77	0.79	0.78	0.0628	0.9	82.2	12.4	12.6	8632.
867	10	0.46	1.87	1.56	0.0385	16.8	153.7	40.4	48.4	1109.
867	20	1.70	1.80	1.78	0.0502	1.0	223.6	35.4	36.0	18048.
867	30	0.28	1.43	1.36	0.0594	4.6	116.7	22.9	24.0	3090.
885	10	0.20	2.08	1.80	0.0352	11.4	203.8	51.0	58.9	1816.
885	40	0.20	2.88	2.83	0.1670	4.3	102.8	16.9	17.2	6688.
885	50	0.45	1.22	1.11	0.0801	15.1	60.9	13.9	15.2	811.
890	10	0.27	2.77	2.24	0.0394	21.1	209.5	56.9	70.3	1313.
890	20	0.98	1.78	1.59	0.0724	16.8	93.0	22.0	24.6	1059.
890	40	0.30	1.71	1.50	0.0976	27.6	63.1	15.4	17.5	621.
898	10	0.64	1.68	1.55	0.0538	8.5	130.0	28.8	31.3	1970.
898	28	1.13	0.77	0.77	0.0397	0.1	171.8	19.4	19.4	133623.
898	35	2.17	0.55	0.55	0.0442	0.0	121.6	12.4	12.4	219839.
909	10	0.14	2.07	2.04	0.0681	1.0	197.8	30.0	30.3	20651.
909	30	1.24	0.72	0.65	0.0318	7.7	85.2	20.3	22.8	936.
909	35	2.50	0.39	0.38	0.0219	0.3	116.3	17.5	17.6	12857.
909	39	2.80	0.61	0.58	0.0553	4.4	53.6	10.6	11.1	1395.

Units Chl a : mg · m<sup>-3</sup>

$P_s^B$  and  $P_{max}^B$  : mgC (mgChl a)<sup>-1</sup> · h<sup>-1</sup>

$\alpha$  : mgC (mgChl a)<sup>-1</sup> ( $\mu E \cdot m^{-2} \cdot s^{-1}$ )<sup>-1</sup>

( $\beta, I_m, I_k, I_s, I_b$ ) :  $\mu E \cdot m^{-2} \cdot s^{-1}$

slope of the linear part of the P/L curve at low light intensities, characterizes photochemical reactions and is related to the quantum efficiency of photosynthesis.  $\alpha$  was fairly constant in the upper 30 meters, but increased markedly below the pycnocline indicating an adaptation to the low light levels found in the deeper part of the euphotic zone.

Table 3. Average and standard deviation of phytoplankton biomass (Chl  $\underline{a}$ ) and photosynthetic parameters at different depth strata in the Barents Sea, August 1985.

Depth Stratum	n	Chl $\underline{a}$	$P_{\max}^{\text{BChl}}$	Chl	$10^4 x$	$I_{\max}$	$I_k$
All depths	28	0.98±0.98	1.38±0.61	0.0581±0.0270	13.0±20.4	127.5±56.3	25.6±12.3
10 meter	8	0.35±0.18	1.82±0.38	0.0500±0.0120	21.0±35.0	173.0±30.1	38.4±11.6
20-30 meter	8	0.89±0.49	1.35±0.49	0.0498±0.0137	10.1±10.0	145.2±67.1	27.3± 8.4
31-40 meter	8	1.79±1.45	1.17±0.82	0.0709±0.0442	11.0±12.3	87.3±28.1	16.3± 4.8
>41 meter	4	0.82±0.46	1.01±0.20	0.0672±0.0161	8.3± 8.4	83.2±18.0	15.6± 3.5

Units: Chl  $\underline{a}$  :  $\text{mg} \cdot \text{m}^{-3}$   
 $P_{\max}^{\text{BChl}}$  :  $\text{mgC} \cdot (\text{mg Chl } \underline{a})^{-1} \cdot \text{h}^{-1}$   
 $\alpha^{\text{Chl}}$  :  $\text{mgC} \cdot (\text{mg Chl } \underline{a})^{-1} (\mu\text{E} \cdot \text{m}^{-2} \cdot \text{s}^{-1})^{-1}$   
 $\beta, I_{\max}, I_k$  :  $\mu\text{E} \cdot \text{m}^{-2} \cdot \text{s}^{-1}$

All three light parameters  $\beta$ ,  $I_{\max}$ , and  $I_k$  decreased steadily with depth. The decrease of  $\beta$ , a parameter that characterizes the photoinhibition of photosynthesis, can be related to the assumption that phytoplankton in the upper layers are more exposed to photoinhibiting intensities of light than those phytoplankton deeper in the water column. This resulted in higher  $\beta$  values for samples near the surface. Both  $I_{\max}$ , the light intensity at which  $P_{\max}$  is reached, and  $I_k$ , the light intensity at the intersect of the linear and plateau parts of the P/L curve, decreased with depth at the same rate as  $P_{\max}$ . Low values of  $I_k$  have been suggested to represent adaptation to low light intensities, and the observed decrease can be seen in this respect. A more detailed quantitative analysis of the parameters of the P/L curve will be carried out at a later date.

The photosynthetic parameters can also be expressed in a carbon to carbon basis as they are shown in Table 4 together with phytoplankton growth rate values.  $P_{\max}^{\text{BC}}$ , normalized to carbon ( $P_{\max}^{\text{BC}}$ ), shows an opposite trend to that normalized to chlorophyll ( $P_{\max}^{\text{Bchl}}$ ), with values increasing slightly with depth. At the same time  $\alpha^{\text{C}}$  also increased with depth but at a much larger rate than  $\alpha^{\text{chl}}$  being 3-4 times greater near the chlorophyll maximum than above the pycnocline. These factors indicate that subsurface phytoplankton are well adapted to low light intensi-

Table 4. Averages and standard deviation of phytoplankton biomass (Cp), photosynthetic parameters (normalized to carbon) and growth rate at different depth strata in the Barents Sea, August 1985.

Depth stratum	n	Cp	BC P <sub>max</sub>	C <sup>c</sup> (x10 <sup>-3</sup> )	u
All depths	28	44.9+40.5	0.0293+0.0153	1.408+1.101	0.74+0.29
10 meter	8	25.5+13.0	0.0246+0.0051	0.670+0.159	0.66+0.12
20-30 meter	8	47.9+32.4	0.0256+0.0092	0.950+0.226	0.65+0.20
31-40 meter	8	73.5+57.5	0.0306+0.0240	1.849+1.347	0.74+0.43
>41 meter	4	20.5+14.9	0.0435+0.0117	2.918+0.967	1.00+0.19

Units	Cp(phytoplankton carbon)	: mg · m <sup>-3</sup>
	P <sub>max</sub> <sup>BC</sup>	: mgC (mgC) <sup>-1</sup> · h <sup>-1</sup>
	α <sup>c</sup>	: mgC (mgC) <sup>-1</sup> (μE · m <sup>-2</sup> · s <sup>-1</sup> ) <sup>-1</sup>
	u(specific growth)	: doublings · day <sup>-1</sup>

ties and indicates greater photosynthetic efficiency than surface phytoplankton. This also can be found for the estimated growth rates that indicate an increase with depth below the pycnocline.

### Zooplankton

The dry weight data of Juday net samples from four transects are presented in Fig. 13. The highest biomass was recorded at st. 855 (15 g·m<sup>-2</sup>, haul depth 160 m). The majority of the zooplankton belonged to the large size fraction (>850 μm), and it seems that the mean ratio between large and small forms varied. The samples from section C (st. 899-912) were dominated by more large organisms compared with the other transects.

The MOCNESS vertical profiles showed great variability with respect to magnitude of biomass and the distribution with depth. The highest observed value was 246 mg dry weight·m<sup>-3</sup> (40-50 m depth at st. 850), and values above 100 mg·m<sup>-3</sup> frequently occurred in the north and the east. The highest

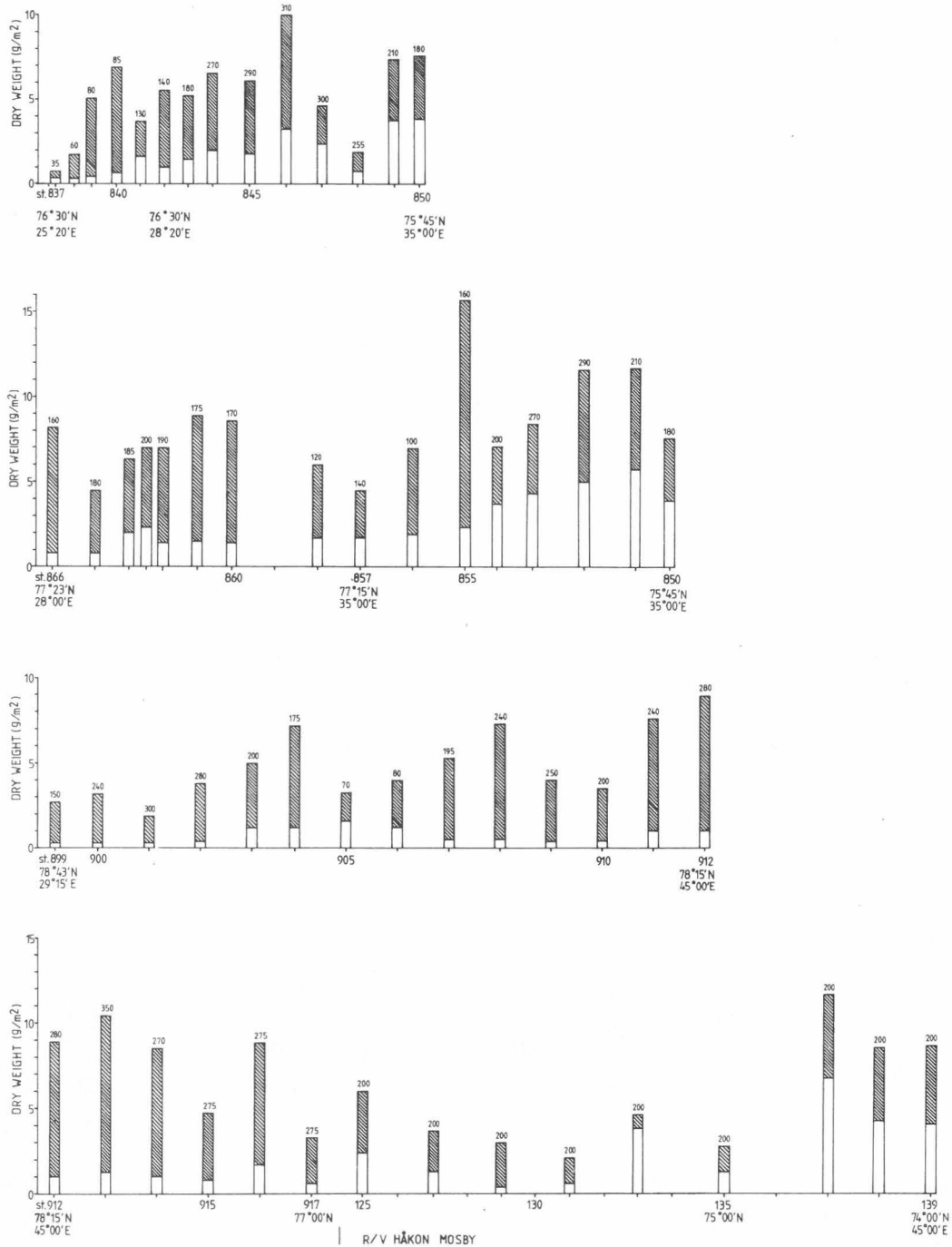


Fig. 13. Zooplankton biomass from selected transects (Juday net data). Haul depths indicated at top of columns. Open bars: small plankton forms (<850 µm), hatched bars: large plankton forms (>850 µm).

concentrations of zooplankton were generally located to the northern area where no capelin were observed (Fig. 14). The zooplankton were less abundant in the central and southern areas where capelin were present (Figs. 15-16). Most of the biomass consisted of large sized plankton, particularly in Arctic water (st. 896, 901, 909, 913).

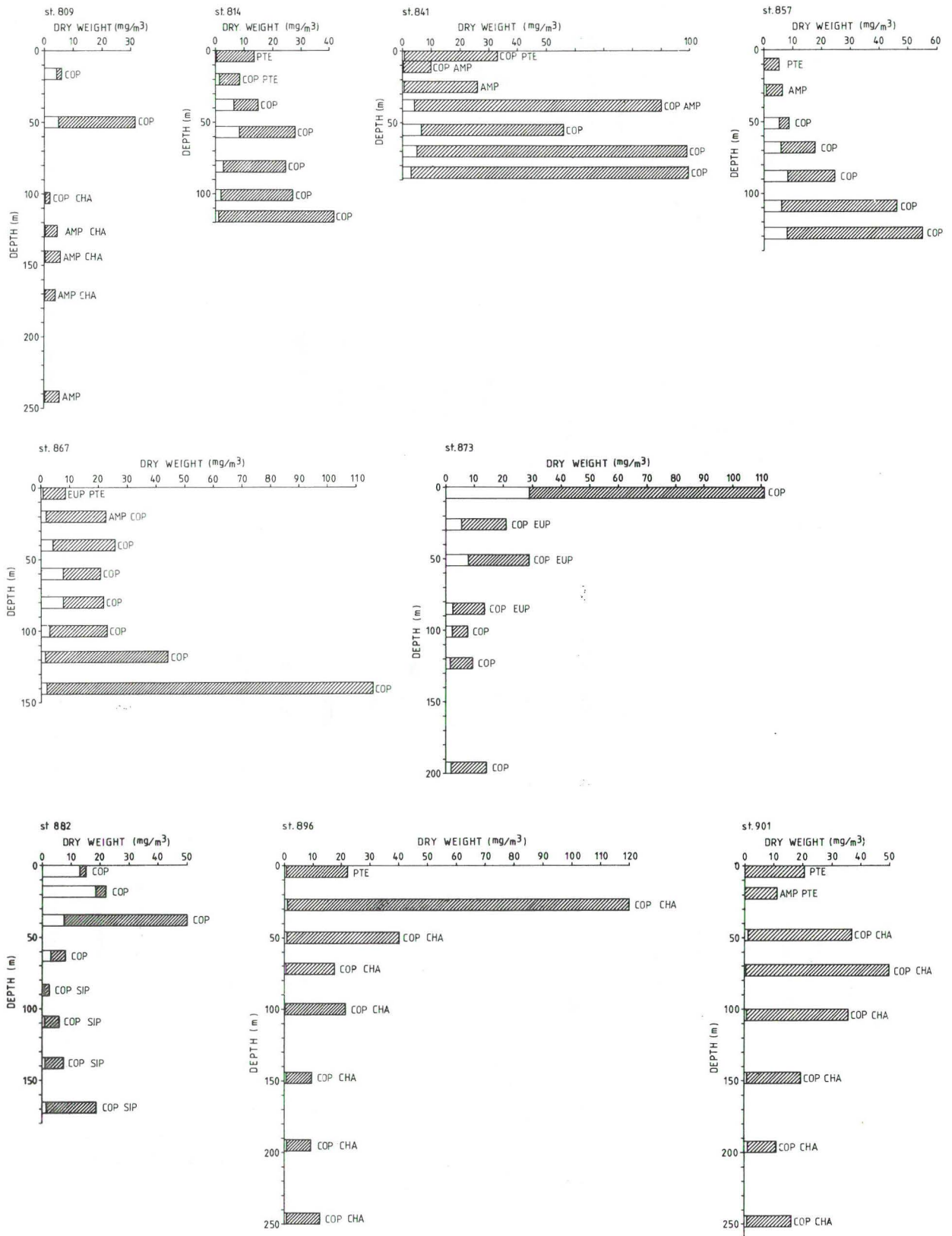


Fig. 14. MOCNESS dry weight depth profiles from stations without capelin registrations. Open bars: small plankton forms (<850 μm). Hatched bars: large plankton forms (>850 μm). Dominating taxonomic groups: PTE=pteropods, COP=copepods, AMP=amphipods, CHA=chaetognaths, EUP=euphausiids, SIP=siphonophores (continues).

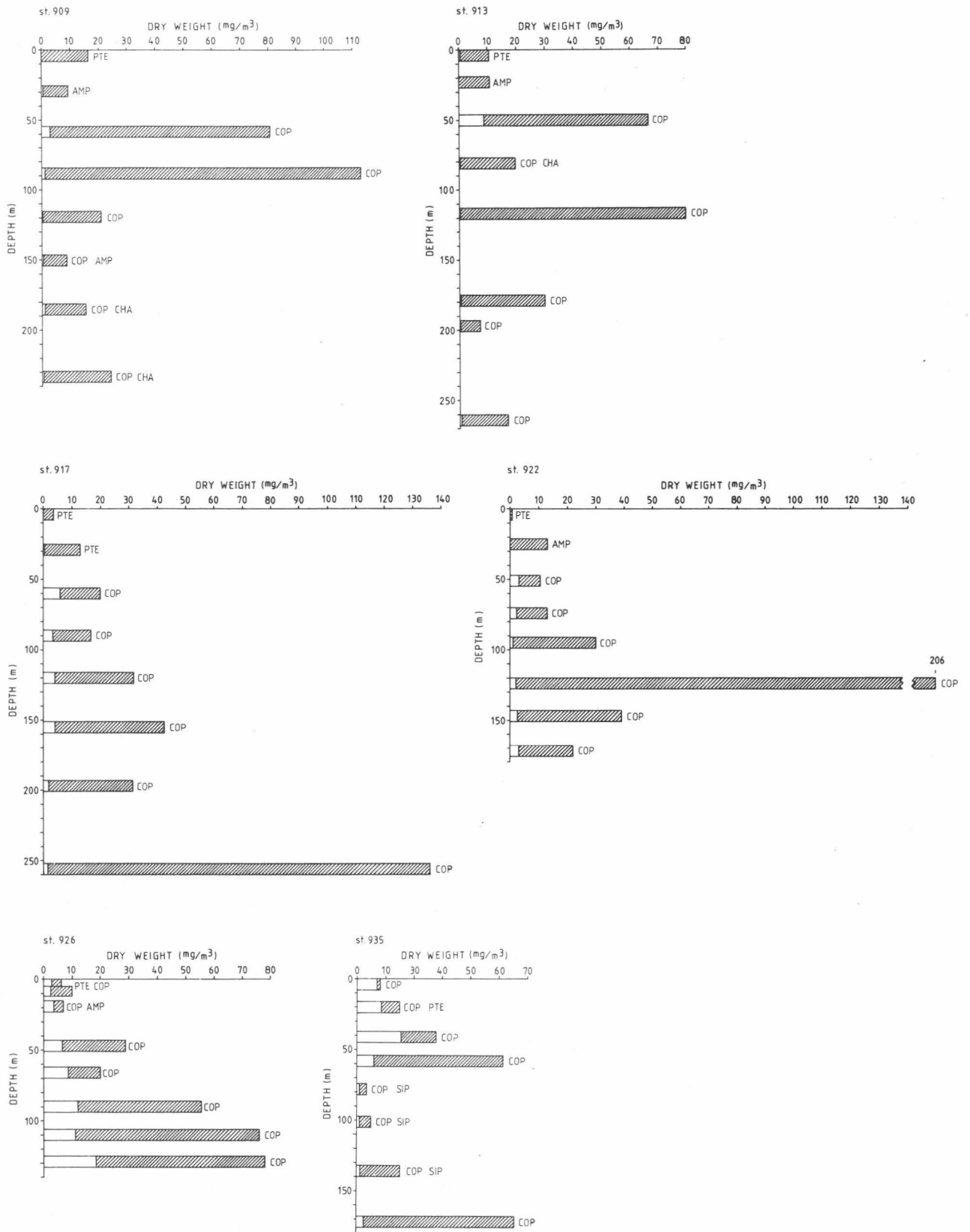


Fig. 14 (continued).

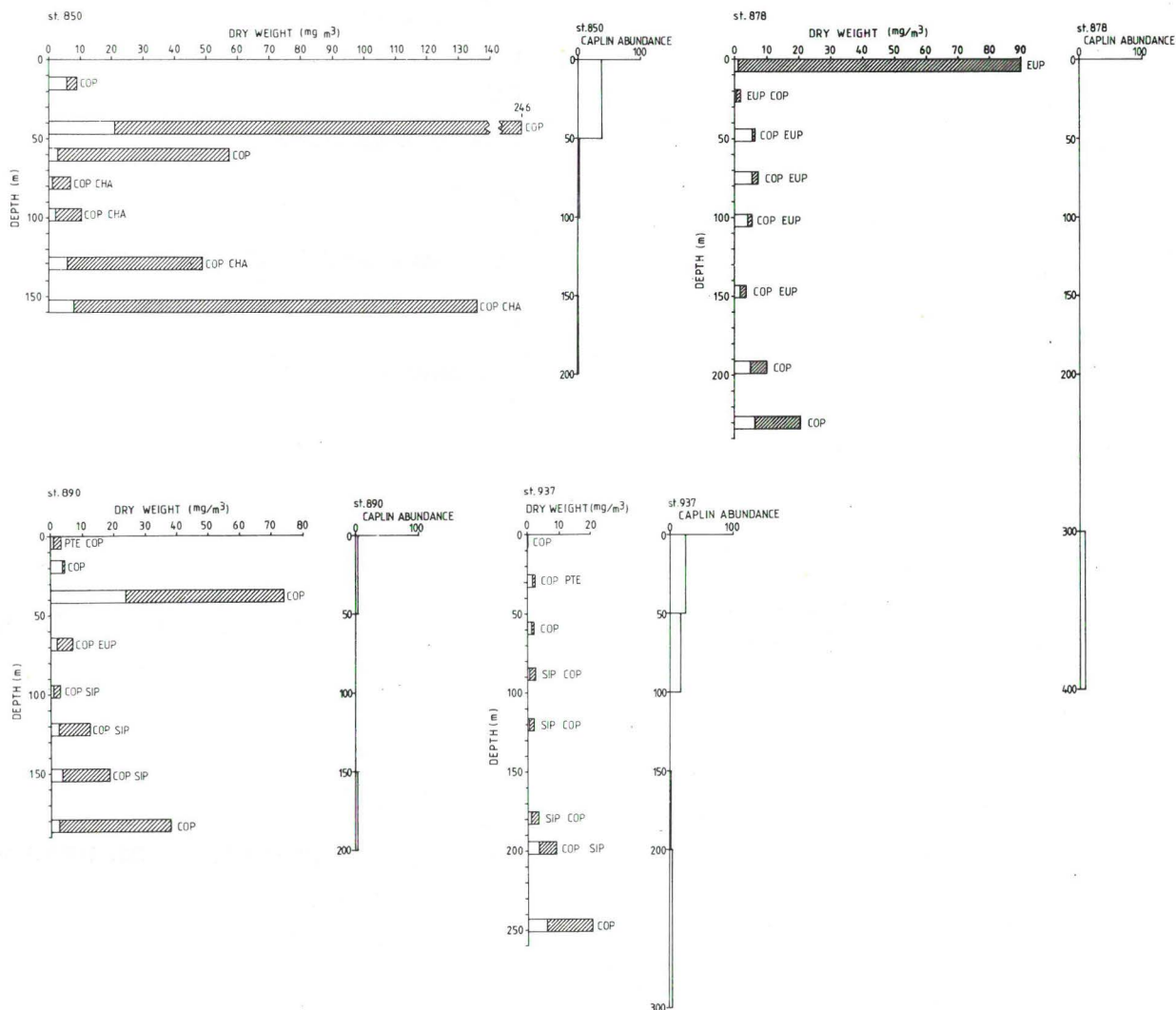


Fig. 15. MOCNESS dry weight and capelin abundance depth profiles from stations with integrated echo intensity  $>0$  and  $<100$ . Capelin abundance units in square meter reflecting target per square nautical mile.

The vertical profiles resulting from pump data are shown in Fig. 17. The highest biomass recorded with the pump was  $1973 \text{ mg} \cdot \text{min}^{-1}$ , or about  $470 \text{ mg} \cdot \text{m}^{-3}$ , at 45 m depth at st. 850.

The distribution of the six dominating taxonomic categories has been indicated in Fig. 14-16. The copepods, consisting mainly of Calanus spp., Metridia longa and Pseudocalanus sp., were common at all stations for most depths. The copepods were especially abundant in the northern and eastern areas, as at st. 901-922, but high concentrations were also found at st. 850. The euphausiids (Thysanoessa spp.) were not observed in



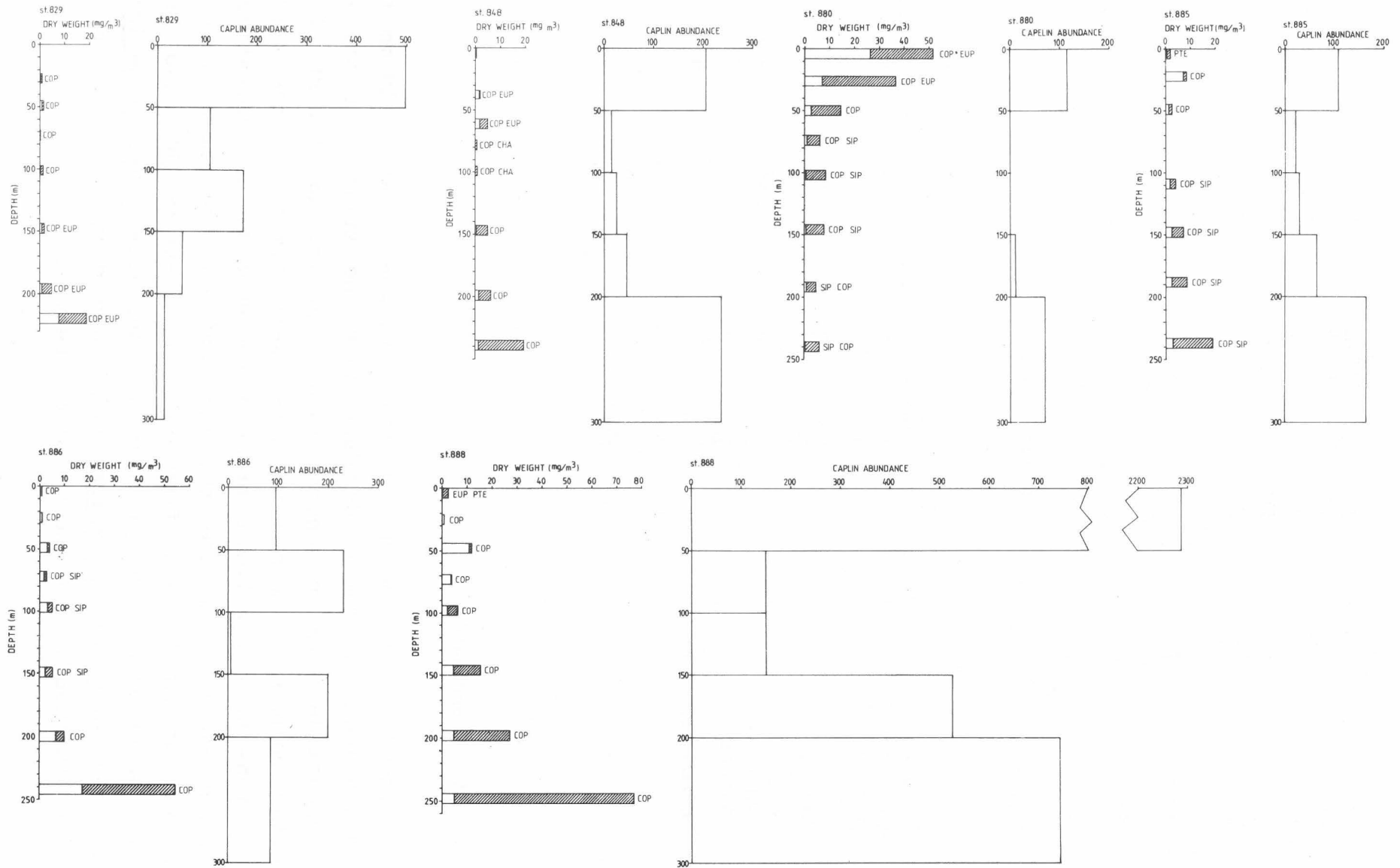


Fig. 16. MOCNESS dry weight and capelin abundance depth profiles from stations with integrated echo intensity >100 (continues).

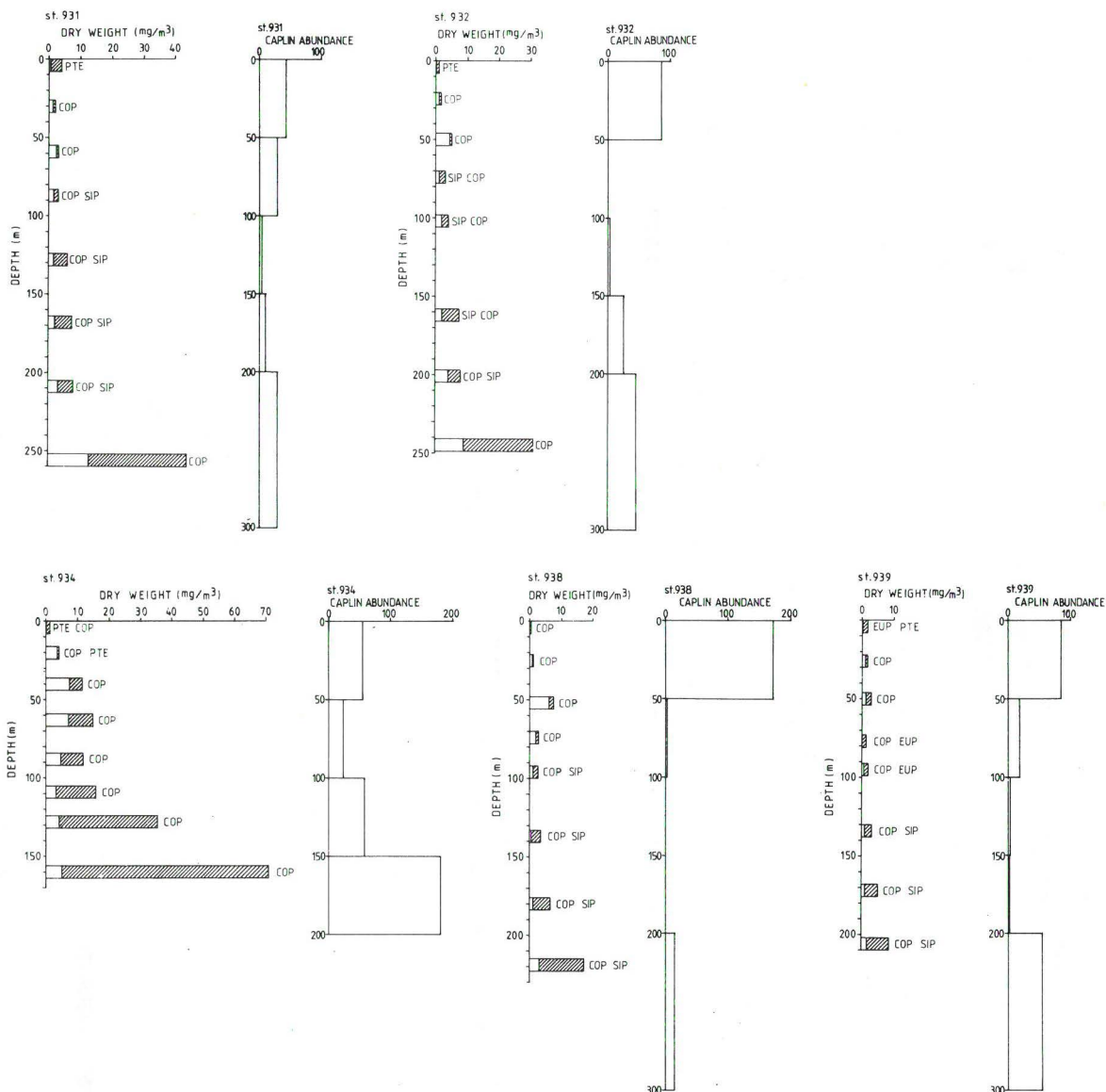


Fig. 16. (continued).

the north-eastern area. Juvenile stages at about 10 mm body length were extremely abundant near the surface at st. 878. Euphausiids were in general located at the upper part of the water column. The siphonophores were common at the central stations near the Polar front and seemed to be dominating in deeper water. Outside the euphausiid-siphonophore area hyperiid amphipods were frequent, and chaetognaths also had a wide occurrence. The pteropods, especially Limacina helicina, as well as Clione limacina, were very distinctive groups and were confined within the upper ten meters.

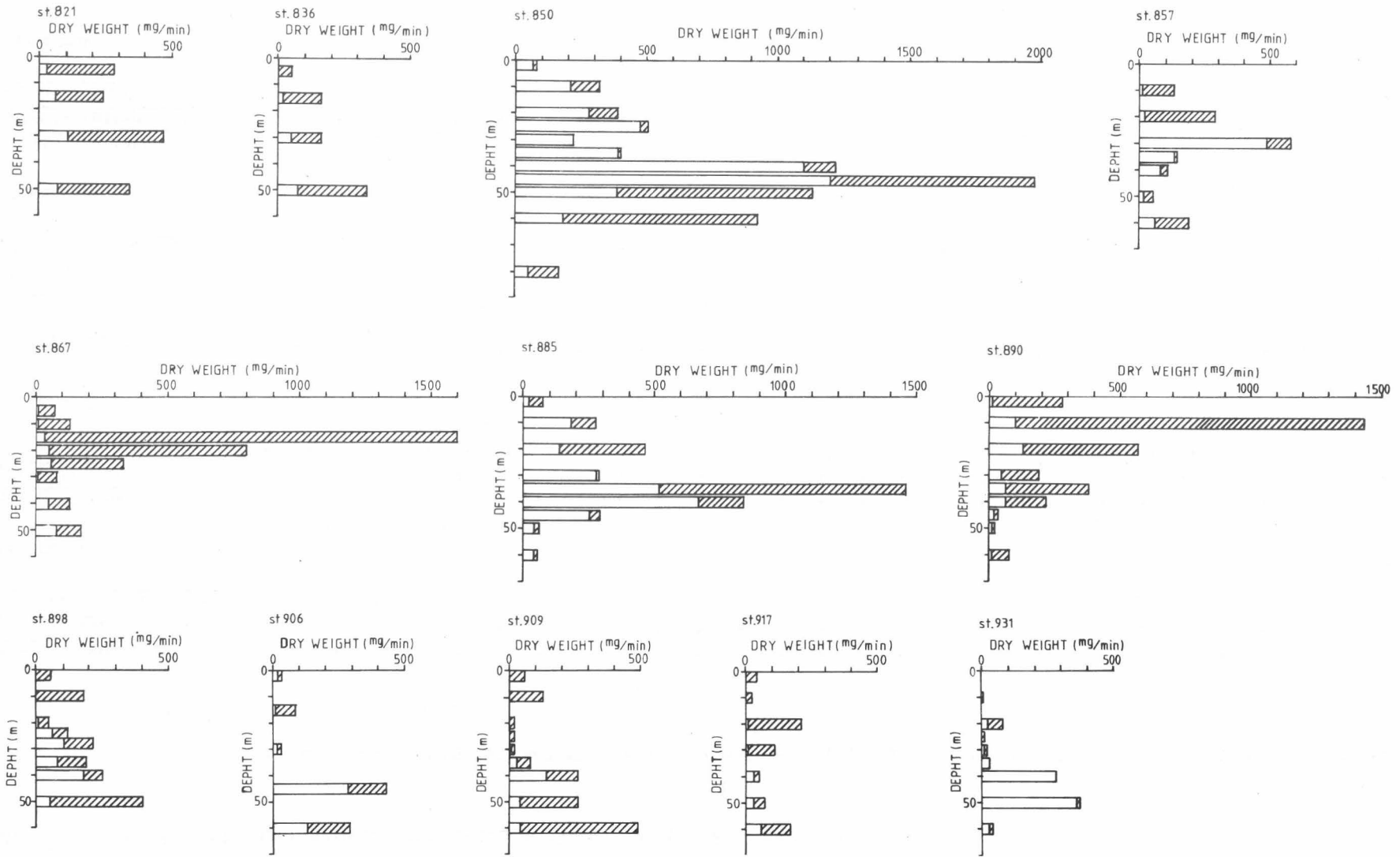


Fig. 17. Zooplankton dry weight depth profiles obtained with plankton pump (mg per minute pumping time). Open bars: small plankton forms, hatched bars: large plankton forms.

Table 5. Species of ctenophores and medusae found in MOCNESS samples.

	809	814	829	840	848	850	857	867	873	878	880	882	885	886	888	890	896	901	909	913	917	922	926	931	932	934	935	937	938	939	
Ctenophora																															
<u>Mertensia ovum</u>		+	+	+		+	+	+	+	+		+	+	+	+	+	+	+	+	+	+	+	+	+	+	+	+	+	+	+	+
<u>Beroë cucumis</u>	+	+	+	+	+	+			+	+	+	+	+	+	+			+	+	+	+	+	+	+	+	+	+	+	+	+	+
<u>Bolinopsis infundibulum</u>					+	+												+				+									
Antomedusae																															
<u>Sarsia princeps</u>		+		+	+	+	+	+		+	+	+	+	+	+	+	+	+	+	+	+	+	+	+	+	+	+	+	+	+	+
<u>Euphysa flammea</u>			+	+	+	+	+	+	+	+	+	+	+	+	+	+	+	+	+	+	+	+	+	+	+	+	+	+	+	+	+
<u>Catablema vesicarium</u>	+	+	+	+	+	+	+	+	+	+	+	+	+	+	+	+								+	+	+	+	+	+	+	+
Trachymedusae																															
<u>Aglantha digitale</u>		+	+	+	+	+	+	+	+	+	+		+		+	+	+	+	+	+	+					+	+	+	+	+	+
Narcomedusae																															
<u>Aeginopsis laurentii</u>			+		+			+		+			+					+		+				+							
Leptomedusae																															
<u>Halopsis ocellata</u>	+				+																										
<u>Tiaropsis multicirrata</u>			+	+		+	+		+	+																					+
<u>Ptychogena lactea</u>									+			+	+	+		+	+					+	+	+			+		+		
Semaestomae																															
<u>Cyanea capillata</u>									+					+											+						

Table 5 lists all species of ctenophores and medusae found in samples from the MOCNESS-hauls. Mertensia ovum and Beroë cucumis were observed at most stations, and among medusae Sarsia princeps, Euphysa flammea, Catablema vesicarium and Aglantha digitale were common. The siphonophores consisting of small Dimophyes arctica have not been properly recorded here and the group is omitted from the table. The horizontal distribution of these species is shown in Fig. 18. The most abundant species, S. princeps, had its maximum concentration in the Polar front area at about 77°N, and E. flammea had a similar distribution. M. ovum had a frequent occurrence in Arctic water, while the other ctenophore B. cucumis seemed to be more linked to Atlantic water.

The vertical distribution of the biomass ( $\text{ml}\cdot\text{m}^{-3}$ ) of the three most important species, M. ovum, B. cucumis, and S. princeps is shown in Fig. 19. The highest concentrations as well as the highest depth integrated quantity of ctenophores and medusa (mainly S. princeps) were observed at st. 926 and 934. From Fig. 19 it is clear that the biomass is found mainly above 50-60 m depth. The different species of ctenophores and medusae were not equally distributed vertically. When data from all MOCNESS stations are averaged, it appears that S. princeps had a numerical maximum above that of E. flammea, and A. digitale was rather abundant at most depth intervals below 40 m (Fig. 20).

#### Distribution of capelin

The geographical distribution of capelin in the investigated area is shown in Fig. 21. The abundance followed the Polar front along the east side of the Svalbard Bank and further to the Central Bank. During the cruise, the capelin moved northwards as indicated in Fig. 22. Unfortunately, the trawl samples were not analyzed during the cruise due to lack of technicians. Therefore all samples were frozen for later analyses which have yet to be made.

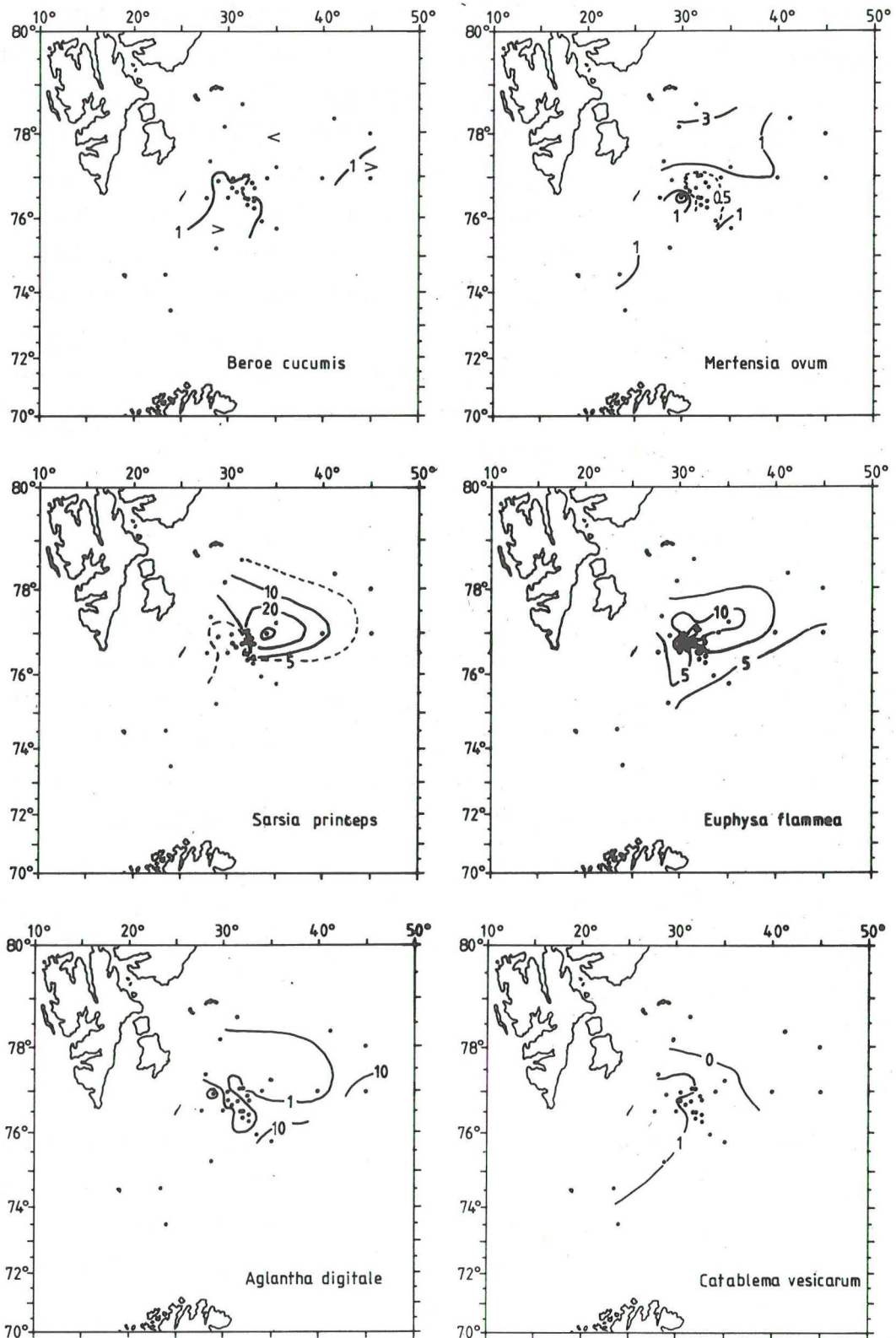


Fig. 18. Horizontal distribution of the most important ctenophores and medusae, as numbers  $\cdot m^{-2}$ .

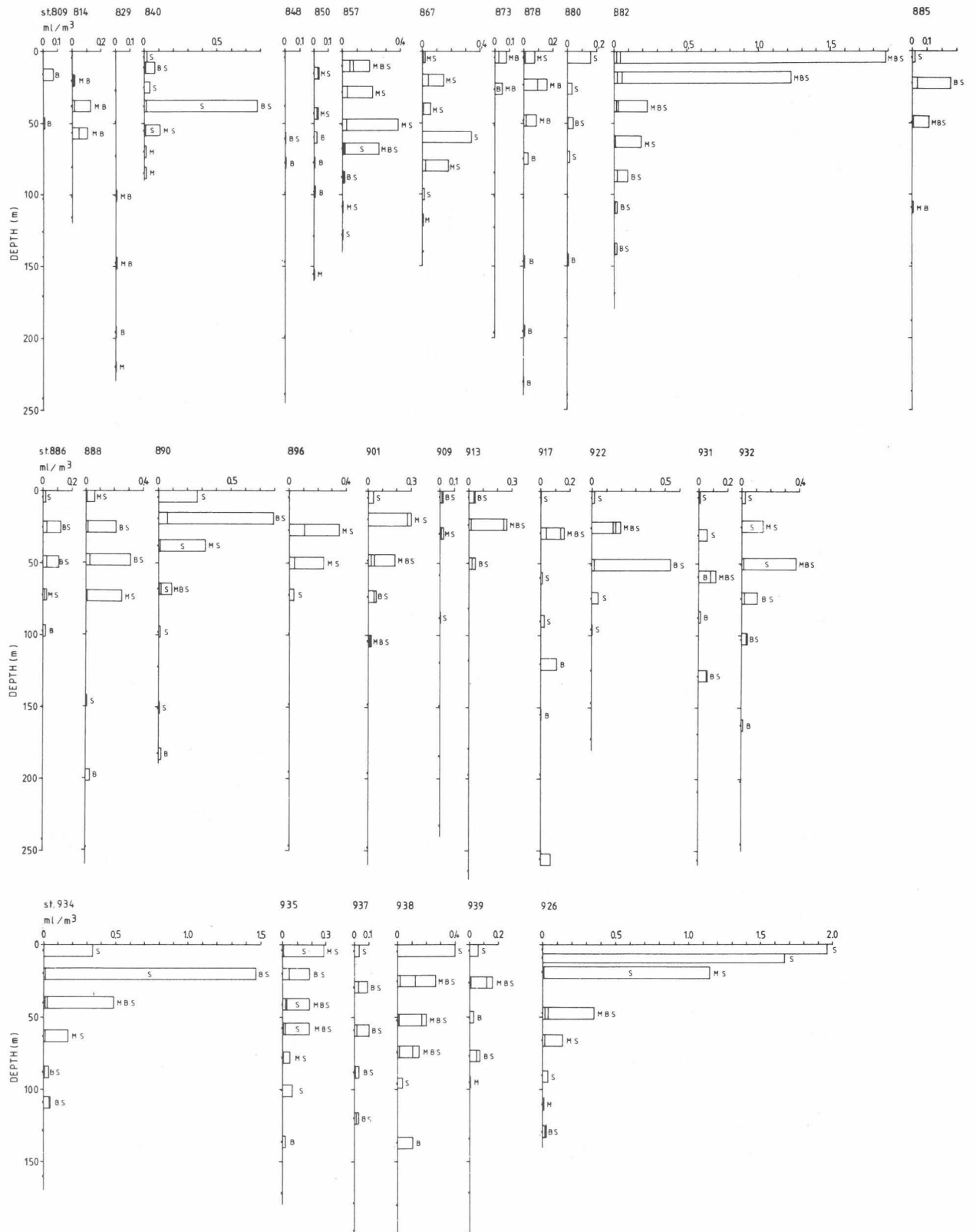


Fig. 19. Vertical wet-biomass (ml/m<sup>3</sup>) distribution of *Mertensia ovum* (M), *Beroë cucumis* (B), and *Sarsia princeps* (S). Data from MOCNESS-samples.

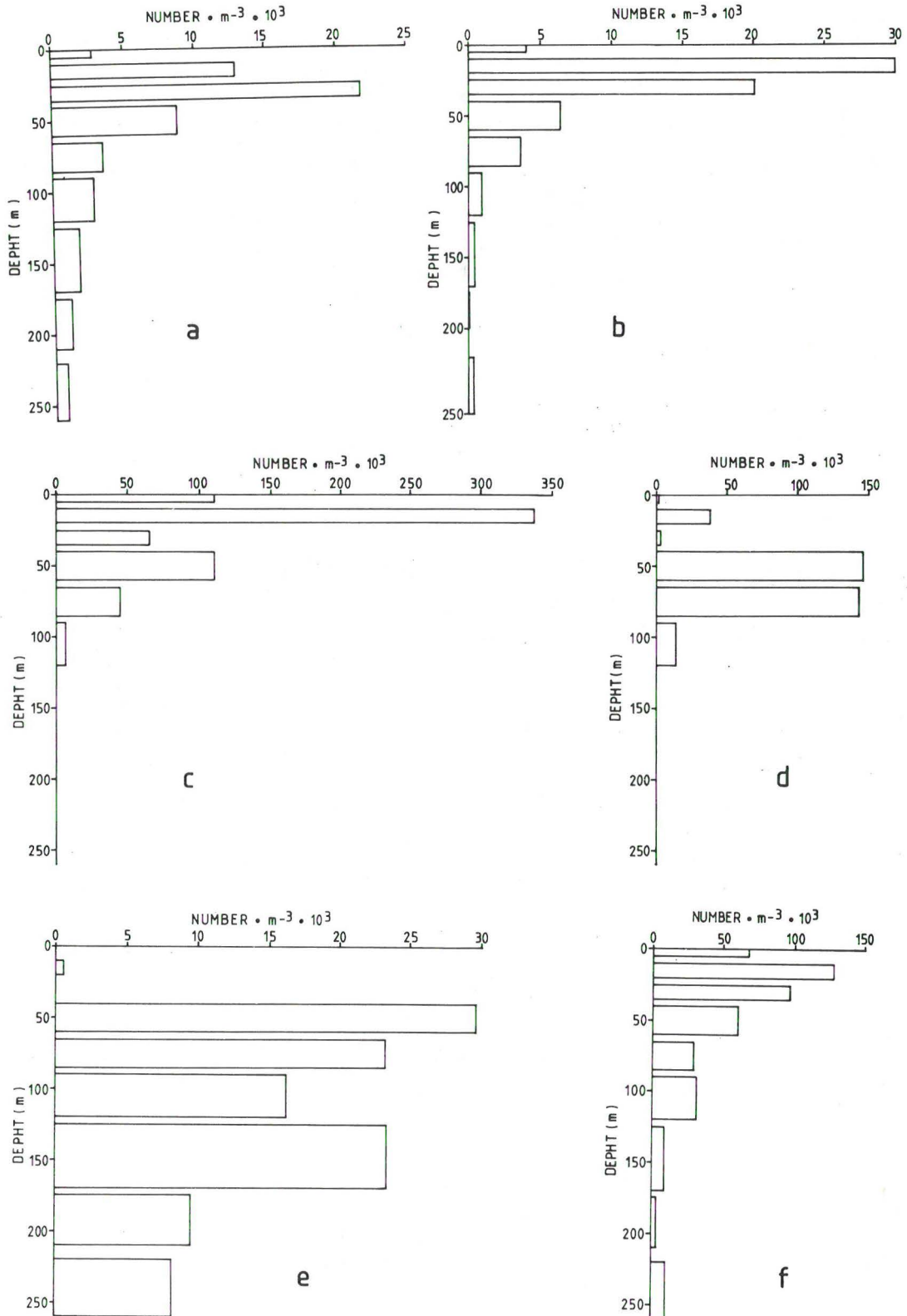


Fig. 20. Vertical distribution of a) *Beroë cucumis*, b) *Mertensia ovum*, c) *Sarsia princeps*, d) *Euphysa flammea*, e) *Aglantha digitale*, f) *Catablema vesicarium*. Mean values of all MOCNESS-stations and depth intervals where the species occurred.



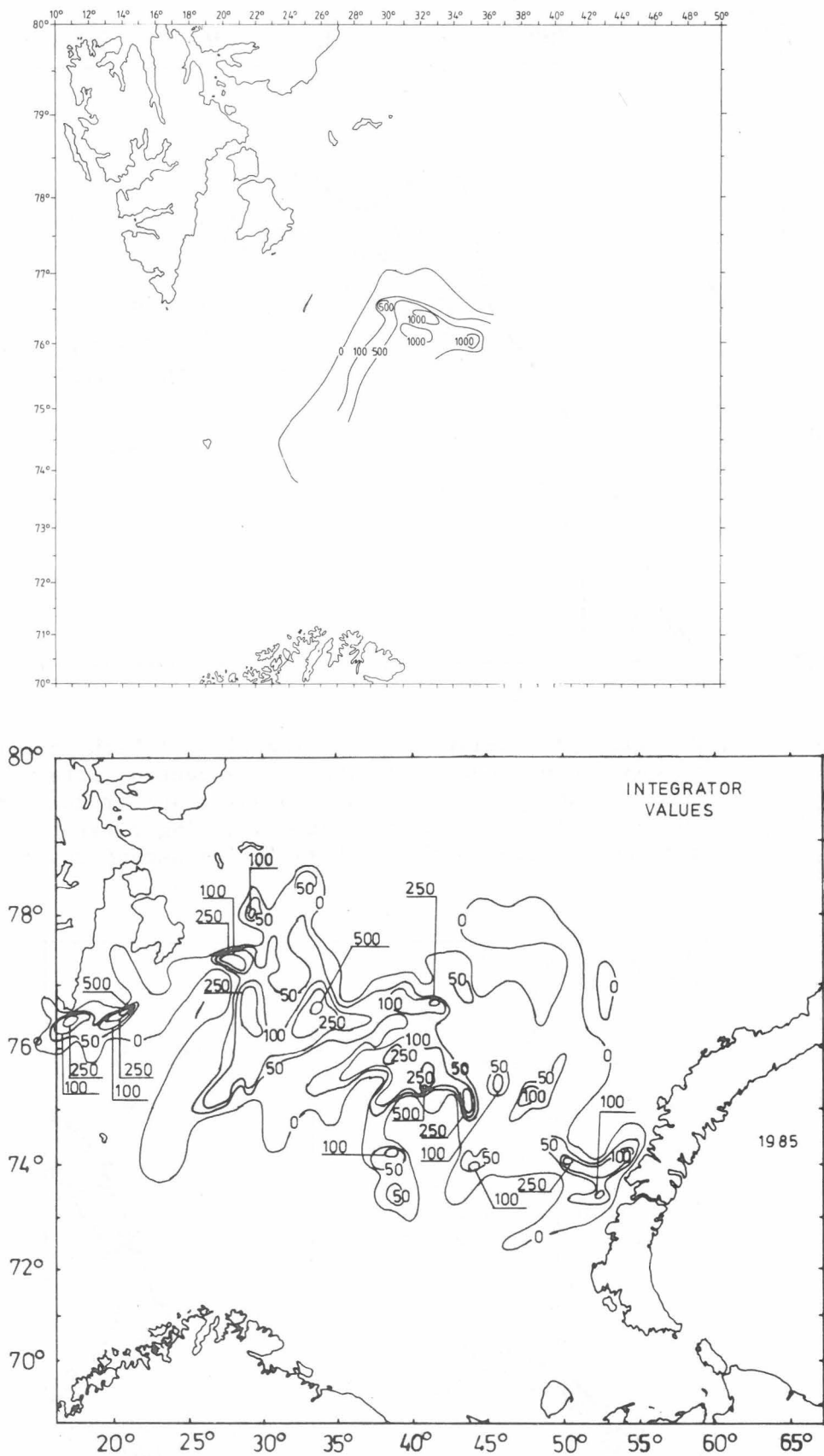


Fig. 21. Geographical distribution of capelin during our cruise in August (upper) and during the Norwegian/USSR survey in September (lower) ( $\text{m}^2$  scattering cross section / (nautical miles) $^2$ ).

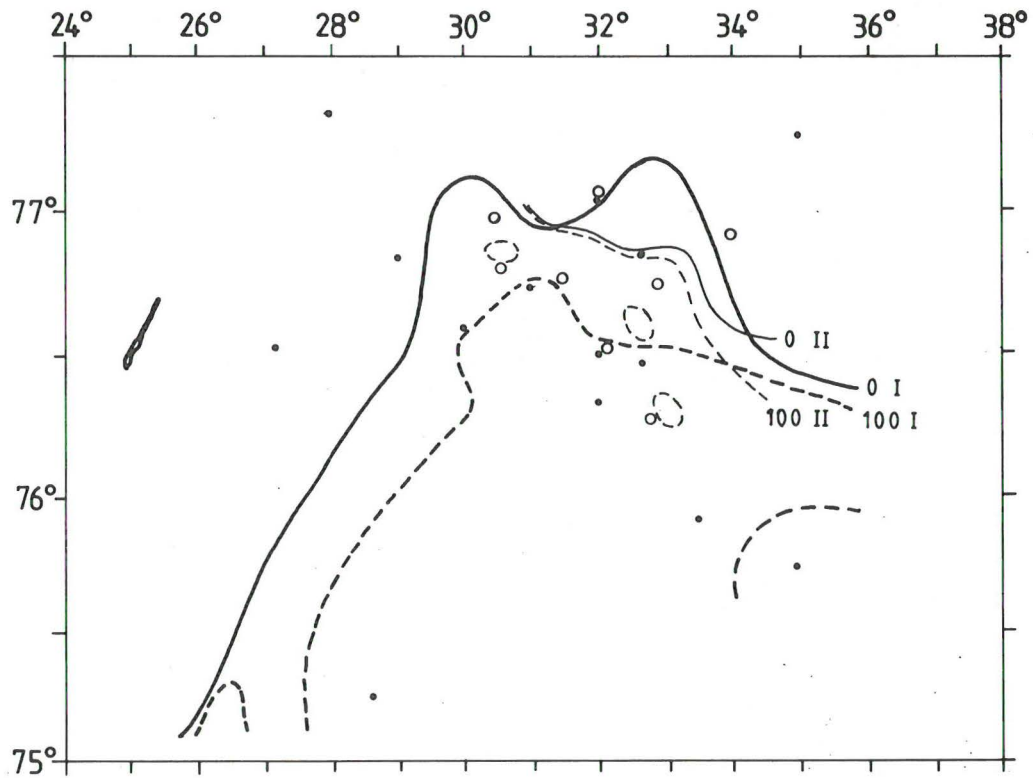


Fig. 22. Position of capelin front during first (thick lines) and second (thin lines) coverage of the central area. 0- and 100-isolines are indicated with solid and broken lines respectively. Dots mark stations during first coverage, and open circles mark stations during second coverage.

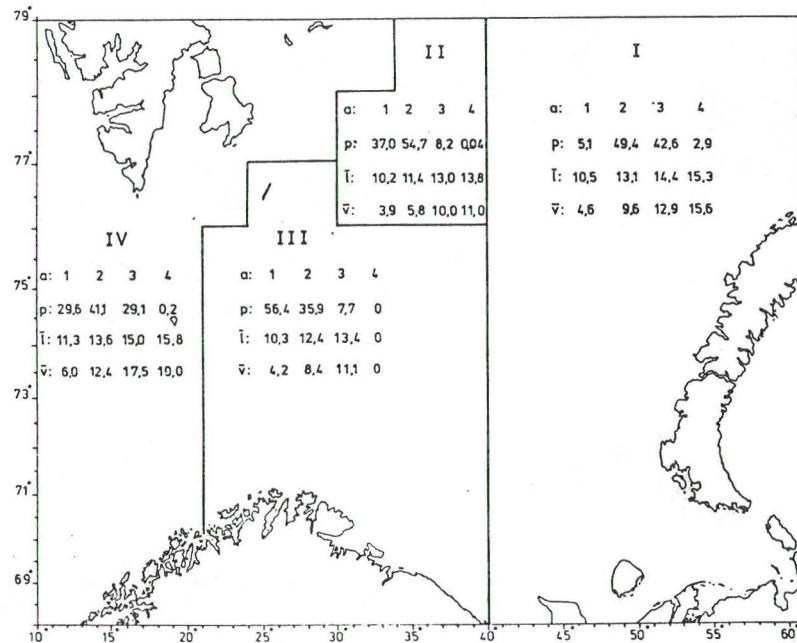


Fig. 23. Biological parameters in four sub-areas used for the acoustic estimate in September 1985. a: age, p: percentage,  $\bar{l}$ : mean length (cm),  $\bar{v}$ : mean volume (ml) (GJØSÆTER and HAMRE 1985).

During the joint Norwegian/USSR acoustic survey of capelin in the Barents Sea in September, the distribution of capelin was as shown in Fig. 21. In the past month there had been a movement northward to Kong Karls Land, but there were still no capelin observed in the cold water masses above the Great Bank. Fig. 23 shows some biological parameters in four sub-areas used for acoustic estimate during the September-cruise. The results from area II and III may, without great error, be used to illustrate the age distribution found during our cruise. It should be noted that less than 10% of the capelin stock were 3 years and older in the area. Mean length and weight of the capelin in these two areas were almost the same as in 1984 (GJØSÆTER and HAMRE 1985).

#### DISCUSSION

The general physical structure found during the present investigation was very similar to those found during the same season in earlier years (HASSEL et al. 1984b; REY and LOENG 1985). However, some differences were observed in the characteristics of the water masses just south of the Polar front in the central part of the Barents Sea. This area is usually dominated by Atlantic water or a mixture of this watermass with Arctic water (LOENG 1985). In August 1985 the temperature of the upper 100 meter layer was about the same as in 1981 but about 2°C lower than in 1984. The salinity in the same layer was slightly higher than in 1981 when salinities were below 35<sup>o</sup>/oo, but essentially lower than 1984 when most of the water column had salinities above 35<sup>o</sup>/oo. These differences are mainly due to variations in the Atlantic inflow to the Barents Sea. However, since the position of the Polar front at the southern edge of the Great Bank had not changed radically, it seems that the variations in the Atlantic inflow have its major effect on the sharpness of the front. The same trend was observed when comparing the hydrography at the eastern section (45<sup>o</sup>E) in 1984 and 1985. The former year presented higher temperatures and salinities than the latter one, while the front was situated at approximately the same place (76<sup>o</sup>N).

In the area north of the Polar front, where the Arctic water dominated, differences observed in 1985 compared to 1981 and 1984 were mainly due to different degrees in the amount of melt water in the surface layer.

The vertical distribution of nutrients in 1985 was also similar to those found in 1981 and 1984, with a very sharp nutricline well below the pycnocline as well as being shallower and stronger in the northern area than in the south. Another feature of importance was the effect of the shallow banks (Svalbard Bank and northern part of the Great Bank) on the physical conditions in the water column and there after on the biological activity in these areas. The presence of eddies on these banks leads to a weakening, or the complete disappearance of the pycnocline, allowing a higher degree of vertical mixing. This resulted in a higher degree of biological production as reflected in the nutrient consumption that reached much deeper compared with oceanic areas.

Most of the phytoplankton in the upper layer was found in the size range less than 10  $\mu\text{m}$ . The same was valid, but in a minor degree, for the subsurface chlorophyll a maximum. This maximum was well distinct at the northernmost stations in the central part of the Barents Sea thus indicating that the main phytoplankton bloom had taken place here later than in the southern part. In the eastern part of the Barents Sea, the subsurface chlorophyll a maximum was weaker than that found in the west. The same trend was found in 1984 (HASSEL et al., 1984b) despite of the fact that the phytoplankton bloom here takes place later than in the western part. This suggests the presence of a short-lived bloom in the east.

The measurements of photosynthesis indicated that the phytoplankton in the deeper layers of the euphotic zone was well adapted to the low light intensities found there. Also, in contrast to the findings in the Canadian Arctic (PLATT et al. 1982), the phytoplankton of the deeper layers appeared to be less susceptible to photoinhibition than those of the upper layer. The reason for these differences are not yet completely understood and will be analyzed at a later stage.

One purpose of this cruise was to examine the interaction between capelin and zooplankton. Previous research in the same area (GJØSÆTER et al. 1983, HASSEL et al. 1984a, HASSEL et al. 1984b) indicated that capelin may graze down the zooplankton to low standing stocks during their northerly food migration in the summer. A strong decline in zooplankton biomass was observed in June 1983 for stations taken along a section from Arctic water southwards through the Polar front to Atlantic water at about  $33^{\circ}\text{E}$ . The same results were obtained in June and August 1984. The northern border of capelin was close to or just south of the plankton gradient. The Polar front separates two different water types, and this may account for the different biomass levels found for Arctic and Atlantic water.

At two different time intervals during this cruise, areas on either side of the northern capelin border were investigated to find if the presence of capelin did cause a measurable decline in the zooplankton stock. During the first coverage, the capelin 0-line was observed just north of  $77^{\circ}\text{N}$  at  $30\text{--}33^{\circ}\text{N}$ . Higher values  $>100$  were found 15-30 nautical miles farther south (Fig. 22). When the area was covered the second time (st. 926-939) the 0-line had moved southwards, while the more massive capelin border (100-line) had changed its position towards the northeast. High capelin abundances were observed at several places in the original 0-100 zone, which thus indicated that an overall northerly migration had taken place. Zooplankton were very poor at st. 938 and 939, and also at st. 937 which lay close to high capelin registrations. The MOCNESS-data indicated that high zooplankton abundance was associated with low capelin registrations. However, we could not return to those stations which were outside the capelin 0-line in order to measure the influence of grazing upon zooplankton. A marked zooplankton decline under these conditions would have been the best proof that capelin are dependant on the zooplankton.

The ctenophores and medusae represent an important group in the Barents Sea ecosystem as predators of zooplankton. It is therefore of interest to obtain a detailed picture of their

horizontal and vertical distribution to learn about the potential of their predation. In terms of wet weight, in many cases, the biomass of ctenophores and medusae far exceeded that of zooplankton, while zooplankton were dominant with respect to dry weight, if a 3-4% dry weight content of medusae was assumed.

Acquirement of correct biomass data for all species and size groups of zooplankton with a single piece of equipment poses a well known methodical problem. The MOCNESS is equipped with a rather coarse net which will not filter the smallest copepods and other juvenile forms, while the heavy net frame is not ideal when catching highly mobile macro-plankton such as adult euphausiids. The ability to catch large zooplankton is even less using the pump, although the finer mesh in the net used is able to retain a higher proportion of the smaller organisms. As depth intervals and sampling positions were different for the pump and the MOCNESS, the corresponding vertical profiles (st. 850, 857, 867, 885, 890, 909, 917 and 931) show poor correspondance, and maxima not apparent from the MOCNESS data were present in the pump data.

#### REFERENCES

- FØYN, L., MAGNUSSEN, M. and SEGLEM, K. 1981. Automatisk analyse av næringssalter med "on line" databehandling. En presentasjon av oppbygging og virkemåte av systemet i bruk på Havforskningsinstituttets båter og i laboratoriet. Fisken Hav. Ser. B, 1981(4): 1-40.
- GJØSÆTER, H., HASSEL, A., LOENG, H., REY, F. and SKJOLDAL, H.R. 1983. Preliminære resultater fra tokt i Barentshavet med M/S "LANCE" og F/F "G.O. SARS" i mai/juni 1983. FO 8310, Havforskningsinstituttet i Bergen. (1-21) (in Norwegian).
- GJØSÆTER, H. and HAMRE, J. 1985. Internal cruise report.

- HASSEL, A., LOENG, H., REY, F. and SKJOLDAL, H.R. 1984a. Preliminære resultater fra tokt med F/F "G.O. SARS" i Barentshavet, 28.5.-18.6.1984. FO 8409, Havforskningsinstituttet i Bergen:(1-34) (in Norwegian).
- HASSEL, A., LOENG, H., REY, F. and SOLBERG, T. 1984b. Resultater fra tokt med F/F "G.O. SARS" i Barentshavet 4.-19.8.1984. FO 8410, Havforskningsinstituttet i Bergen:(1-32) (in Norwegian).
- HASSEL, A., LOENG, H. and SKJOLDAL, H.R. 1986. Marinøkologiske undersøkelser i Barentshavet i januar 1985. Havforskningsinstituttet, rapport FO 8603.
- LOENG, H. 1985. Ecological Features of the Barents Sea. The 6th International Conference of Comité Arctique: Marine Living Systems of the Far North. Fairbanks, Alaska, May 1985: 55 pp. (in press).
- LORENZEN, C.J. 1966. A method for the continuous measurement of in vivo chlorophyll concentrations. Deep-Sea Res., 26(6A): 601-621.
- PLATT, T., GALLEGOS, C.L. and HARRISON, W.G. 1980. Photoinhibition of photosynthesis in natural assemblages of marine phytoplankton. J. Mar. Res., 38(4): 687-701.
- PLATT, T., HARRISON, W.G., IRWIN, B., HORNE, E.P. and GALLEGOS, C.L. 1982. Photosynthesis and photo adaptation of marine phytoplankton in the Arctic. Deep-Sea Res., 29(10A): 1159-1170.
- REY, F. and LOENG, H. 1985. The influence of ice and hydrographic conditions on the development of phytoplankton in the Barents Sea. pp. 49-63 in Gray, J.S. and Christiansen, M.E. (eds.). Marine Biology of Polar Regions, and Effects of Stress on Marine Organisms. John Wiley & Sons Ltd.

SOLEMDAL, P. and ELLERTSEN, B. 1984. Sampling fish larvae with large pumps; quantitative and qualitative comparisons with traditional gear. Flødevigen rapportser. 1, 1984. ISSN 0333-2594. The propagation of cod Gadus morhua L.



## Appendix A

Table A1. List of stations for R/V "G.O. Sars" during the period 29 July-19 August 1985. Stations marked with B were common for all participating scientists. A more extensive program was carried out to provide a fairly detailed description of the vertical structure of chemical and biological properties. The stations marked B, are described as "selected stations" on page 26 (continues).

St.no.	Position		CTD	Water-samples	Q-fluor.	Juday 36	HUFSA	MOCNESS
	N	E						
806	72° 00'	22° 12'	X	X	X	X		
807	72° 30'	22° 46'	X	X	X	X		
808	73° 00'	23° 22'	X	X	X	X		
809	73° 30'	23° 56'	X	X	X	X		X
810	74° 07'	24° 42'	X	X	X	X		
811	74° 15'	24° 18'	X	X				
812	74° 22'	23° 55'	X	X		X		
B 813	74° 33'	23° 20'	X	X	X			
814	74° 33'	23° 20'	X	X	X	X		X
815	74° 39'	22° 59'	X		X	X		
816	74° 44'	22° 44'	X	X	X	X		
817	74° 52'	22° 20'	X	X	X	X		
818	75° 04'	21° 44'	X	X	X	X		
819	75° 15'	21° 08'	X	X	X			
820	75° 15'	22° 00'	X	X	X	X		
821	75° 15'	22° 40'	X	X	X	X	X	
822	75° 15'	23° 20'	X	X	X	X		
823	75° 15'	24° 00'	X	X	X	X		
824	75° 15'	24° 40'	X	X	X	X		
825	75° 15'	25° 20'	X	X	X	X		
826	75° 15'	26° 00'	X	X	X	X		
827	75° 15'	26° 40'	X	X	X	X		
828	75° 15'	27° 40'	X	X	X	X		
B 829	75° 15'	28° 40'	X	X	X	X		X
830	75° 28'	28° 07'	X	X	X	X		
831	75° 40'	27° 34'	X	X	X	X		
832	75° 49'	27° 12'	X	X	X	X		
833	75° 57'	26° 49'	X	X	X	X		
834	76° 05'	26° 27'	X	X	X	X		
835	76° 13'	26° 05'	X	X	X	X		
836	76° 21'	25° 43'	X	X	X	X	X	
837	76° 30'	25° 20'	X	X	X	X		

Table A1 continued.

St.no.	Position		CTD	Water- samples	Q- fluor.	Juday 36	HUFSA	MOCNESS
	N	E						
838	76° 30'	25° 50'	X	X	X	X		
839	76° 30'	26° 20'	X	X	X	X		
840	76° 30'	27° 00'	X	X	X	X		
841	76° 30'	27° 40'	X	X	X	X		X
842	76° 30'	28° 20'	X	X	X	X		
843	76° 26'	28° 58'	X	X	X	X		
844	76° 22'	29° 36'	X	X	X	X		
845	76° 15'	30° 33'	X	X	X	X		
846	76° 09'	31° 30'	X	X	X	X		
847	76° 02'	32° 30'	X	X	X	X		
848	75° 56'	33° 27'	X	X	X	X		X
849	75° 50'	34° 21'	X	X	X	X		
B 850	75° 45'	35° 00'	X	X	X	X		X
851	75° 55'	35° 00'	X	X	X	X		
852	76° 10'	35° 00'	X	X	X	X		
853	76° 25'	35° 00'	X	X	X	X		
854	76° 35'	35° 00'	X	X	X	X		
855	76° 45'	35° 00'	X	X	X	X		
856	77° 00'	35° 00'	X	X	X	X		
B 857	77° 15'	35° 00'	X	X	X	X	X	X
858	77° 16'	34° 00'	X	X	X	X		
859	77° 18'	33° 00'	X	X	X			
860	77° 20'	32° 00'	X	X	X	X		
861	77° 21'	31° 15'	X	X	X	X		
862	77° 22'	30° 32'	X	X	X	X		
863	77° 23'	30° 10'	X	X	X	X		
864	77° 23'	29° 46'	X	X	X	X		
865	77° 23'	29° 00'	X	X	X	X		
866	77° 23'	28° 00'	X					
B 867	77° 23'	28° 00'	X	X	X	X	X	X
868	77° 15'	28° 00'	X	X	X	X		
869	77° 05'	28° 00'	X	X	X	X		
870	76° 55'	28° 00'	X	X	X	X		
871	76° 45'	28° 00'	X	X	X	X		
872	76° 39'	29° 00'	X	X	X	X		
873	76° 55'	29° 00'	X	X	X	X		X
874	77° 10'	29° 00'	X	X	X	X		
875	77° 10'	30° 00'	X	X	X	X		
876	76° 55'	30° 00'	X	X	X	X		
877	76° 45'	30° 00'	X	X	X	X		
878	76° 32'	30° 00'	X	X	X	X		X
879	76° 26'	31° 00'	X	X	X	X		
880	76° 40'	31° 00'	X	X	X	X		X

Table A1 continued.

St.no.	Position		CTD	Water- samples	Q- fluor.	Juday 36	HUFSA	MOCNESS
	N	E						
881	76° 55'	31° 00'	X	X	X	X		
882	77° 05'	32° 00'	X	X	X	X		X
883	76° 50'	32° 00'	X	X	X	X		
884	76° 40'	32° 00'	X	X	X	X		
B 885	76° 30'	32° 00'	X	X	X	X	X	X
886	76° 20'	32° 00'	X	X	X	X		X
887	76° 16'	32° 40'	X	X	X	X		
888	76° 25'	32° 40'	X	X	X	X		X
889	76° 35'	32° 40'	X	X	X	X		
B 890	76° 45'	32° 40'	X	X	X	X	X	X
891	76° 55'	32° 40'	X	X	X	X		
892	77° 05'	32° 40'	X	X	X	X		
893	77° 30'	31° 32'	X	X	X	X		
894	77° 40'	31° 04'	X	X	X	X		
895	77° 55'	30° 22'	X	X	X	X		
896	78° 10'	29° 40'	X	X	X	X		X
897	78° 25'	28° 58'	X	X	X	X		
B 898	78° 35'	28° 29'	X	X	X	X	X	
899	78° 43'	29° 15'	X	X	X	X		
900	78° 39'	30° 15'	X	X	X	X		
901	78° 37'	31° 30'	X	X	X	X		X
902	78° 35'	32° 45'	X	X	X	X		
903	78° 33'	34° 00'	X	X	X	X		
904	78° 31'	35° 00'	X	X	X	X		
905	78° 29'	36° 15'	X	X	X	X		
906	78° 27'	37° 30'	X	X	X	X	X	
907	78° 25'	38° 45'	X	X	X	X		
908	78° 23'	40° 00'	X	X	X	X		
B 909	78° 21'	41° 15'	X	X	X	X	X	X
910	78° 19'	42° 30'	X	X	X	X		
911	78° 17'	43° 45'	X	X	X	X		
912	78° 15'	45° 00'	X	X	X	X		
913	78° 00'	45° 00'	X	X	X	X		X
914	77° 45'	45° 00'	X	X	X	X		
915	77° 30'	45° 00'	X	X	X	X		
916	77° 15'	45° 00'	X	X	X	X		
917	77° 00'	45° 00'	X	X	X	X	X	X
918	77° 00'	43° 45'	X	X	X	X		
919	77° 00'	42° 30'	X	X	X	X		
920	77° 00'	41° 15'	X	X	X	X		
921	77° 00'	40° 00'	X	X	X	X	X	X
922	77° 00'	38° 45'	X	X	X	X		
923	77° 00'	37° 30'	X	X	X	X		

Table A1 continued.

St.no.	Position		CTD	Water- samples	Q- fluor.	Juday 36	HUFSA	MOCNESS
	N	E						
924	77° 00'	36° 15'	X	X	X	X		
925	77° 00'	35° 00'	X	X	X	X		
926	77° 00'	34° 00'	X	X	X	X		X
927	76° 50'	34° 00'	X	X	X	X		
928	76° 40'	34° 00'	X	X	X	X		
929	76° 30'	34° 00'	X	X	X	X		
930	76° 23'	33° 20'	X	X	X	X		
B 931	76° 16'	32° 40'	X	X	X	X	X	X
932	76° 31'	32° 01'	X	X	X	X		X
933	76° 41'	33° 03'	X	X	X	X		
934	76° 52'	32° 35'	X	X	X	X		X
935	77° 04'	32° 01'	X	X	X	X		X
936	76° 59'	31° 30'	X	X	X	X		
937	76° 45'	31° 30'	X	X	X	X		X
938	76° 45'	30° 30'	X	X	X	X		X
939	77° 00'	30° 30'	X					X

NITROGEN CYCLING IN THE BARENTS SEA, JULY-AUGUST 1985

By

SVEIN KRISTIANSEN and TOVE FARBROT  
University of Oslo  
Department of Biology, Marine Botany  
P.O. Box 1069 Blindern  
N-0316 Oslo 3, Norway

SUMMARY

The purpose of this project is to measure uptake rates and remineralization rates of nitrogen in the Barents Sea.

The concentrations of  $\text{NH}_4$  and urea, and the uptake rates of  $^{15}\text{NO}_3$ ,  $^{15}\text{NH}_4$  and  $^{15}\text{urea}$  were measured as described by PAASCHE and KRISTIANSEN 1982; KRISTIANSEN 1983). Remineralization of  $\text{NH}_4$  was measured by isotope dilution (PAASCHE and KRISTIANSEN 1982b) but  $\text{NH}_4$  was stripped from the water by a solvent extraction procedure (DUDEK *et al.* in prep.) instead of steam distillation. The samples from the cruise are not yet worked up. The parameters measured are given in Table 1.

REFERENCES

DUDEK, N., M.A. BRZEZINSKI and P.A. WHEELER. In prep. Recovery of ammonium nitrogen by solvent extraction for the determination of relative  $^{15}\text{N}$  abundance in regeneration experiments. Submitted to Marine Chemistry.

KRISTIANSEN, S. 1983. Urea as a nitrogen source for the phytoplankton in the Oslofjord. Mar. Biol. 74: 17-24.

PAASCHE, E. and S. KRISTIANSEN. 1982a. Nitrogen nutrition of the phytoplankton of the Oslofjord. Estuarine, Coastal and Shelf Sci. 14: 237-249.

PAASCHE, E. and S. KRISTIANSEN. 1982b. Ammonium regeneration by microzooplankton in the Oslofjord. Mar. Biol. 69: 55-63.

Table 1. Parameters measured in the Barents Sea in July-August 1985. The concentrations of  $\text{NH}_4$  and of urea are given in  $\mu\text{g-atoms N l}^{-1}$ . x = measured, - = not measured.

Station	Depth m	Nutrients		Nitrogen uptake	$\text{NH}_4$ remin	
		$\text{NH}_4$	Urea		tot	63 $\mu\text{m}$
807	5	-	-	x	-	-
807	20	-	-	x	x	x
813	10	-	-	x	x	x
813	25	-	-	x	x	-
813	35	-	-	x	x	-
829	10	0.2	0.6	x	x	x
829	30	0.1	0.8	x	x	-
829	50	0.4	0.2	x	x	-
838	10	0.3	0.2	x	-	-
850	10	0.2	0.6	x	x	x
850	35	0.2	0.5	x	x	-
850	45	1.1	0.5	x	x	-
857	10	0.3	0.4	x	x	x
857	27	0.4	0.4	x	-	-
857	40	0.7	<0.1	x	x	-
857	60	0.4	0.4	x	x	-
867	10	0.2	0.1	-	-	-
867	20	0.3	<0.1	x	-	-
885	10	0.2	0.4	x	x	x
885	40	0.4	0.2	x	x	-
885	50	1.3	0.3	x	x	-
890	10	0.2	0.3	x	x	x
890	20	0.2	0.3	x	x	-
890	40	1.0	0.2	x	x	-
898	28	0.4	0.2	x	-	-
898	35	0.3	0.2	x	-	-
898	150	0.2	0.3	-	-	-
909	10	0.2	<0.1	x	-	-
909	30	0.2	0.3	x	x	-
909	39	0.7	0.1	x	-	-
931	10	0.4	<0.1	x	x	-
931	33	0.2	<0.1	x	x	-
931	37	0.6	0.4	x	x	-
936	40	1.0	0.1	x	-	-

## NANOPLANKTON BIOMASS IN THE BARENTS SEA

By

CHRISTOPHER D. HEWES

Polar Research Program

Scripps Institution of Oceanography

La Jolla, California, U.S.A., 92093

### INTRODUCTION

The dogma of food-webs for the world ocean has changed greatly in the past five years. It is now generally recognized that the bulk of both phytoplankton biomass and primary production of pelagic waters occurs in population of cells which pass through 10  $\mu\text{m}$  screens (MALONE, 1980). This may have tremendous impact on the way we interpret data and develop models of food webs for the Barents Sea. For example, it is hypothesized that a large proportion of total primary production for the Antarctic ocean occurs in the nanoplankton, and this is consumed and recycled within a sizable protozoan community (HEWES, et al., 1985). Much of this photosynthesis may occur in a size range of particulates which is too small to be effectively grazed by net-zooplankton (copepodes, krill, etc.). Thus, not only do zooplankton graze directly upon diatoms, but also upon the protozoan stocks which had preyed upon a smaller phytoplankton. As a result, some of the food consumed by net-zooplankton is additionally through secondary or tertiary production sources (i.e. the grazing upon other grazers). Therefore, it is important to estimate the biomass of phytoplankton passing through 10  $\mu\text{m}$  screens. It is also relevant to obtain some idea of how large the protozoan biomass is with respect to that of larger animals. The significance of

this information is that this may indicate the extent which organic carbon is recycled in the lower portion of the food-web, and thus, the efficiency by which the flux of primary production is transported upwards to higher trophic levels.

#### MATERIALS AND METHODS

The best method to obtain the biomass of phytoplankton is through a microscopical approach. The major difficulties encountered with traditional methods are the time which is involved in the actual analysis of each sample, and the distinction of plant from animal micro-organisms. Furthermore, there is a limited amount of time after which samples can be examined with regard to the nutritional mode of these organisms in order to obtain quantitative data, therefore the analysis must be made on board ship. Some of these difficulties are greatly resolved through the use of the Filter-Transfer-Freeze (FTF) method of sample preparation (HEWES and HOLM-HANSEN, 1983; HEWES et al., 1984). This method of microscopical analysis was used to obtain cell densities of autotrophic and heterotrophic eucaryotes contained in 10  $\mu\text{m}$  Nitex prescreened water samples. Biomass was estimated using the conversion of cell volume to biomass as described by STRATHMANN (1967).

Unfortunately, only a few samples can be analyzed by FTF methodology with respect to the number of stations obtained during any expedition. However, by determining specific relationships between autotrophic carbon and other biological factors for given ecological areas, biomass can be extrapolated. Chlorophyll (Chl) can be an excellent parameter through which plant carbon can be estimated, but only if the appropriate Carbon:Chl value is known. Traditionally, values for Carbon:Chl are derived from linear relationships between Particulate Organic Carbon and Chlorophyll, and as a result, may be in considerable error. On the other hand, Carbon:Chl values extrapolated from autotrophic biomass obtained microscopically and Chlorophyll show a non-linear relationship, and may be much more precise (HEWES, SAKSHAUG, and HOLM-HANSEN,



in preparation). Therefore, a significant amount of my work was done in conjunction with the phytoplankton group (i.e., F.Rey) so that the relationship between autotrophic carbon and Chl with respect to various physical factors might be determined.

## RESULTS AND DISCUSSION

During the August expedition, 30 euphotic zone water samples for 8 major stations were analyzed microscopically and the respective biomasses for autotrophic and heterotrophic nanoplankton communities estimated while on board "G.O.Sars" (See Table 1). The average biomass for autotrophic nano-

TABLE 1. Summary of nanoplankton biomass estimates in the Barents Sea during August 1985.

YEAR	STATION NUMBER	DEPTH	<10 um BIOMASS ug C/liter phyto- protozoan plankton		CHLOROPHYLL			PLANT CARBON to CHLOROPHYLL
					ug CHL/liter <10 um	percent TOTAL	percent <10 um	
1985	813	10	22	9	0,30	0,40	77	70,82
1985	813	25	18	6	0,30	0,31	95	58,53
1985	813	35	79	11	0,85	1,07	80	92,74
1985	829	10	12	22	0,19	0,15	129	62,74
1985	829	30	18	27	0,45	0,50	90	40,07
1985	829	50	11	14	0,54	0,58	92	20,32
1985	850	10	37	10	0,40	0,47	83	93,16
1985	850	35	51	21	0,78	0,85	93	64,69
1985	857	10	3	15	0,01	0,18	6	258,00
1985	857	25	127	86	0,41	0,70	59	309,00
1985	857	27	118	48	0,99	1,18	84	119,27
1985	857	30	34	14	0,62	0,94	66	54,24
1985	857	35	24	63	0,80	1,22	66	30,59
1985	857	40	35	51	1,72	4,42	39	20,45
1985	885	10	12	45	0,20	0,20	100	61,05
1985	885	40	8	34	0,16	0,20	78	54,42
1985	885	50	10	15	0,45	0,49	92	22,98
1985	890	10	7	21	0,20	0,27	75	33,70
1985	890	20	30	53	0,70	0,98	72	43,04
1985	890	40	32	73	0,25	0,34	74	128,52
1985	898	10	13	46	0,69	0,77	90	18,46
1985	898	23	12	16	0,30	0,33	90	39,69
1985	898	28	59	43	1,36	1,51	90	43,35
1985	898	35	103	74	1,79	1,99	90	57,48
1985	931	10	28	13	0,22	0,28	77	99,54
1985	931	30	24	35	0,23	0,30	77	78,38
1985	931	33	35	40	0,31	0,36	88	98,71
1985	931	36	53	35	0,31	0,35	88	153,71
1985	931	39	133	48	1,52	3,53	43	37,71
1985	931	45	126	57	1,63	3,79	43	33,27

plankton was 42  $\mu\text{g C/liter}$ , as compared to 35  $\mu\text{g C/liter}$  heterotrophic biomass (average nanoplankton Chl for these samples was 0.62  $\mu\text{g/liter}$ ). This amounts to an average of >40% of the total nanoplankton standing stock being represented by heterotrophic (and presumably grazing) microbial organisms). This would suggest that the secondary production by protozoans was the same magnitude as that of the higher trophic levels (see LOENG et al. this report).

The estimates of biomass for the autotrophic nanoplankton methods were compared with Chl values obtained from the August 1984 and August 1985 Pro Mare expeditions (Table 2). The

TABLE 2. Average values for euphotic zone biomass and biomass parameters from August, 1984, and August, 1985, PRO MARE expeditions.

Year	NUMBER of SAMPLES	<10 $\mu\text{m}$ BIOMASS $\mu\text{gC/liter}$ phyto- protozoan plankton		CHLOROPHYLL			PLANT CARBON to CHLOROPHYLL
				$\mu\text{g Chl/liter}$ <10 $\mu\text{m}$	percent TOTAL	<10 $\mu\text{m}$	
1984	12	33	21	0,66	1,41	59	54
1985	30	42	35	0,62	0,96	77	77
TOTAL	42	39	31	0,63	1,10	72	70

relationship found is demonstrated in Fig. 1. This relationship is similar to that obtained for Antarctic waters (HEWES, SAKSHAUG, and HOLM-HANSEN, in preparation). The similarity for the relationship of autotrophic biomass and Chlorophyll concentration between the two polar regions would be more or less expected because Carbon:Chl values are, in part, regulated by the ambient light regime which is nearly equal during the respective austral summers. That a non-linear relationship between autotrophic biomass and Chlorophyll does occur for the Barents Sea phytoplankton stocks is further substantiated by supplemental data obtained from earlier (pre-PRO MARE expeditions obtained by F.Rey, Institute of Marine Reserach).

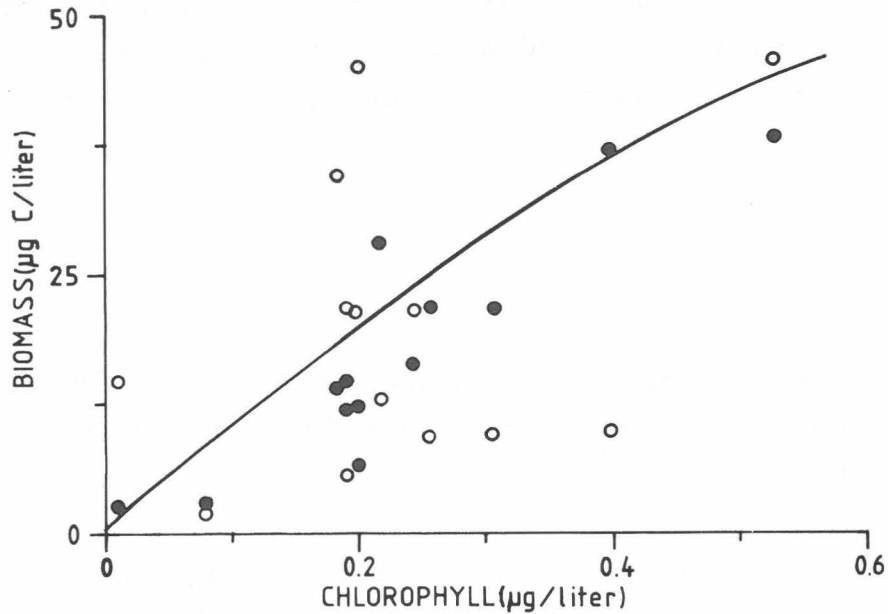


FIGURE 1. The relationship found between chlorophyll concentration and autotrophic biomass for nanoplankton samples taken at 10 meter depths during the August, 1984, and 1985, PRO MARE expeditions. Filled circles represent autotrophic biomass, and open circles represent heterotrophic biomass.

The data which has been analyzed so far indicates that:

- 1) Carbon: Chl values vary greatly for surface populations (60-100). but those obtained from deeper waters (i.e. >40 meters) are more stable (about 20).
- 2) Phytoplankton growth rates (obtained by combining data from C14 uptake and autotrophic biomass have been found near the theoretical maximum possible for the temperature and ambient light of the area (0,5-2,0 divisions/day).
- 3) Near surface (10 meter) phytoplankton populations have lower rates of growth than do those found deeper in the water column.
- 4) Growth rates of phytoplankton do not appear to be limited by nutrient supply. In spite of the low nitrate concentrations found in the surface waters, no correlation between growth rate or biomass, and nitrate has yet been found. It is possible that

ammonia, resulting from excretion by the large protozoan stocks, is utilized as a nitrogen source for phytoplankton production in nitrate depleted water.

## REFERENCES

- LOENG, H., A. HASSEL, F. REY and H.R. SKJOLDAL, 1986. Physical and biological oceanography and capelin front study. Pp. 5-60 in this report.
- HEWES, C.D. and O.HOLM-Hansen (1983). A method for recovering nanoplankton from filters for identification with the microscope. The filter-transfer-freeze (FTF) technique. *Limnol.Oceanogr.*, 28(2): 389-394.
- HEWES, C.D., F.M.H.REID and O.HOLM-HANSEN (1984). The quantitative analysis of nanoplankton: a study of methods. *J.Plankt.Res.*, 6(4):601-613.
- HEWES, C.D., O.HOLM-HANSEN, and E.SAKSHAUG (1985). Alternate Carbon Pathways at Lower Trophic Levels in the Antarctic Food Web. Pp. 277-283 in (SIEGFRIED, W.R., P.R. CONDY, and R.M. LAWS, Eds.) Antarctic Nutrient Cycles and Food Webs. Springer-Verlag, Berlin. 700 pg.
- MALONE, T.C. 1980. Algal Size. Pp 433-463 in (Morris, Ed.), The Physiological Ecology of Phytoplankton. Blackwell Scientific Publications, Oxford. 625 p.
- STRATHMANN, R.R. 1967. Estimating the organic carbon content of phytoplankton from cell or plasma volume. *Limnol Oceanogr.* 12(3): 411-418.

## BIO-OPTICAL PROPERTIES OF THE BARENTS SEA DURING SUMMER

By

W. SEAN CHAMBERLIN

Dept. Biological Sciences  
University of southern California  
Los Angeles, California, U.S.A.

### INTRODUCTION

This investigation of the Barents Sea was undertaken with three major goals: 1) to survey the spectral absorption and fluorescence excitation properties of marine phytoplankton and particulate matter in the Barents Sea with particular reference to the major water masses; 2) to provide information on the photoadaptive state of phytoplankton in the vertical structure of water column; and 3) to make a detailed examination of the chlorophyll maximum in an attempt to discern the pigment assemblages comprising this feature.

### METHODS

The methods used involve measurements of spectral absorption and fluorescence, excitation of natural populations collected on glass fiber filters, and have been largely described by KIEFER and SOOHOO (1982) and MITCHELL and KIEFER (1984). In this study, spectral absorption between 370 and 700 nm. was determined with a Shimadzu UV 240 spectrophotometer and graphically recorded. Spectral fluorescence excitation between 350 and 550 nm. was

determined using a tungsten light source and single grating monochromator from Bausch and Lomb, a vertical light path sampling compartment, A Gamma Scientific photomultiplier, and an Aminco-Bowman photometer interfaced through a Remote Measurements ADC-1 to a Macintosh 512K computer. A 680 nm. bandpass filter was placed before the photomultiplier to discriminate between fluoresced and reflected light. Once collected, the spectral data was averaged, smoothed, and corrected using commercially available software.

## RESULTS AND DISCUSSION

Though strictly qualitative at this time, preliminary results for seven of the thirty-one stations sampled reveal distinct geographic and vertical differences. Three stations, 867, 885, and 890, representative of a mixed Atlantic-Arctic water mass, appear most similar, both with respect to the shapes of the fluorescence and absorption spectra, and the trends of these spectra in the vertical structure. The most pronounced feature of the fluorescence spectra is the increase in fluorescence excitation with depth at 480 nm. relative to the chlorophyll a fluorescence at 445 nm. (Fig.1). According to NEORI et al. (1984), this feature may be interpreted as photoadaptation, the increase in blue-green fluorescence being attributed to an increase in accessory pigments in deeper waters, yet differences in species composition in different layers of the water column cannot be excluded until microscopical counts in these layers are completed. In the absorption spectra, a small but distinct peak occurs at 585 nm (Fig.2) below the pycnocline, and is still visible at 265 m. at Station 885, but whether this absorption is due to phycobiliproteins or a chl a-chl c complex protein is uncertain (Rey, pers. comm.). One additional feature in the absorption spectra of these stations is the increased absorption in the chl. c regions at 465 nm and 645 nm (see Fig. 2) in samples closely associated with the chlorophyll maximum, particularly at Stations 885 and 890. This feature is not as pronounced at similar depths in other stations, and may

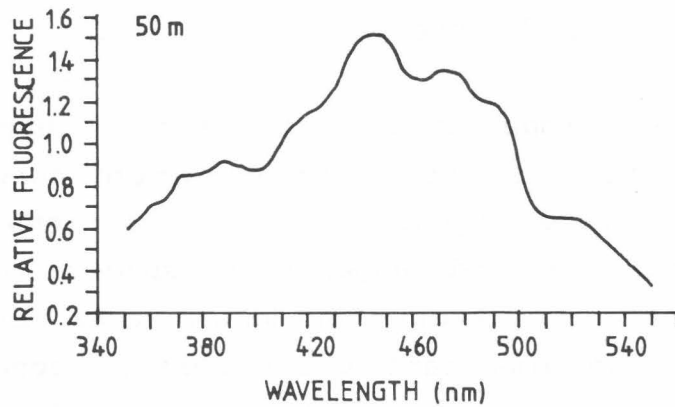
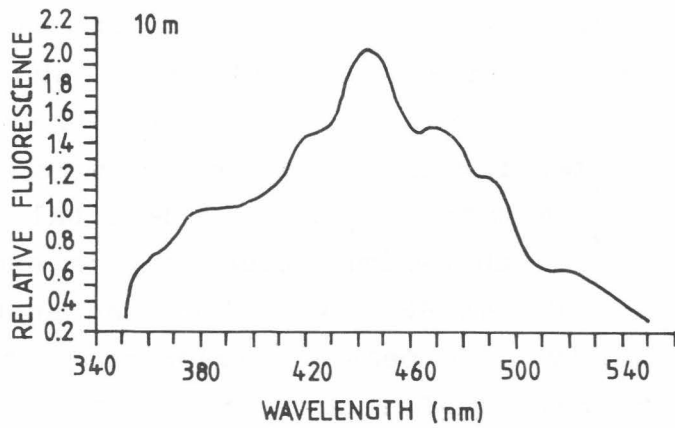


Fig.1. Representative fluorescence excitation spectra for Station 885 at two depths. Note the increase in accessory pigment fluorescence at 480 nm to chl.a fluorescence at 440 nm.

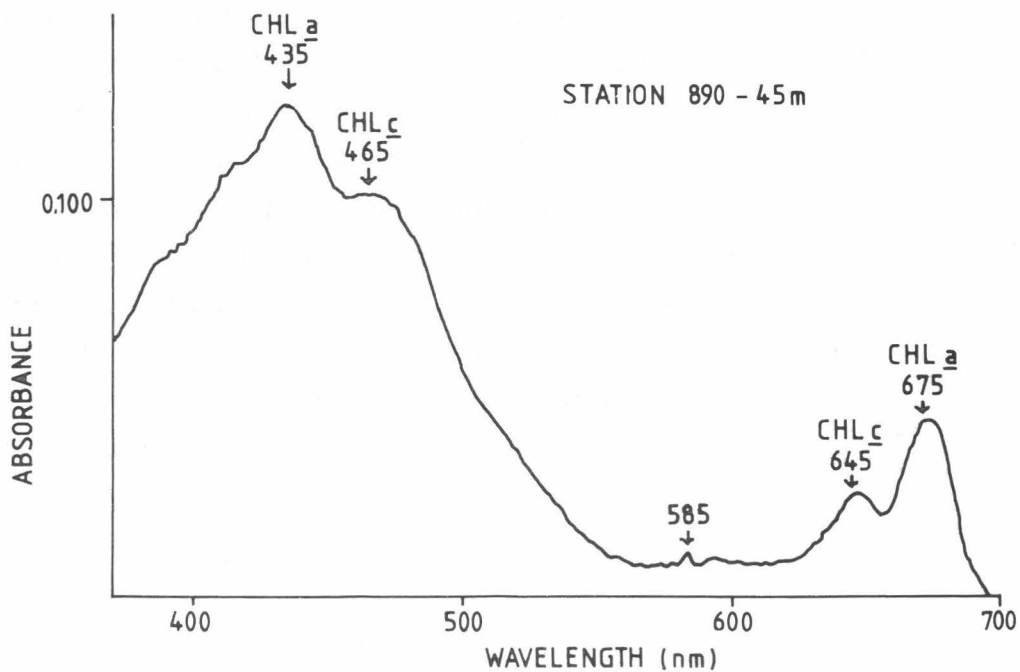


Fig. 2. Representative absorption spectra for Station 890 at 45 m. Chl.a. absorption is visible at 435 and 675 nm; chl c at 465 and 645 nm. Note the small peak at 585 nm.

reflect either changes in species composition, or changes in the successional or development state of the species present. Of the other locations, Stations 898 near Kong Karl's Island, representing an Arctic water mass, is most different. consisting almost entirely of detrital pigments in the surface waters with maximal fluorescence excitation at 410 nm. Detrital 857 at 40 m and 60 m, and Station 909 at 39 m. Additionally, the peak in absorption at 585 nm appears at Stations 850, an Atlantic watermass, and 857, a mixed water mass, but not as distinct at Stations 898 and 909, consisting of Arctic water.

Verification of the importance of these differences will require further analysis, but some tentative conclusions may be drawn: 1) there appear to be correlations in the types of fluorescence and absorption spectra observed relative to the Atlantic, Arctic and mixed water masses; 2) photoadaptation may be important under certain conditions, s but quantitative estimation of fluorescence efficiencies and microscopical analysis of species abundances must be performed before this hypothesis can be evaluated; and 3) it appears that different pigment assemblages can comprise the chlorophyll maximum.

The response of the phytoplankton to photosynthetically available light represents an important process in the dynamics of the formation and maintenance of the chlorophyll maximum. Further work in this area should include measurements of the spectral light field in the vertical structure, and would be greatly enhanced by chromatographic analysis of phytoplankton pigments. With an understanding of the interaction between light and nutrients in the chlorophyll maximum, a predictive ecological model of this feature may be formulated.



## ACKNOWLEDGEMENTS

The author wishes to express his thanks to the captain and crew of the "G.O.Sars"; Harald Loeng for the physical data and much humor; Hein-Rune Skjoldal for valuable discussions and "big" stations after breakfast; and especially to Francisco "Pancho" Rey for technical assistance, nutrient and chlorophyll data, many stimulating discussions, and lots of scientific and moral support.

## REFERENCES

- KIEFER, D.A., and J.B. SOOHOO. 1982. Spectral absorption by marine particles of coastal waters of Baja California. Limnol.Oceanogr. 27(3): 492-499.
- MITCHELL, B.G., and D.A. KIEFER. 1984. Determination of absorption and fluorescence excitation spectra for phytoplankton. P 157-169 in O.Holm-Hansen, L.Bolis, and R.Gilles (eds.) Marine Phytoplankton and Productivity. Springer-Verlag, Berlin, New York.
- NEORI, AMIR, O.HOLM-HANSEN, B.G.MITCHELL, and D.A.KIEFER. 1984. Photoadaptation in marine phytoplankton. Plant Physiol. 76: 518-524.



## MICROBIAL HETEROTROPHIC ACTIVITY

By

T.F. THINGSTAD, ØYVIND ENGER and EVY FOSS SKJOLDAL  
Dept. of Microbiology & Plant Physiology  
University of Bergen,  
5000 Bergen, Norway

### INTRODUCTION

The objective of the microbiological work was to quantify the transfer of matter through the bacterial link of the ecosystem and, if possible, to relate this to variations in other parameters such as type of water mass, phytoplankton and others.

Participants on the cruise were cand.mag. Ø. Enger and 1.-amanuensis T.F. Thingstad. E. Foss Skjoldal assisted in preparations, and in working up the samples.

The investigations reported here are based on previous work earlier in the project; done in cooperation with cand.real. Bente Pengerud.

Reservations are taken that work up and data analysis is not completed. Conversion factors may be changed and improved statistical analysis is planned. Use of the data therefore requires contact with, and permission from the authors.

## SHORT DESCRIPTION OF STATIONS

A first characterization of the stations was done before water sampling by the use of a CTD-sonde and an in situ fluorometer. Those measurements are more thoroughly described elsewhere. Therefore, only a short description is included for stations on which any microbiological investigations were carried out.

Such investigations were carried out on 16 stations (Table 1). Of these were (Fig. 1):

Station 807 and station "F" in the coastal current.

Station 810 and 829 in atlantic water south of the polar front.

Station 850 on Storbanken.

Station 838 on Svalbardbanken, north of the polar front.

The various measurements for bacterial biomass and activity are drawn in depth profiles together with fluorescence and the differential of sigma-t, in order to reveal possible patterns in the relationship between bacterial activity, pycnocline and fluorescence maximum.

On stations with a distinct fluorescence maximum, the water samplers were arranged to give at least one sample above, one in, and at least one below the maximum.

## BACTERIAL NUMBERS, BIOMASS AND FRACTION ON PARTICLES

Methods

Bacterial numbers are determined by epi-fluorescence microscopy using DAPI as stain and polycarbonate filters of 0.2  $\mu\text{m}$  pore size. Bacterial volumes are determined on shore after the cruise by direct measurements in the microscope or by measurements on projected photographic slides.

C-biomass is estimated using a fixed volume to carbon conversion factor of  $5.6 \cdot 10^{-13} \text{ gC}/\mu\text{m}^3$ .

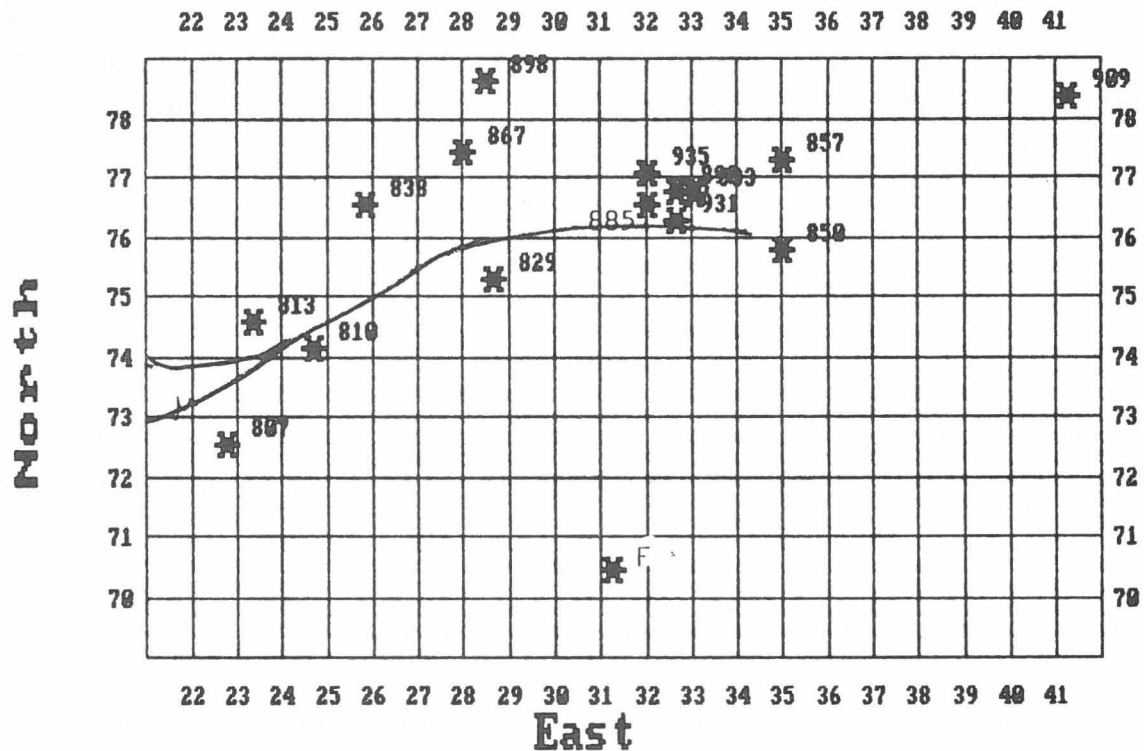


Fig. 1. Station map. Stations at which microbiological investigations were carried out.

Table 1. Stations at which microbiological investigations were carried out.

Station	date	latitude	longitude	Comment
807	2.08	72°30'	22°46'	Coastal water down to 20-30m
810	3.08	74°07'	24°42'	Atlantic water
813	3.08	74°33'	23°20'	Polar water
829	4.08	75°15'	28°40'	Polar water to 20-30m
838	5.08	76°30'	25°50'	Mixed w.column, Svalbardbank
850	6.08	75°45'	35°00'	Sentralbanken, "local water", melt water above approx 30m.
857	7.08	77°15'	35°00'	Polar water, melt water above ca. 20m
867	8.08	77°23'	28°00'	Polar water
885	10.08	76°30'	32°00'	Polar water, Capelin front
890	11.08	76°45'	32°40'	Polar water, Before C.front
898	12.08	78°35'	28°29'	Polar water, Kong Karls land
909	13.08	78°21'	41°15'	F.water. Most NE'ly stonion. <u>Phaeocystis</u> at lower fl.max.
931	15.08	76°16'	32°40'	Coastal water down to 20-30m Some <u>Phaeocystis</u>
933	16.08	76°41'	33°03'	Polar water. Picopl.dominated
935	16.08	77°04'	32°01'	Polar water
F	17.08	70°25'	31°15'	Coastal water, Vardl.

As an indicator of possible particle-bound bacteria, the number of bacteria retained on polycarbonate filters of 1  $\mu\text{m}$  pore size was also counted. Fraction retained of total population is computed.

### Results

Results are given in Table 2.

Bacterial numbers vary from  $1.6 \cdot 10^5 \text{ml}^{-1}$  to  $2.5 \cdot 10^6 \text{ml}^{-1}$ , i.e. within the range which seem to be normal in pelagic water masses.

Mean volume varies within the range 0.08 to  $0.33 \mu\text{m}^3$ .

Total C-biomass of bacteria varies within the range 8 to 150  $\mu\text{gmC/l}$ .

% of bacterial numbers retained on 1  $\mu\text{m}$  filters varied from 1 to 55<sup>0</sup>/oo.

While the bacterial density can be determined fairly precisely, there are large uncertainties tied both to the computation of volumes and to conversion from volume to carbon. Adjustments in these values may therefore be necessary during subsequent work with the results.

The observed pattern in these parameters varied extensively from station to station (Figs. 2 and 3). At the moment it seems difficult to point to clear generalizations. There are stations where the bacterial number apparently decreases with depth (885, 867, 898), a station with high bacterial density at the pycnocline (935) and stations where bacterial density is highest at the fluorescence maximum (909, 931). It is interesting to note that the station with the highest density of bacteria (933) had a relatively low in situ fluorescence without marked peaks in the profile.

Table 2. Bacterial densities (DAPI), proportion retained on 1  $\mu$ m filters, mean volumes and estimates of bacterial C-biomass. Measurements of size are done either directly in the microscope (m) or on photographs (p). More measurements of volume will be available.

stasj	dyp	bakt	%lu	MeanV	method	ugC/l
807	5	4.40E+5	nd			
807	20	4.40E+5	nd			
813	10	6.73E+5	1.90	.18	m	67.84
813	25	5.92E+5	2.50	.09	m	29.84
813	35	4.82E+5	3.90	.16	m	43.19
813	50	4.71E+5	4.70	.15	m	39.56
829	10	1.64E+5	6		nd	
829	30	4.92E+5	2.20		nd	
829	50	5.08E+5	1.70		nd	
829	60	3.76E+5	2.50		nd	
850	10	4.15E+5	2.60	.22	p	50.20
850	35	4.81E+5	3.50	.17	p	46.87
850	45	4.22E+5	1.30	.14	p	31.90
850	60	3.62E+5	1.90	.15	p	30.41
857	10	5.66E+5	.40	.12	p	39.30
857	27	4.66E+5	10.40	.19	p	50.10
857	40	6.56E+5	3.70	.24	p	89.27
857	60	1.09E+5	7.50	.19	p	11.29
867	10	1.51E+6	1.30	.18	p	150.52
867	20	5.29E+5	3.70	.08	p	47.40
867	30	5.66E+5	2.60	.16	p	50.71
885	10	5.77E+5	4	.13	p	42.33
885	40	5.87E+5	2.50	.33	p	108.48
885	50	4.61E+5	9.90	.10	p	26.59
885	60	4.17E+5	9.90	.11	p	25.69
885	80	2.36E+5	16.60	.16	p	20.48
890	10	6.65E+5	9.50	.23	p	84.72
890	20	6.10E+5	55.30	.22	p	75.15
890	40	4.92E+5	9.90	.16	p	44.91
890	60	6.24E+5	11.40	.17	p	60.63
898	10	5.87E+5	7.90		nd	
898	28	3.31E+5	11.40		nd	
898	50	1.94E+5	5.10		nd	
898	60	2.31E+5	7.30		nd	
898	80	1.42E+5	4.30		nd	
909	10	1.02E+5	2.10	.14	m	8.00
909	20	1.82E+5	2.80	.12	m	12.23
909	30	1.69E+5	4.60	.09	m	8.52
909	39	7.72E+5	30.40	.20	m	86.46
909	50	7.39E+5	26.70	.11	m	45.52
909	80	1.63E+5	2.20	.09	m	8.22
931	10	3.58E+5	2.30		nd	
931	25	2.98E+5	32		nd	
931	33	3.45E+5	11.40		nd	
931	36	3.80E+5	22.90		nd	
931	39	5.76E+5	33.70		nd	
931	45	5.70E+5	9.20		nd	
931	60	4.37E+5	8.50		nd	
933	20	2.39E+6	17.40		nd	
933	30	2.52E+6	19.20		nd	
933	40	1.49E+6	1.49		nd	
935	10	4.26E+5	3.10		nd	
935	20	1.37E+6	1		nd	
935	30	5.85E+5	2.20		nd	
935	40	5.12E+5	1.90		nd	

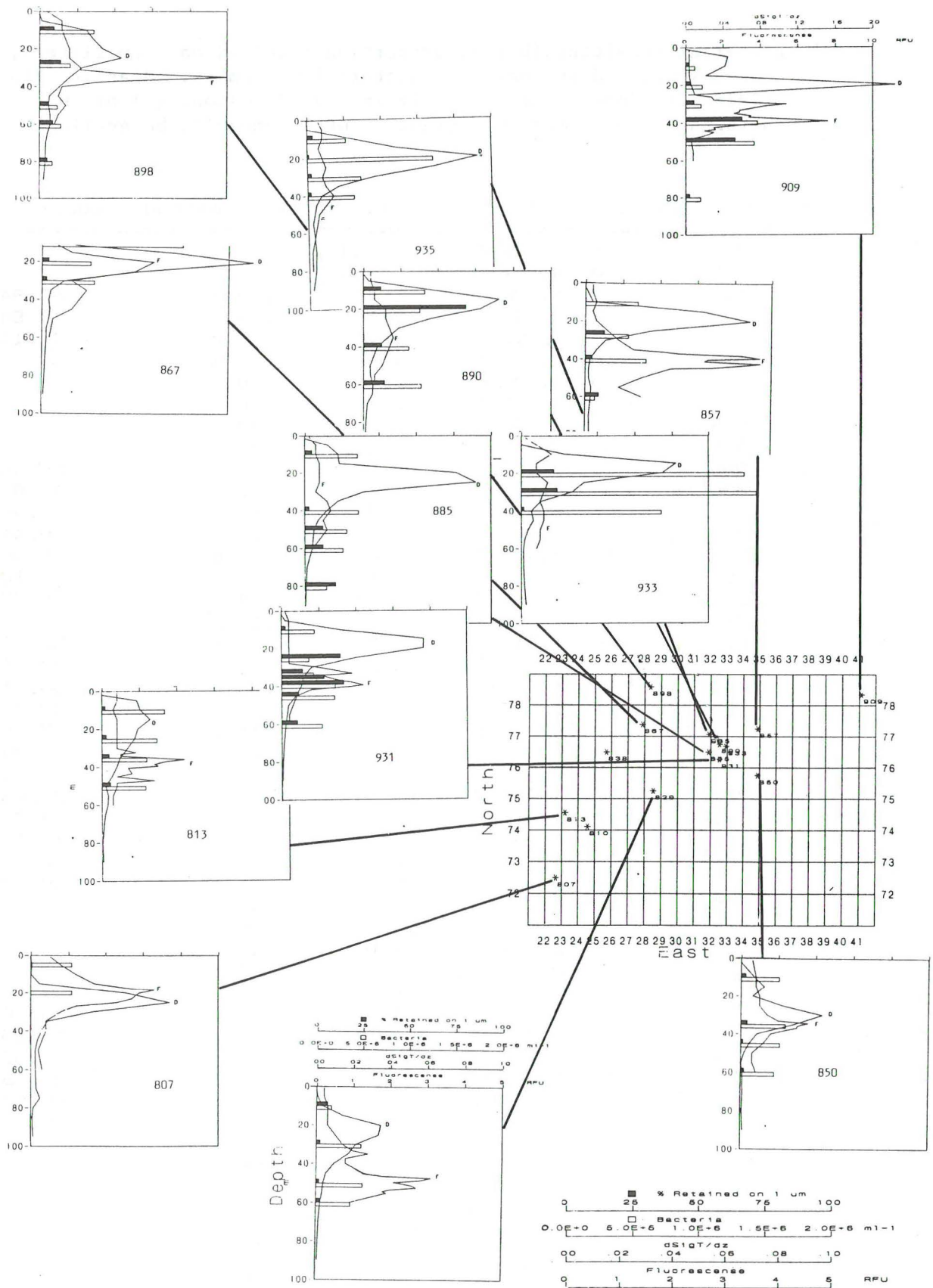


Fig. 2. Depth profiles for bacterial densities (open bars) and fraction of bacteria retained on 1  $\mu\text{m}$  filters (filled bars), plotted together with depth profiles of *in-situ* fluorescence and the differential of sigma-t. Scale on axes are identical for all stations except 909 where the scale values for both fluorescence and  $d/dz$  (sigma-t) are doubled.



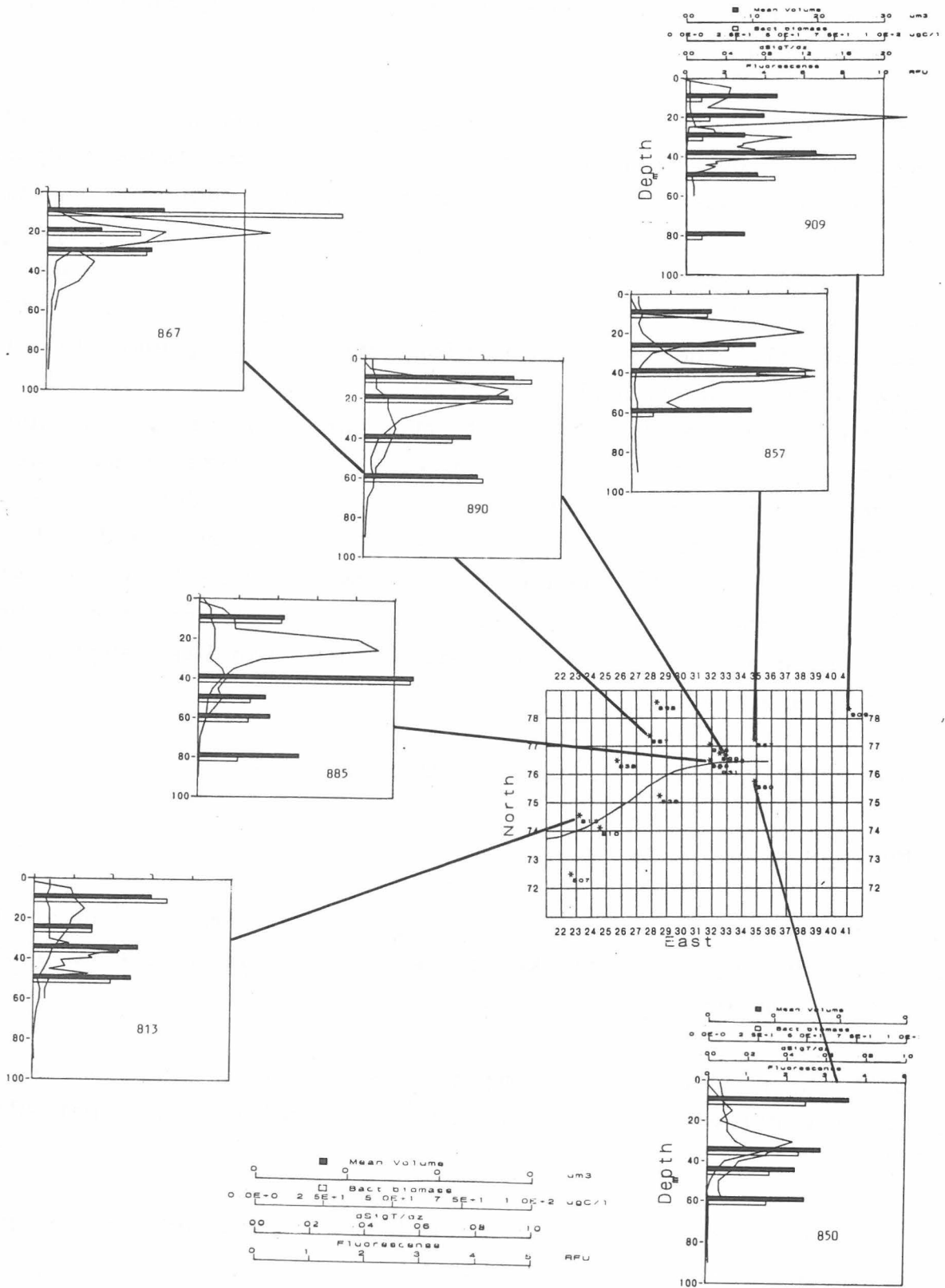


Fig. 3. Mean bacterial volumes (filled bars) and bacterial C-biomass. Refer to text figure 2.

Any direct conclusions may of course not be drawn from high bacterial numbers to high activities. High bacterial density may equally well be a consequence of low predation pressure on the bacteria.

On several stations a high retention of bacteria on 1  $\mu\text{m}$ -filters was observed. This is not a consequence of large bacterial sizes, but due to the attachment of the bacteria to slime particles (marine snow). The size of these particles in situ is unknown due to the procedures used for water sampling, prefiltering, fixation and specimen preparation. On stations 909 and 931, the close connection between this phenomenon and a Phaeocystis dominated phytoplankton community around 39 m depth, strongly suggest that the carbohydrate production of this algae was the origin of this slime. There were, however, also stations (890, 933) where the Phaeocystis density was much smaller, but where high retention still was observed. It may seem as if the phenomenon could be more coupled to the pycnocline on these stations. The possibility of marine snow being generated at fronts between water masses has been suggested in the literature.

#### BACTERIAL PRODUCTION AND GENERATION TIME

##### Methods

Bacterial production in cells/ml·day (24 hrs) is determined using the thymidine uptake method. Incubations were done at in situ temperature  $\pm 1^{\circ}\text{C}$ .

Generation time  $t_g$  is computed as  $\ln 2 \cdot N/P$ , where  $N$  is cell density per ml and  $P$  is production in cells formed per ml per day.

Bacterial production in  $\mu\text{gC/l}\cdot\text{day}$  is computed as  $\ln 2 \cdot M/t_g$ , where  $M$  is C-biomass in  $\mu\text{gC/l}$ .

## Results

Results are given in Table 3. Generation times vary from 0.7 to 9.2 days, from which values of bacterial production in the range 3-70  $\mu\text{gC}/\text{l}\cdot\text{day}$  are computed.

Taking the low water temperatures (+2 - -2°C) into consideration, these estimates of bacterial production seem interestingly high.

A reasonable estimate for bacterial respiration seem to be that 80% of the substrate-C is converted to  $\text{CO}_2$ . If this value is used, estimates of total bacterial C-consumption will be in the range 15-350  $\mu\text{gC}/\text{l}\cdot\text{day}$ .

Since data for primary production and particulate C were not available during the writing of this report, I have not yet been able to make the obviously interesting comparisons which are possible at this point. With present methods, it seems to be a general problem that estimates of bacterial C-consumption may exceed the estimates of primary production.

Depth profiles for station 909 are shown in Fig. 4. Bacterial production seemed to be concentrated in the layer of maximum Phaeocystis population at 39 m depth.

As for bacterial numbers and biomass, the data does not invite to general conclusions concerning the pattern of depth profiles and/or variation between water masses.

## SOURCES OF BACTERIAL SUBSTRATES

### Rationale and methods

It seems reasonable to hypothesize that the source of carbon for bacterial growth varies with depth in the water column. One possibility is that the phytoplankters above the fluorescence maximum are stressed due to limited supply of available mineral nutrients, and that this may cause excretion of carbo-

Table 3. Bacterial production in cells/ml·day, biomass production in  $\mu\text{gC}/\text{l}\cdot\text{day}$ , and bacterial generation time in days.

stasi	dyp	bakt	prod	biom	biomprod	tg
	m	ml <sup>-1</sup>	ml <sup>-1</sup> day <sup>-1</sup>	$\mu\text{gC}/\text{l}$	$\mu\text{gC}/\text{l}\cdot\text{day}$	days
807	5	4.40E+5	1.42E+5			2.15
807	20	4.40E+5	2.27E+5			1.34
813	10	6.73E+5	2.72E+5	67.84	27.46	1.71
813	25	5.92E+5	2.61E+5	29.84	13.16	1.57
813	35	4.82E+5	2.16E+5	43.19	19.33	1.55
850	10	4.15E+5	7.49E+4	50.20	9.06	3.84
850	35	4.81E+5	3.86E+4	46.87	3.76	8.64
850	45	4.22E+5	9.08E+4	31.90	6.86	3.22
850	60	3.62E+5	3.86E+4	30.41	3.24	6.50
857	10	5.66E+5	1.76E+5	39.30	12.22	2.23
857	27	4.66E+5	5.11E+4	50.10	5.49	6.32
857	40	6.56E+5	5.11E+5	89.27	69.51	.89
857	60	1.09E+5	7.95E+4	11.29	8.23	.95
867	10	1.51E+6	1.14E+5	150.52	11.31	9.22
867	20	5.29E+5	1.99E+5	47.40	17.80	1.85
867	30	5.66E+5	4.54E+4	50.71	4.07	8.64
885	10	5.77E+5	1.87E+5	42.33	13.74	2.14
885	40	5.87E+5	9.93E+4	108.48	18.36	4.10
885	50	4.61E+5	6.24E+4	26.59	3.60	5.12
885	60	4.17E+5	9.65E+4	25.69	5.94	3.00
890	10	6.65E+5	1.84E+5	20.48	5.68	2.50
890	20	6.10E+5	4.11E+5	84.72	57.15	1.03
890	40	4.92E+5	7.09E+4	75.15	10.84	4.81
890	60	6.24E+5	7.09E+4	44.91	5.11	6.10
898	10	5.87E+5	1.76E+5			2.31
898	28	3.31E+5	5.68E+4			4.04
898	50	1.94E+5	1.08E+5			1.25
898	60	2.31E+5	7.38E+4			2.17
898	80	1.42E+5	6.24E+4			1.58
909	10	1.02E+5	1.02E+5	8.00	8.01	.69
909	20	1.82E+5	9.08E+4	12.23	6.10	1.39
909	30	1.69E+5	1.02E+5	8.52	5.15	1.15
909	39	7.72E+5	5.39E+5	86.46	60.39	.99
909	50	7.39E+5	1.14E+5	45.52	6.99	4.51
935	10	4.26E+5	2.27E+5			1.30
935	20	1.37E+6	1.28E+5			7.44
935	30	5.85E+5	1.28E+5			3.18
935	40	5.12E+5	5.68E+4			6.25

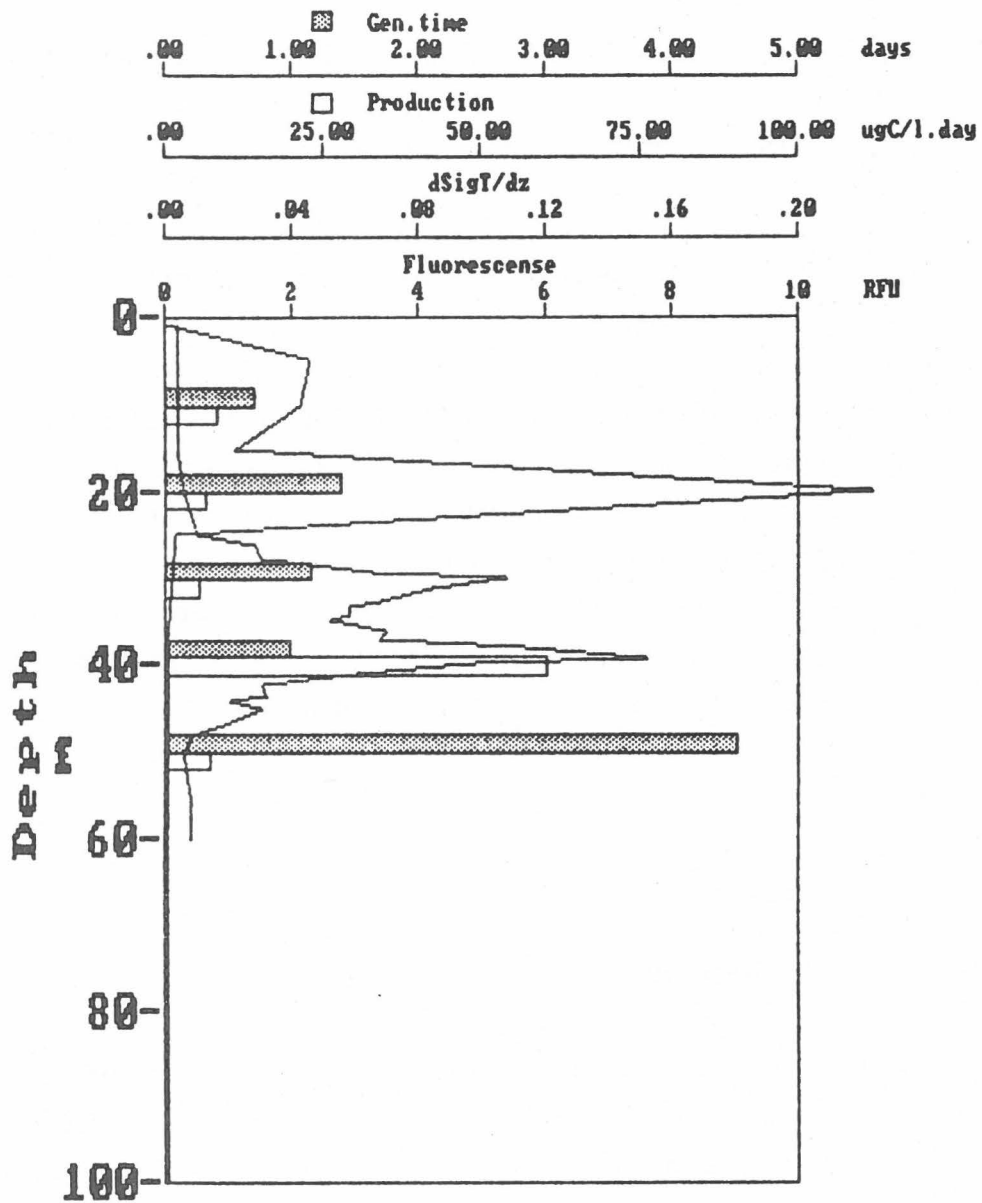


Fig. 4. Depth profiles for bacterial production in  $\mu\text{gC}/\text{l}\cdot\text{day}$  and bacterial generation time at station 909. Bacterial production was mainly concentrated in the Phaeocystis dominated layer (39 m). Below this layer, bacterial generation time increases.

hydrate enriched organic material. In the layer below the fluorescence maximum, however, it seems more reasonable that a "rain" of dead or senescent organisms, i.e. protein containing particles, provides the source of bacterial substrates. This picture would suggest that indicators of bacterial utilization of carbohydrate/glucose versus protein/amino acids, would change downwards in the water column, especially as one passes from above to below the fluorescence maximum.

Three different methods were attempted as such indicators:

- Most Probable Number (MPN) determination of the density of organisms growing on media containing protein and glucose respectively as C-source.
- Uptake of  $^{14}\text{C}$ -labelled amino-acids and glucose.
- Enzyme capacity for exoglucosidases and exoproteases respectively.

In the form attempted, the method for determination of exoglucosidase capacity was not sufficiently sensitive. In addition, the fluorometer broke down in the middle of the cruise, prohibiting further attempts to refine the method and also limiting the number of measurements carried out for exoprotease capacity. Calibration was also prohibited and values are given in Relative Fluorescence Units (RFU) only.

### Results

Results are given in Table 4.

#### MPN-glucose/MPN-protein -----

There was a variation in nearly three orders of magnitude in MPN-values, from 4 to  $>1600 \text{ ml}^{-1}$ . There is a high degree of correlation between MPN-values on glucose and on protein-based media (Fig. 5a). The reason why station 829:60 m and 898:28 m deviates from the general pattern is unknown.

No coherent picture in variation with depth was found. Stations 885 and 890 both had minima in MPN at 40 m, while stations 850 and 857 both had their largest MPN-values at 10 m, while at 829 the largest values were at the fluorescence maximum (50 m).

Table 4. Indicators of substrate specificity in the bacterial community, MPN on glucose (MPN<sub>glu</sub>) and protein (MPN<sub>pro</sub>) containing media, incorporation of <sup>14</sup>C from labelled glucose (DPM<sub>glu</sub>) and protein (DPM<sub>aa</sub>) and enzyme capacity of exoproteases (Exoprot).

Stasj	dyp	MPN <sub>glu</sub>	MPN <sub>pro</sub>	DPM <sub>glu</sub>	DPMAa	Exoprot
=====						RFU
	m	ml-1	ml-1			
807	5	17	17			
	20	33	23			
813	10	70	130	1528	2208	
	35	50	80	1171	6343	
	60	30	27	170	826	
829	10	70	50	366	7067	
	50	500	900	531	3444	
	60	4	170	448	7614	
850	10	1600	1600	894	6772	.72
	35	500	1600	848	4079	.75
	60	30	90	328	1032	.25
857	10	1600	3000	1428	11950	1.95
	27					1.98
	40	110	240	2555	31621	3.15
	60	170	220	247	6359	.42
867	10			76	2520	.62
	20			400	10354	2.22
	30			276	3459	.90
885	10	>1600	>1600	1888	11540	
	40	110	80	975	7927	
	50	1600	1600	413	5008	
890	10	1600	>1600	1496	13994	
	20	54	500	3421	14524	
	40	300	>1600	103	6476	
898	10	missing	50	2185	12290	
	23			1136	5596	
	28	4	500	1748	5832	
	35	50	500	1819	10475	
	50			1211	5049	
	60			1799	4869	
909	10			1205	8409	
	20			692	5175	
	30			1163	9027	
	35			1422	34787	
	39			3317	19791	
	50			540	5726	
931	80			1278	116	
	10			983	8715	
	25			601	6818	
	33			1028	11069	
	36			798	7986	
	39			798	8092	
935	45			259	4407	
	60			490	1021	
	10			2905	14759	
	20			3049	16963	
	30			1588	17657	
	40			1153	6674	

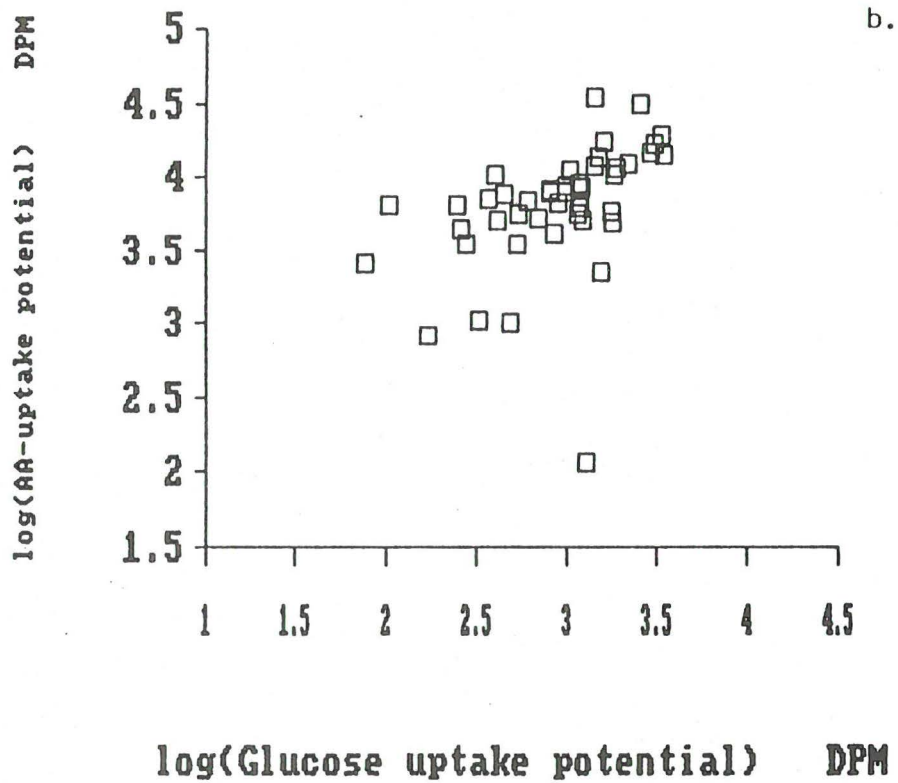
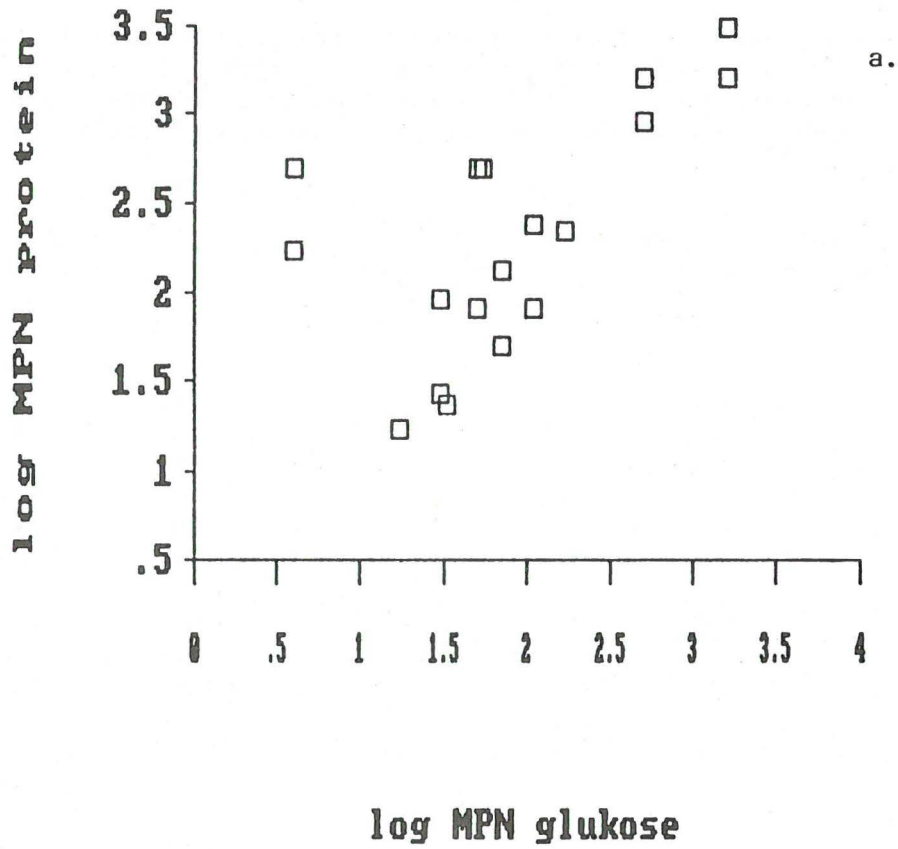


Fig. 5a-b. Scatterdiagrams for observations of MPN (Fig. 5a) and  $^{14}\text{C}$ -uptake (Fig. 5b) on glucose (x-axes) versus protein/amino-acids (y-axes). Each point represents one sample (i.e. one station-one depth).



Uptake of  $^{14}\text{C}$ -glucose/ $^{14}\text{C}$ -aminoacids

-----

In this case there is also a tendency towards covariation of these two measurements (Fig. 5b), but not as marked as was the case for the MPN-values. Station 909:80 m departs from the standard pattern for unknown reasons. At station 909 (Fig. 6), the maximum in amino acid uptake was found in the layer between the two peaks in the fluorescence profile, while glucose uptake maximum coincided with the lower, Phaeocystis-dominated peak.

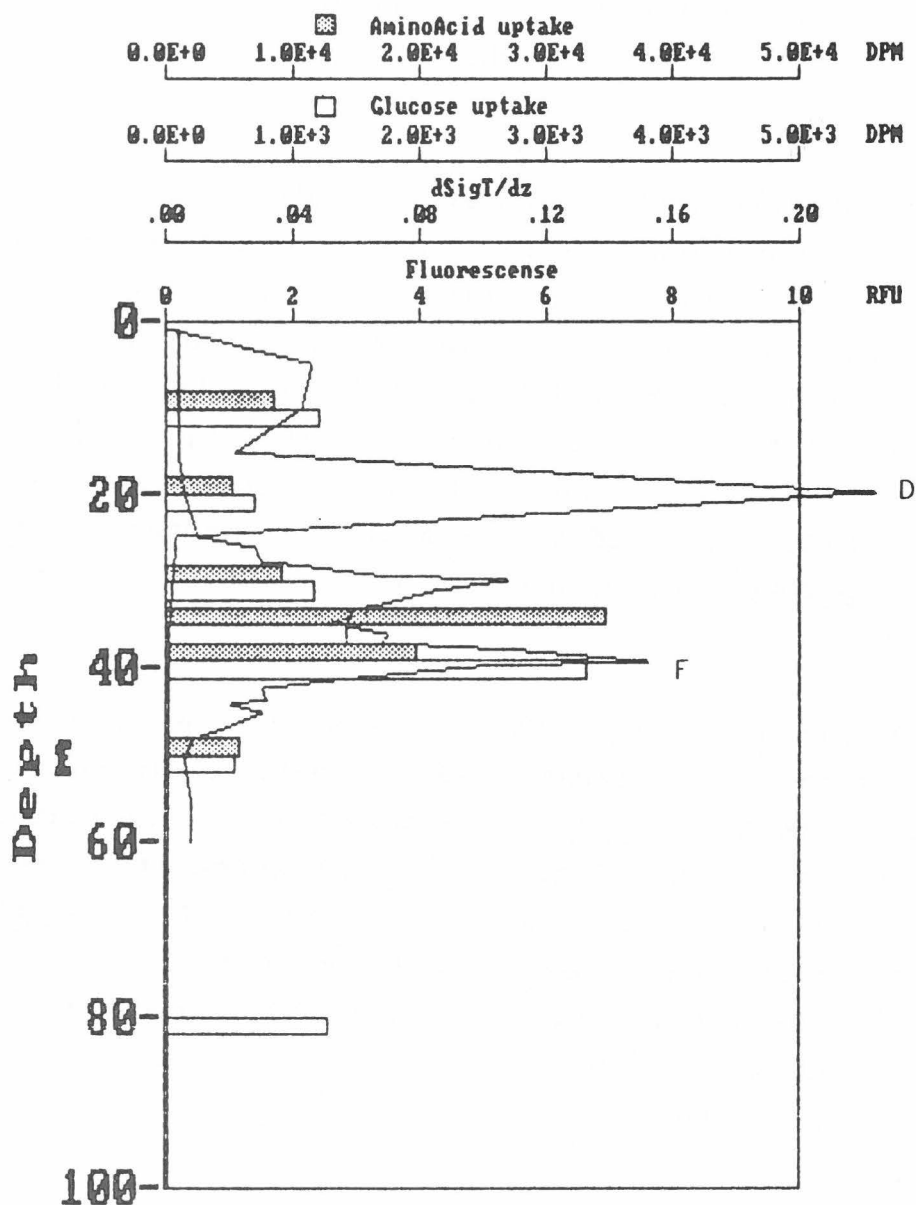


Fig. 6. Uptake potentials for  $^{14}\text{C}$ -glucose (open bars) and amino-acids (filled bars) on station 909. Note the difference in depth of maximum uptake potentials.

An interesting pattern taking the assumed carbohydrate excretion from Phaeocystis into consideration. At station 931, which also had a marked Phaeocystis population at the lower peak in the fluorescence profile, both glucose and amino acid uptake coincided at the upper (33m) peak of the fluorescence profile.

#### Exoprotease

-----

At two of the three stations where these measurements are available, the peak in activity coincides with the fluorescence maximum (857 and 867), while there is no such effect at station 850.

The potentials for amino acid uptake and protease activity were found to correlate (Fig. 7a), a relationship previously shown in the literature and also found by ourselves in other situations. The data also suggest a linear relationship between amino-acid uptake potential and bacterial production estimates based on thymidine uptake potential (Fig. 7b). The interesting possibility emerging from these relationships is that the extremely rapid and simple method of protease activity measurement perhaps may be used as an indicator of bacterial productivity.

Comparisons of the MPN-values with the uptake of the corresponding  $^{14}\text{C}$ -substrates (Fig. 8a-b) indicates that these two measurements, a priori assumed to be indicators of similar characteristics of the microbial community, are uncorrelated. This set of data suggest that the ability to grow in culture media (MPN-technique) reflects one property or group of properties (the two MPN-measures are correlated) while the activity and substrate-type indicators (exo-enzyme and  $^{14}\text{C}$ -uptake) reflects another.

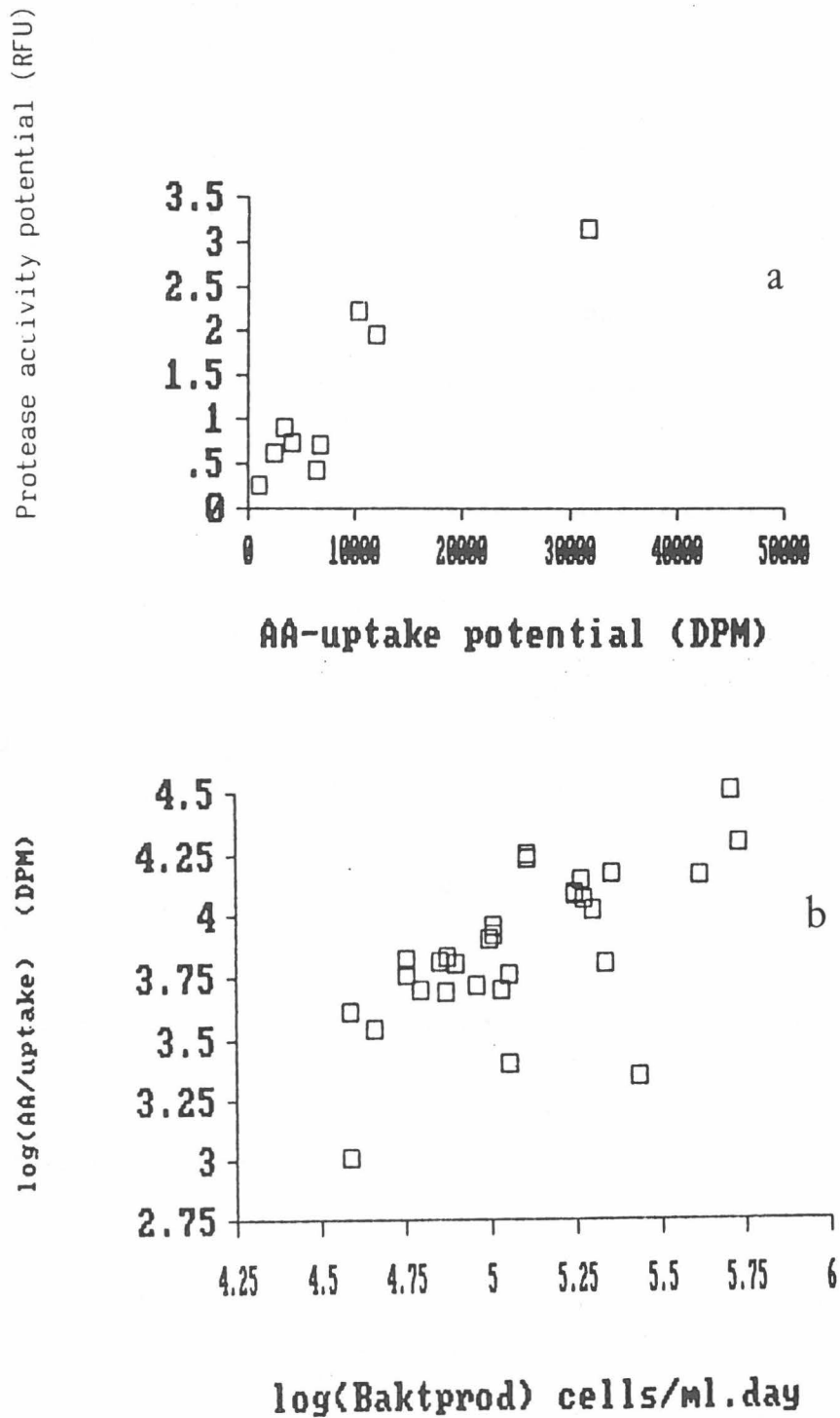


Fig. 7a-b. Scatterdiagram of measurements of protease-activity versus amino-acid uptake (Fig. 7a) and amino acid uptake versus bacterial production based on thymidine uptake (Fig. 7b).

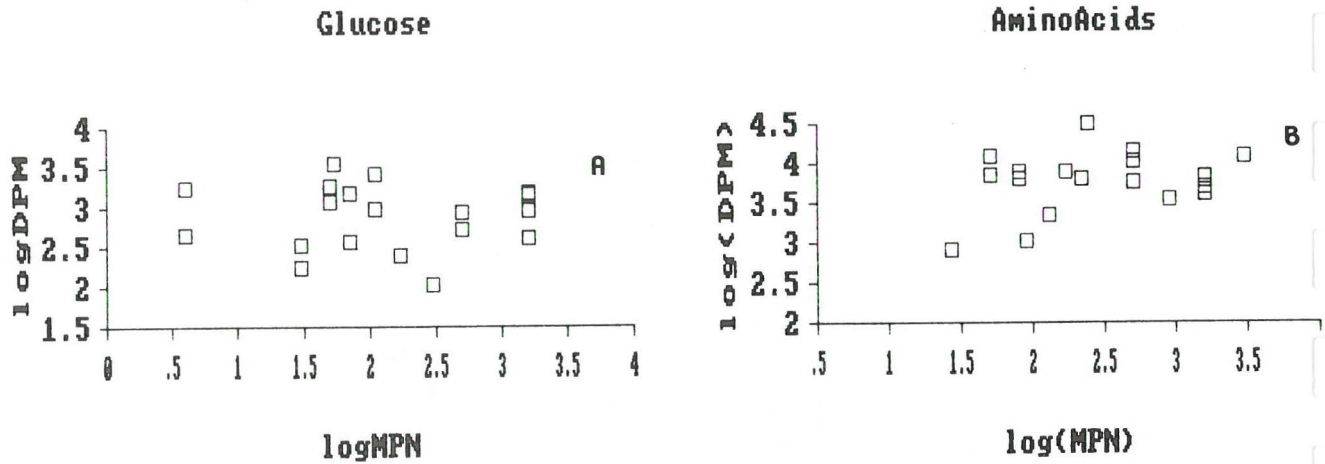


Fig. 8a-b. Scatterdiagram of uptake potentials (DPM) against MPN for glucose (a) and amino acids/protein (b).

#### AUTO- AND HETEROTROPHIC NANOPLANKTON (<math>10\mu\text{m}</math>)

##### Methods

Auto- (Anano) and heterotrophic (Hnano) nanoplankton was determined using epifluorescence microscopy of formalin fixed samplers concentrated on polycarbonate filters of  $1\mu\text{m}$  pore size. The specimens were stained with DAPI and Primulin and examined using a 100x Zeiss neofluar objective. All preparations were stored frozen and examined within three days. In cases of doubt, spots were identified as organisms by the presence of a DAPI-stained nucleus, cells with chlorophyll fluorescence were classified as autotrophic and their size measured using the fluorescence from primuline. C-content is computed from volume using the Strathmann equation (UNESCO phytoplankton manual). No corrections are made for possible shrinkage during fixation or losses due to unrecognizable organisms. Only organisms  $<10\mu\text{m}$  are included.

##### Results

Number and C-biomass of Anano and Hnano are given in Table 5. Estimates of nanoplankton biomass are in the same order of magnitude as the estimates for bacterial biomass. The covariation between bacterial and nanoplankton biomass is however

Table 5. Cell density, mean volume, and C-biomass for autotrophic (Anano) and heterotrophic (Hnano) nanoplankton < 10  $\mu\text{m}$ .

Stasj	dyp	cell numb		mean vol		biomass	
		$10^3 \text{ml}^{-1}$		$\mu\text{m}^3$		$\mu\text{gC/l}$	
	m	Anano	Hnano	Anano	Hnano	Anano	Hnano
807	5	5.50	1.40	-	-	-	-
	20	3.70	3.20	-	-	-	-
829	10	.70	.70	-	-	-	-
	30	.80	.80	-	-	-	-
	50	1.50	.70	-	-	-	-
	60	.60	.70	-	-	-	-
850	10	3.40	.90	-	-	-	-
	35	1.90	1	122	68	42	13
	45	1	1.60	105	63	19	8
	60	.40	.50	90	60	7	5
857	10	.90	1.20	119	73	19	17
	27	1.70	.60	115	49	37	6
	40	5.20	2.40	189	50	18	23
	60	.50	.60	89	51	8	6
867	10	.60	1.90	122	56	14	20
	20	2.30	.60	181	19	74	2.40
	30	.30	.20	114	105	7	4
885	10	7.10	2.10	2.70	25	4	10
	40	9.30	1.90	1.40	13	3	5
	50	7.80	1.20	2.40	56	4	12
	60	1	.30	1.40	26	.30	2
	80	.50	.50	11	7	1.10	.80
890	10	3.10	1.20	17	26	10	6
	20	15.50	2.20	2	86	8	36
	40	7.90	1	19	24	27	4
	60	1.60	.50	7	19	2	2
898	10	1.90	1.40	37	50	14	14
	28	1.70	1.40	407	79	114	21
	35	2	1.90	182	54	66	20
	50	.20	.90	342	80	12	14
	60	.05	1.60	~4	15	.02	15
	80	.05	1.80	~4	15	.02	15
909	10	1.10	1.50	79	89	15	24
	20	1.60	1.90	53	27	16	10
	30	1.20	.90	1200	74	211	11
	39	6.10	.60	133	64	148	7
	50	.80	.30	36	22	5	1
	80	.30	.40	60	25	4	2
931	10	.60	1.40	34	66	4	18
	25	1.60	1.10	79	5	23	1
	33	2	.80	49	38	18	6
	36	4.30	3.40	159	38	115	24
	39	9.90	3.60	34	47	65	32
	60	1.10	.60	78	55	15	6
933	20	.80	2.30	2.20	11	.40	5
	30	1.20	1.90	17	60	4	20
	40	2.90	.40	2.90	132	2	9
935	10	.70	1.20	33	25	5	6
	20	4.80	1.10	89	12	71	3
	30	5.40	.90	5	31	6	6
	40	3.20	.60	19	44	11	5

small (Fig. 9). Many of the bacterial biomass estimates are larger than the estimates of nanoplankton biomass in the same water sample. It must be stressed, however, that methodological uncertainties are attached to the estimates of both bacterial and nanoplankton biomass.

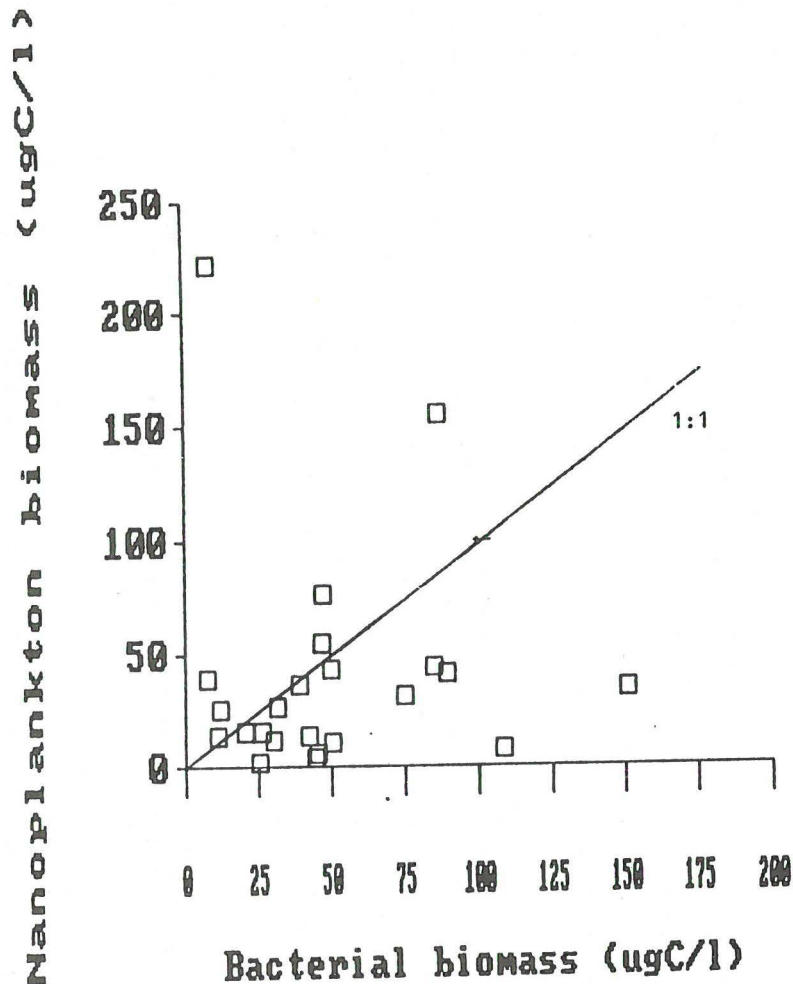


Fig. 9. Scatterdiagram of nanoplankton (Anano + Hnano) against bacterial biomass estimates.

Fig. 10 shows the scatter diagram for our nanoplankton estimates against the corresponding estimates made by Christopher Hewes on the same samples.

Due to variations in the species composition of the nanoplankton community, large variations between samples were found in the mean volumes of both Hnano and Anano. An interesting extreme was station 885 with a dominating population of small,

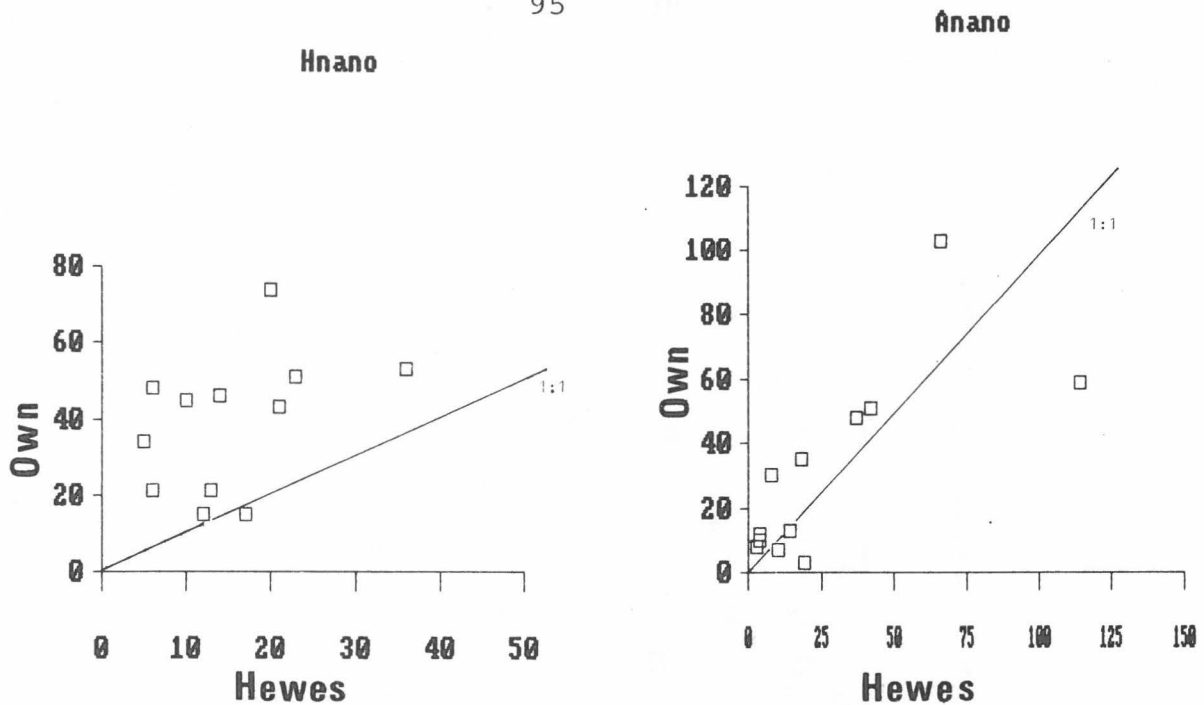


Fig. 10. Scatter diagram of our own biomass estimates of Hnano and Anano against corresponding estimates made by Christopher Hewes using a slightly different technique.

presumably eucaryotic, picoplankton giving a mean volume of  $1.4 - 2.7 \mu\text{m}^3$  for Anano. The other extreme in Anano mean volume,  $1200 \mu\text{m}^3$ , was found at station 909:30m (upper peak of fluorescence profile).

Despite the large uncertainties linked to volume estimation and conversion to carbon units, attempts to use numbers only as a measure of nanoplankton biomass, would seem to be of limited value in this area.

In samples taken close to the maximum of the fluorescence profile, estimates of Anano biomass exceeded those of Hnano. At other depths, however, Hnano biomass usually exceeded Anano biomass estimates (Fig. 11).

#### CYANOBACTERIA

Cyanobacteria with yellow-red autofluorescence (Synecoccus-type) were quantified on separate, non-stained preparations. These were made by filtering 25 ml of water sample on a 22 mm polycarbonate filter. The preparations were store frozen and counted within three days. Except for the two stations with coastal water, the numbers were insignificant. In the coastal

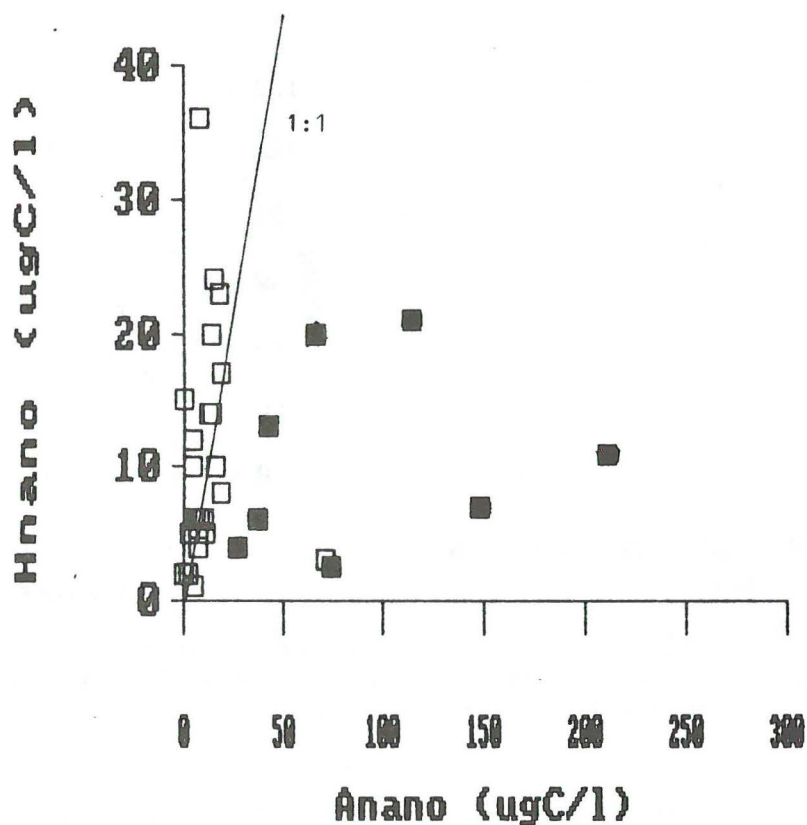


Fig. 11. Scatter diagram of Hnano versus Anano biomass estimates. Filled squares represents samples at fluorescence maximum.

water was found  $9 \cdot 10^3 \text{ ml}^{-1}$  (807:5 m and 20 m) and  $9 \cdot 10^3 \text{ ml}^{-1}$  (Station F:5 m). The water sample at station F was taken from a continuously running seawater intake at 5 m depth. Position: close to Vardø. On all other stations the 10m samples was examined.

#### PHOSPHORUS. CONCENTRATIONS AND UPTAKE

##### Methods

Total phosphorus (TP) was measured after wet oxidation with acid persulfate. Particulate phosphorus (PP) in the size fractions from  $0.2 \mu\text{m}$  to  $1.0 \mu\text{m}$  and greater than  $1.0 \mu\text{m}$  were measured after serial filtration through polycarbonate filters and subsequent ignition. Values of soluble reactive phosphorus (SRP) measured by autoanalyzer have been kindly supplied by M.Hagebø, Institute of Marine Research. Dissolved organic phosphorus (DOP) is estimated as



$$\text{DOP} = \text{TP} - (\text{PP} + \text{SRP})$$

Uptake of ortophosphate in the two size fractions are determined after addiditon of carrier-free  $^{32}\text{P}$ -ortophosphate, incubation and serial filtration on polycarbonate filters. Radioactivity on filters was determined by scintillation counting.

% of isotope taken up pr hr is estimated by linear fit to 3 points within a maximum incubation time of 4 hours.

Organisms in both size fractions are assumed to have access to the same pool of free orthophosphate in the water and the measured SRP-values are assumed to be representative of this pool.

### Results

Results are given in Table 6.

At all stations measured, TP-values were low in the layer above fluorescence maximum, supposedly as a result of previous sedimentation of P-containing material out of the euphotic zone. An interesting profile for TP was found at station 909, having a maximum in TP just below the lower peak in the fluorescence profile (Fig 12). Among the stations investigated, 909 probably represents the "youngest" stage in the succession following the ice-edge bloom. The peak in TP could be interpreted as a relatively rapid release of P from praticulate matter sedimenting out of the fluorescence maximum.

The fraction  $>1\mu\text{m}$  contained the largest fraction of PP, from 51 to 82%.

The distribution of phosphorus between SRP,PP and DOP shows that the main part of P is in the form of SRP below the fluorescence maximum. A large part (up to 49%) does, however, seem to be in the form of DOP in the upper layers. The contribution of PP varies from 6 to 40%.

Table 6. Phosphorus. Concentration of total (TOTP), particulate (PartP), percentage of particulate retained on 1  $\mu$ m-filters, soluble reactive phosphorus (SRP), distribution in per cent between SRP, PartP and DOP, uptake, % of uptake retained on 1  $\mu$ m-filters and "generation-times" ( $t_g$ ) of particulate P in the two size fractions.

Stasj	Dyp	TOTP	PartP	>1u	SRP	%SRP	%PartP	%DOP	Poppt	>1u	tg>1u	tg<1u
		m ugat/l		%	ugat/L		%		10 <sup>-3</sup> ugat/l.h	%	dcgn	dcgn
807	5								.22	82		
	20								.33	87		
813	25								.16	51		
829	10	.154	.062	69	.030	19.	40.	40.	.07	24	78.0	11.1
	30	.210	.072	63	.050	24.	34.	42.	.07	27	73.5	16.0
	50	.196	.067	63	.110	56.	34.	10.	.14	62	13.8	13.3
	60	.262	.091	72	.170	65.	35.	0.	.60	73	4.4	4.6
838	10	.273			.220	81.						
	20	.333			.120	36.						
	40	.304			.170	56.						
850	10	.208	.074	67	.09	43.	36.	21.	.76	15	12.6	1.1
	35	.256	.063	65	.11	43.	25.	32.	.41	14	20.6	1.8
	45	.390	.086	67	.22	56.	22.	22.	.99	36	4.7	1.3
	60	.483	.040	55	.75	155.	8.	-64.	1.58	9	4.5	.4
857	10	.240	.097	63	.06	25	40.	35.	.09	34	61.1	18.5
	20	.204			.08	39.			.02	30		
	27	.567	.133	71	.26	46.	23.	31.	.64	35	12.2	2.7
	40	.769	.180	75	.63	82.	23.	-5.	.82	41	11.6	2.7
	50								.56	38		
	60	.735	.104	54	.70	95.	14.	-	.82	30	6.6	2.4
	100	.773			.88	114.						
	135	.894			.80	89.						
885	10	.246	.088	59	.08	33.	36.	32.	.37	15	27.2	3.3
	20	.312			.10	32.						
	40	.565	.104	58	.42	74.	18.	7.	2.06	19	4.4	.8
	50	.848	.053	51	.81	96.	6.	-2.	.54	10	14.4	1.5
	60	.827			.87	105.			3.88	5		
	80	.906			.92	102.						
	100	.881			.91	103.						
890	10	.399	.113	56	.05	13.	28.	59.				
	20	.496	.193	58	.09	18.	39.	43.	.61	16	33.2	4.6
	30	.599			.38	63.						
	40	.880	.297	82	.66	75	34.	-9.	1.21	26	22.4	1.7
	60	.874			.81	93.						
	80	.901			.88	98.						
	100	.934			.88	94.						
898	10	.370	.137	64	.13	35.	37.	28.				
	23	.381			.08	21.						
	28	.434	.103	66	.13	30.	24.	46.				
	35	.506	.128	68	.16	32.	25.	43.				
	50	.689	.107	63	.55	80.	16.	5.				
	60	.691			.62	90.						
	80	.751			.65	87.						
909	10	.321	.119	57	.05	16.	37.	47.	.11	69	24.9	41.8
	20	.333			.07	21.			.06	51		
	30								.29	51		
	35	.498	.120	64	.51	102.	24.	-27.	.46	36	13.4	4.2
	39	.800	.147	63	.65	81.	18.	0.	.29	25	36.9	7.2
	45	.981			.66	67.			.13	16		
	60	.806			.63	78.						
	80	.796			.69	87.						
931	10	.352			.08	23.						
	25	.393			.15	38.						
	33	.407			.17	42.						
	39	.626			.40	64.						
	45	.623			.31	50.						
	60	.951			.82	86.						
	80	1.026			.88	86.						

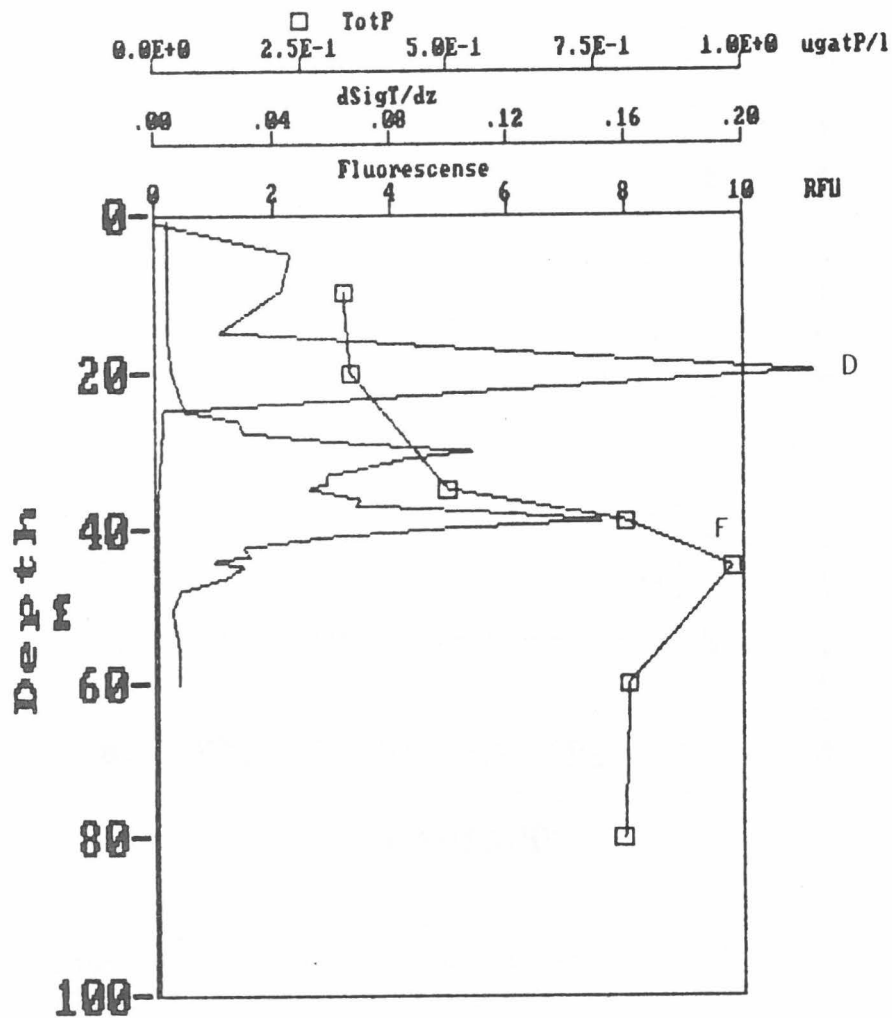


Fig. 12. Depth profile for total-P, station 909.

In some samples the SRP-values exceeds the TP-values, leading to negative estimates for DOP. The reason for this obviously incorrect result is not clear.

The distribution of orthophosphate uptake between the two size fractions varies over an extremely large range, from 87 to 5% retained by the 1 $\mu$ m-filter.

"Generation times" are calculated for the two size fractions. These may be compared to the biological generation times of the populations if

- the phosphorus collected on the filters is free of detrital P.

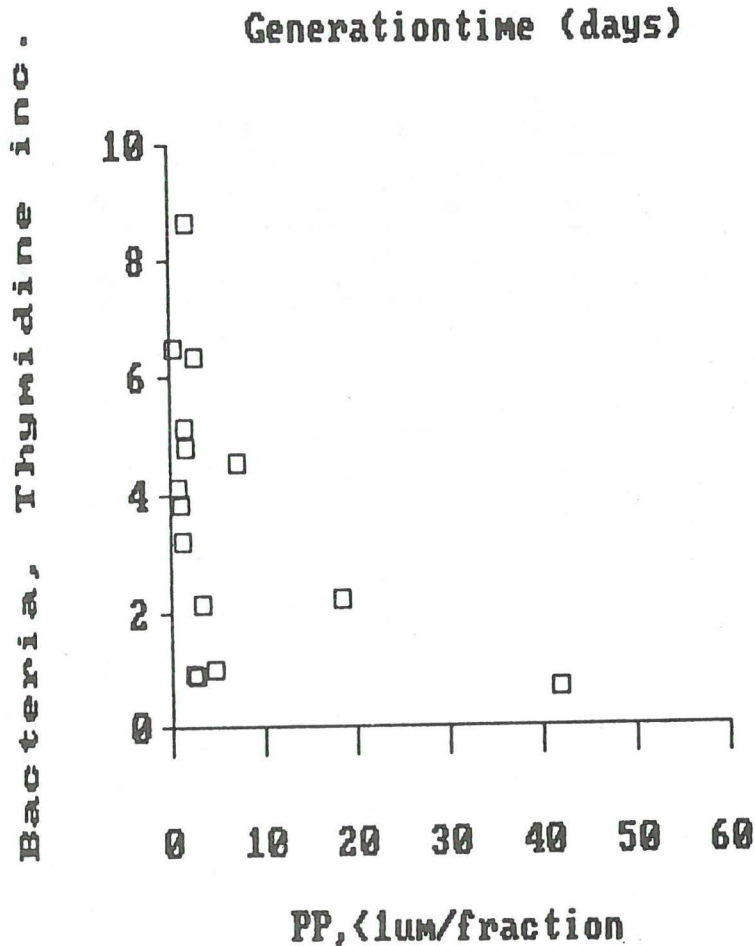


Fig. 13. Scatterdiagram for bacterial generation times estimated from thymidine uptake, versus "generation times" for particulate P in the size fraction from 0.2  $\mu\text{m}$  to 1.0  $\mu\text{m}$ . Values on both axes in days.

- the uptake and the growth of the organisms are in balance.

"Generation time" for the fraction from 0.2  $\mu\text{m}$  to 1.0  $\mu\text{m}$  is of the same order of magnitude as the generation times estimated for bacteria as described earlier. The degree of covariation is, however, small (Fig. 13).

#### MAIN CONCLUSIONS

For some stations, interesting relationships seem to exist between phytoplankton and bacterial activities. This is most pronounced in conjunction with Phaeocystis community at 909:39m.

Another interesting feature is the "normality" of the bacterial generation time estimates, despite the low water temperatures.

The demonstration of large parts of the bacteria being attached to "marine snow" is interesting and departs from the present dogma of marine microbiology, assuming most pelagic bacteria to be free living in the water masses.

At the present stage of data analysis it is difficult to point to further obvious general relationships between biomass/activity of the bacteria and their environment.

The presumably "youngest" station, station 909, exhibited several special and interesting features. It may therefore be speculated as to whether the picture of bacterial activity as a function of ecosystem "age" could have been clearer if stations further north towards the ice-edge with "younger" ecosystems had been included.



## MICROPLANKTON IN THE BARENTS SEA IN AUGUST 1985

By

TORBJØRN DALE

Institute of Marine Biology  
N-5065 Blomsterdalen, Norway

### INTRODUCTION

The importance of microzooplankton, especially the ciliates, in the planktonic food web has been recognized in recent years (MARGALEFF 1963, BEERS and STEWART 1969, PORTER *et al.* 1979). Most of our knowledge on this topic is, however, derived from studies from temperate and boreal regions (SOROKIN 1977, HEINBOKEL and BEERS 1979, BEERS *et al.* 1980, SMETACEK 1981, TANIGUCHI 1983). Only a few papers exist on the densities in polar regions (WULFF 1919, JOHANSEN 1976, BROCKEL 1981, TUMANTSEVA 1982, TANIGUCHI 1984) and to my knowledge there is only three papers dealing with the growth rates of polar ciliates (LEE and FENCHEL 1972, JOHANSEN 1976, GIFFORD 1985).

The present study aims at increasing the knowledge of the ecological roles of the ciliates and other microzooplankters in the Barents Sea and is a part of the multidisiplinary ecological project "PRO MARE". The main emphasis in the present study has been put on the density-distribution of ciliates as well as other microplankters which could be of importance for the ciliates. Some emphasis has also been put on the study of the filtration and growth rates of the ciliates.

## METHODS AND METHODS

This investigation was concentrated on the upper 100 m. The sampling depths on each station were chosen on basis of the vertical in situ fluorescence profile kon each station. Usually approximately 10 depths were sampled. On basis of the fluorescence profile, three main depths from above, in and below the fluorescence maximum were sampled with a 30 l Niskin sampler. The remaining depths were sampled with 2.5 l Niskin samplers. The samples from the three main depths were screened through 250  $\mu\text{m}$  prior to subsampling. Two sets of subsamples were taken for the enumeration of the microplankton. The first set was taken from all depths and subsampled in 250 ml opaque plastic bottles. These will be referred to as the unconcentrated samples. The second set was only taken from the main depths and were subsampled in 1 l opaque plastic bottles. These will be referred to as the concentrated samples. Both the unconcentrated and concentrated subsamples were usually taken within 10-30 minutes after the sampling. The unconcentrated subsamples were stored in the dark in a thermobox, usually no longer than 6-8 hours prior to the analysis. The sampling, subsampling and storing technique caused the temperature to increase in the coldest samples from approximately  $-1.5^{\circ}\text{C}$  to  $2-3^{\circ}\text{C}$ . The increase was less in the warmer samples.

The numbers of live ciliates were determined usually in two unconcentrated subsamples of 4.74 ml each, at x 25 magnification by means of a dark field stereo-microscope, according to the technique described by DALE and BURKILL (1982). The larger and less abundant species such as tintinnids, Ceratium spp., Dinobryon sp., nauplii, copepodites, rotifers, appendicularia, bipinnaria, and veliger larvae of gastropods and bivalvia were quantified in the concentrated samples from the main depths. These subsamples which were stored at  $4-5^{\circ}\text{C}$ , were concentrated to 20-40 ml by means of a 20  $\mu\text{m}$  screen just prior to examination in the stereomicroscope, usually within 8-10 hours after the sampling. All subsamples were carefully mixed prior to each sub-subsampling.



Usually some concentrated and unconcentrated subsamples from each of the stations were fixed in Bouin's (COATS and HEINBOKEL 1982) for later staining with silver-protargol in order to identify the ciliates. Some unconcentrated samples were also fixed in formalin.

Some attempts were done to determine the in situ growth rates of ciliates by means of incubation of natural samples in cages (short tubes equipped with 10 or 20  $\mu\text{m}$  plankton mesh on the ends, diam. 12.5 cm, depth 2 cm, volume 245 ml), in regular plastic bags (vol. ca 500 ml) or in plastic bottles (vol. ca. 750 ml) suspended in tanks flushed with sea water from the boats pump system.

It was also tried to establish monocultures of some of the ciliate species. Samples with high densities of ciliates were inoculated in 50 ml Nunclon plastic bottles enriched with various monocultures of algae (Prorocentrum minimum, P. micans, P. balticum, Heterocapsa triquetra, Scrippsiella trochoidea, Isochrysis tahiti) as well as bacteria grown on rice grains. The algae had been grown at 15°C, but had been gradually acclimatized to approximately 7°C over a period of 5 days. The algal stock cultures were contained in 750 ml Nunclon plastic bottles and stored in a large tank with sea water on deck and exposed to the natural light. The cultures were enriched with nutrients by adding filtered sea water from 50-100 m approximately once a week.

Selected samples with high densities of ciliates were also inoculated with fluorescent latex beads (0.57, 1.04 and 5.18  $\mu\text{m}$ ) in order to study uptake rates according to the technique described by (BØRSHEIM 1984).

Table 1 shows the sampling program in more detail.

Table 1. The main samples taken or experiments done.

date	stn	Vert.profile		incubations			gen. time. exp.			Fixed samples	
		uncon.	con.	bact.	beads	algae	cage	bag	bottl.	Bouin Form.	diverse
2.8	807	v	v					1		v	
3.8	813/814	v	v					1	2	v	
4.8	829	v	v	1	1			2	3	v	v
5.8	838	v	v	2	2	1				v	v - comparison of
5.8	843	v									technique for
6.8	850	v	v							v	estimation of
											densities
7.8	857	v	v	3		2				v	- experiments with
8.8	867	v	v							v	<u>S. strobilus</u>
9.8											
10.8	885	v	v	4		3				v	
11.8	890	v	v		3	4				v	v
12.8	898	v	v		4	5				v	v
13.8	909	v	v	5	5,6			1		v	v - microscopical
15.8	931	v	v	6	7					v	v examination of
16.6	935	v	v							v	contents of sedi-
											ment-traps

## RESULTS

Heterotrophic ciliates.

The average density of the heterotrophic ciliates (mainly Strombidium spp., <40-50  $\mu$ m) in the samples from 50 m and above was 3.2 per ml (n=87, range 0.2-12.9 ciliates per ml) compared to 0.6 per ml (n=29, range 0-1.8 per ml) in the samples from 55-100 m. The highest densities of 12.9 and 10.0 ciliates per ml were found at st. 807 (0 m) and 867 (20 m) respectively. The tintinnid population was dominated by Parafavella denticulata and Ptychocylis sp. but some Salpingella sp., Acantostomella sp. and Leprotintinnus pellucidus were also observed. The density of the tintinnids in the upper 50 m were 0.062 tintinnids per ml (n=32, range 0-0.66 per ml) or only 1.9% of the total density of the heterotrophic ciliates. The

highest densities of the tintinnids were 0.66 and 0.37 per ml found at st. 898 at 10 and 28 m, respectively. Some other ciliates (Didinium spp. 2 species, Prorodon spp., Monodinium (?) sp.) were also observed in the concentrated samples. The density of these forms averaged 0.005 cells per ml in the upper 50 m (n=33, range 0-0.047 cells per ml) with Didinium spp. as the most abundant. The density of the non-oligotrichs averaged 1.5% of the total ciliate population. The highest density of the non-oligotrichs was found at st. 909 (10 m). This station was also unusual with respect to the total population of the ciliates as a marked subsurface maximum was seen at 39 and 45 m (Fig. 1).

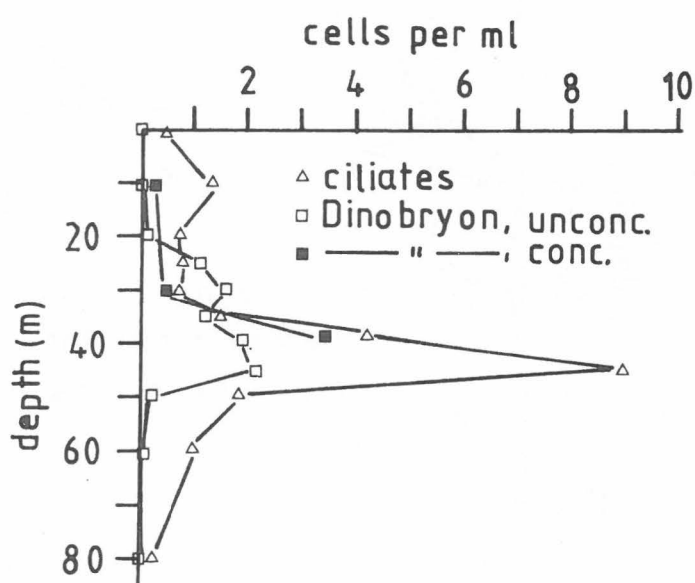


Fig. 1. Depth distributions of heterotrophic ciliates and colonies of Dinobryon sp. (from both unconcentrated and concentrated samples) at st. 909, 13 Aug. 1985 in the Barents Sea.

#### Mesodinium rubrum.

The average density of the autotrophic ciliate M. rubrum in the samples from above 50 m was 0.44 cells per ml (n=87, range 0-8.9 cells per ml) compared to the average density in the samples between 55 m and 100 m of 0.03 cells per ml (n=29, range 0-0.3 cells per ml). M. rubrum were not observed or only in low densities (<0.2 cells per ml) at st. 807, 829, 850, 885,

898 and 935. Generally the highest densities were found at st. 813/814, 857, 867 and 890. The maximum of 8.9 cells per ml was found at st. 857 at 25 m (Fig. 2). With the exception of st. 890 which had no well defined fluorescence maximum, the peaks of *M. rubrum* at st. 813/814, 857 and 867 were found above the fluorescence maximum, but did not coincide with any of the main sampling depths.

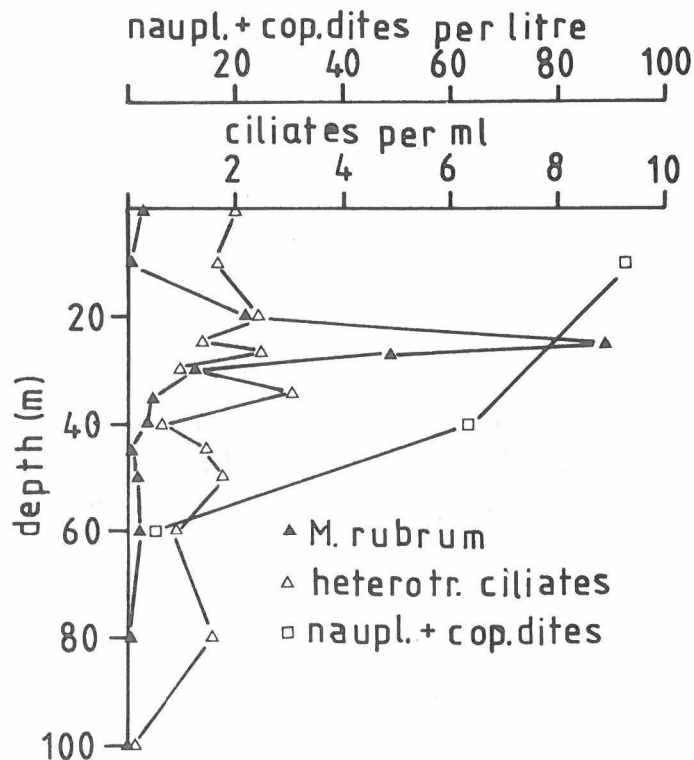


Fig. 2. Depth distributions of heterotrophic ciliates, *M. rubrum* and nauplii/copepodites at st. 857, 7 Aug. 1985 in the Barents Sea.

### Ceratium spp.

*Ceratium "tripos"* was the most common of the ceratia. *C. fusus* and *C. furca* were much less frequent. The average density of *Ceratium* spp. in the samples from the upper 50 m was 0.05 per ml (n=31, range 0-0.25 per ml). The highest densities were usually found in the upper 30 m and the peak values of 0.25 and 0.24 cells per ml, were found at st. 931 (10 m) and 885 (10 m), respectively. Stations 807, 813/814 and 898 were characterized

by low densities ( $<0.01$  per ml) of the ceratia, whereas st. 829, 850, 885, 890 and 931 had high densities ( $>0.10$  per ml).

#### Dinobryon sp.

The estimation of the densities of the colonial autotrophic flagellate Dinobryon sp. was complicated by fragmentation of the colonies as well as some difficulties to decide whether the colonies consisted mainly of empty loricas or loricas with living cells. Because of these problems the estimates must be considered carefully and should be regarded as semiquantitative. The average densities of the colonies in the samples from the upper 50 m was 0.19 colonies per ml (n=32, range 0-3.36 colonies per ml). The highest density of 3.36 colonies per ml was found at st. 909 (39 m) (Fig. 1), but these consisted mainly of dead colonies. The colonies at 30 m (0.57 colonies per ml), however, consisted mainly of living cells. St. 807, 813/814, 838 and 867 were characterized by low ( $<0.01$  colonies per ml) densities of Dinobryon sp. whereas the stations 857, 890, 898, 909 and 931 were characterized by high densities ( $>0.2$  colonies per ml) in some of the main depths.

#### Nauplii and copepodites.

The densities of the copepodites have probably been somewhat overestimated as some carried egg sacs. These must therefore have been adults, but of small species which passed through the prescreening mesh of 250  $\mu\text{m}$ . The average density of the nauplii in the samples from the upper 50 m was 35.0 ind. per litre (n=33, range 0-184 ind. per l) compared to 12.3 ind. per litre (n=33, range 0-35 per l) for the copepodites. The highest densities of nauplii and copepodites were found at st. 931 (10 m) and st. 885 (10 m), respectively. St. 807, 813/814 and 834 were characterized by low densities ( $<10$  ind. per l) of nauplii whereas densities above 100 ind. per l were only found at st. 850 and 931. The densities of the copepodites varied less than the nauplii. The densities of both groups appeared to be highest in the samples from above 30 m.

Other metazoan.

The metazoans listed in table 2 were only recorded in low densities and in only 1-8 samples of a total of 34 samples. The given densities must therefore be regarded more as indications than true estimates.

Table 2. The densities of some metazoan microplanktes in the samples from the Barents Sea, June 1985, based on a total of 34 samples (n = number of samples in which a given group was observed).

	n	ind./litre
Rotifers ( <u>Synchaeta</u> ?)	2	0.41
Appendicularians	2	0.28
bipinnaria larvae	1	0.03
gastropod veliger	4	0.61
bivalvia veliger	8	0.88

Both the gastropod and the bivalvia veligers appeared to be most frequent in the samples between 30-40 m depth.

Growth rate experiments.

A total of 2, 3 and 1 experiments were performed with cages, plastic bags and bottles respectively in order to measure the growth rates of natural assemblages of planktonic ciliates. None of these experiments succeeded as the density of the ciliates always declined so rapidly that the ciliates were almost gone within two days after incubation.

Cultivation of planktonic ciliates.

A total of 5 attempts (2-6 inoculations per attempt) were made in order to establish ciliate cultures. After some days, some ciliate species appeared to grow well on some of the algae which had been given to the samples. At the end of the cruise, these samples were brought to Inst. of Marine Biology by airplane in an insulated box where the temperature were kept around 4-5°C. The samples were then kept in a room at 4°C with

a light and dark cycle of 16/8 hours. On basis of these crude cultures I was able to isolate two species of naked oligotrichs, Strombidium sp. (sphaerical, ca. 50-60  $\mu\text{m}$ ) and Strombidinopsis sp. (conical, length ca. 75  $\mu\text{m}$ ). Both these species were growing well on the dinoflagellate Heterocapsa trochoidea (ca. 18  $\mu\text{m}$ ). The doubling time at 4°C was 2 days for both species.

Six attempts were done in order to isolate possible planktonic bacterivorous ciliates from the water samples. The bacteria were grown on rice grains as a substrate. None of these experiments succeeded, but this could possibly be due to flagellates as these probably also occurred in the samples. The flagellates might have outcompeted the ciliates by being more efficient grazers on the bacteria than the ciliates.

#### Filtration rates.

A total of 7 inoculations with fluorescent latex beads were also performed in order to study the uptake rates of particles with different diameters. So far only one of these samples have been inspected. From this sample, however, it was evident that a small abundant Strombidium sp. (ca. 25-30  $\mu\text{m}$ ), did not take up bacteria-sized beads (0.57  $\mu\text{m}$ ).

#### Various experiments.

Some experiments were performed on storing and shaking of the water samples in order to study the effects on the density of the ciliates within the samples. The density of the heterotrophic ciliates (mainly oligotrichs) in the unshaken sample declined 81% and 87% after 15 and 18 hours of storing respectively or equivalent to approximately 4.7% per hour. In the sample which were carefully shaken and subsampled every 5 minutes, however, the density declined with as much as between 27 and 40% per period of shaking. As indicated by both experiments, however, the supposedly very fragile ciliate Mesodinium rubrum were much less negatively effected by the experimental conditions than the rest of the ciliates.

One experiment (in cooperation with F. Rey) were performed in order to test if the ciliate Strombidium strobilius contained photosynthetically active chloroplasts. The experiment was done with samples from st. 867 (20 m) where the density of S. strobilus was 2.7 cells per ml. The C-14 uptake were tested on replicate water samples treated in three different ways,

- a): natural sample,
- b): fraction > 20  $\mu\text{m}$  concentrated with respect to volume by a factor of ca. 8.2 and with respect to S. strobilus by a factor of approximately 5,
- c): unconcentrated water screened through 20  $\mu\text{m}$ .

The preliminary results indicates that the C-14 uptake in the concentrated sample was approximately 50% higher than in the natural sample.

If one assumes that the increased uptake was only due to S. strobilus, then it follows from a simple calculation that

S. strobilus could have accounted for approximately 12.5% of the uptake in the untreated sample.

$$x + y = 1; \quad 5x + y = 1.5;$$

x = photosynthesis of S. strobilus

y = photosynthesis of the other organisms.

Replicates of these samples have been fixed and more certain conclusions regarding the contribution of the C-14 uptake by S. strobilus cannot be drawn until it has been verified from microscopical examinations that the concentrated sample did not contain any other larger organisms than S. strobilus that might have accounted for the increased C-14 uptake in the concentrated sample.

S. strobilus is yellowish-brown. By means of a special technique (see S. Chamberlain's section) it was possible to measure the absorption spectra of filtrates of S. strobilus on Millepore filters from

- a): the natural sample,
- b): the >20  $\mu\text{m}$  concentrated sample and
- c): the <20  $\mu\text{m}$  unconcentrated sample.



However, it was not possible to detect any pigments in the concentrated sample which were markedly different from the two other samples, indicating that the yellow pigments of S. strobilus was similar to that of the phytoplankton in the sample.

#### DISCUSSION

This report is only a preliminary treatment of some of the samples collected and experiments performed during the cruise with "G.O. Sars" to the Barents Sea in August 1985.

The average densities of the heterotrophic ciliates and M. rubrum were 3.2 and 0.44 cells per ml, respectively. This is in the same range as reported from the Barents Sea in June 1984 (DALE 1984). In comparison TANIGUCHI (1984) reported densities of naked ciliates to be in the range 0.5-1.0 cells per ml to be common values in the arctic and subarctic Pacific ocean in summer. The present samples were clearly dominated by the naked oligotrichs as the densities of the tintinnids (loricated oligotrichs) and the non-oligotrichous ciliates averaged only 1.9 and 1.5% respectively of the total ciliate population in samples from the upper 50 m. The naked oligotrichs seem also to be of greater importance than tintinnids and other ciliates in eastern Canadian waters (JOHANSEN 1976).

The densities of the heterotrophic ciliates and M. rubrum were 5 and 14 times, respectively, higher in the 0-50 m layer than in the 55-100 m layer. This probably reflects the tight coupling between the distribution of the heterotrophic ciliates and the phytoplankton and the need of light for the autotrophic ciliate M. rubrum.

The density of the voracious ciliates Didinium spp. averaged approximately 1% of the total ciliate population. Its freshwater relative is known to specialize on feeding on other ciliates. MEUNIER (1910), however, has shown that the marine forms in the Barents Sea may also feed on dinoflagellates, small tintinnids and even fecal pellets.

It is interesting to note that the peaks of M. rubrum usually were observed above the fluorescence maximum. This indicates that the main distribution of M. rubrum were higher in the water than most of the algae contributing to the fluorescence maximum. This could in turn indicate that M. rubrum possibly because of its algal symbionts were able to stay in an environment with lower concentrations of nutrients than the algae found in the fluorescence maximum. (Could it be related to f.ex.  $\text{NH}_3$  ?)

Additionally, this observation indicates that a biologically interesting layer has not been included within the three main depths selected at the stations during the cruise.

The average density of nauplii in the Barents Sea in August in the present investigation was 35 per litre. In comparison DALE (1984) found by applying the same technique on 7 samples from 1 m depth from Haltenbanken in late July, 1982, that the average density of nauplii was only 3 per litre. TANIGUCHI (1984), however, found values in the Bering Sea in July which frequently exceeded 100 per litre.

At present it is not possible to compare the densities of the ciliates with the densities of potential food organisms such as algae or bacteria. In this respect, however, st. 909 appears to be of interest. The high densities of heterotrophic ciliates at 39 and 45 m were coincident with the highest densities of Dinobryon sp. observed during the present cruise. Whether these ciliates were feeding on living or decaying Dinobryon sp. or other organisms associated with Dinobryon is not known. However, if they were feeding on bacteria, this could hopefully be demonstrated by replicate samples which were incubated with bacteria sized beads. These samples, however, has not been inspected yet. In freshwater, Dinobryon is characteristic for oligotrophic water (SLEIGH 1971).

Little is known about the predators of the ciliates in the Barents Sea. However, fig. 3 which shows the densities of the naupli/copepodites versus the densities of the ciliates includ-

ing M. rubrum, suggests a predator-prey relationship between the crustaceans and the ciliates.

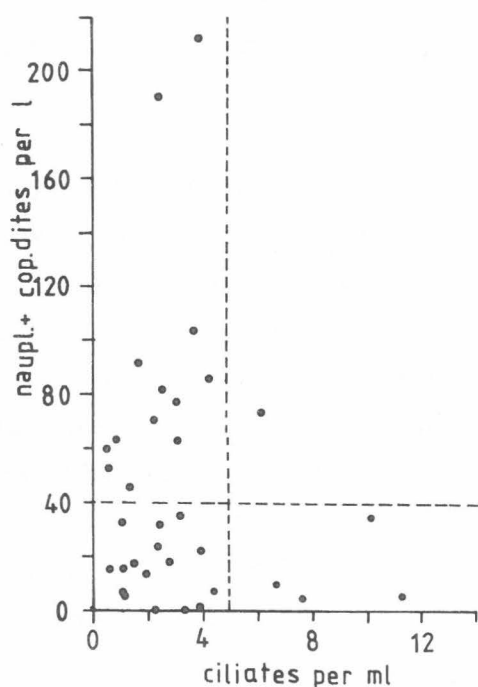


Fig. 3. The densities of ciliates (heterotrophic and M. rubrum) versus nauplii/copepodites.

That the nauplii might eat ciliates is clear, as I have made one observation of a nauplie (ca. 150  $\mu$ m) which was eating the yellow ciliate S. strobilus (ca. 100  $\mu$ m). The graph is not all too convincing, but the suggested relationship might have been obscured in this graph by several factors. Firstly, the naupliar stages 1 and 2 does not eat; these stages have probably also been included in my counts. Secondly, the impact of a copepodite on the densities of the ciliates is probably greater than the impact of a nauplie; this is not reflected in the present graph. Thirdly, the densities of the larger copepods and thereby their impact is not known. Fourthly, low densities of ciliates also occurs when their food supply is exhausted. In support of the suggested relationship SMETACEK (1981) has shown an inverse relationship between the densities of the protozooplankton and the zooplankton in the Kieler Bight and BERK et al. (1977) has shown that copepods were able to feed on the small ciliate Uronema sp. (ca. 20  $\mu$ m).

The densities of the other metazoans (rotifers, veliger larvae of bivalvia and gastropods, appendicularians) ranged between 0.4-0.9 ind. per litre. These estimates have been done on 1 litre samples per depth. Clearly, it appears necessary to use at least 10 l of water per depth to obtain better precision on the estimates of these organisms.

STOECKER et al. (1983) has successfully used cages to measure in situ growth rates of the large tintinnid Favella sp. Why my experiments failed is not clear but is in accordance with earlier experiments (DALE, unpubl.). One explanation could be related to the fragility of the organisms. The storing and shaking experiments has shown that the naked oligotrichs which dominated in my samples were very fragile and sensitive to shaking. It is conceivable that the tintinnids are better protected against mechanical stresses in the cages than the naked forms. Exhaustion of food might be another explanation.

The doubling time at 4°C of the two oligotrich species isolated from the Barents Sea was 2 days. In comparison JOHANSEN (1976) reported an average doubling time for tintinnids grown at 10°C of 4 days. GIFFORD (1985), however, found a minimum doubling time of approximately 1.5 days at 6°C for a small Strombidium sp. (length 40 µm).

#### REFERENCES

- BEERS, J.R.; F.M.H. REID and G.L. STEWART 1980. Microplankton population structure in Southern California nearshore waters in late spring. Mar. Biol. 60: 209-226.
- BEERS, J.R. and G.L. STEWART 1969. Microzooplankton and its abundance relative to the larger zooplankton and other seston components. Mar. Biol. 4: 182-189.

- BERK, S.G., D.C. BROWNLEE, D.R. HEINLE, H.J. KLING and R.R. COLWELL 1977. Ciliates as food source for marine planktonic copepods. Microb. Ecol. 4: 27-40.
- BROCKEL, K.V. 1981. The importance of nanoplankton within the pelagic Antarctic ecosystem. Kieler Meeresforsch. Sonderh. 5: 61-67.
- BØRSHEIM, K.Y. 1984. Clearance rates of bacteria-sized particles by freshwater ciliates, measured with monodisperse fluorescent latex beads. Oecologia (Berlin) 63: 286-288.
- COATS, D.W. and J.F. HEINBOKEL 1982. A study of reproduction and other life cycle phenomena in planktonic protists using an acridine orange fluorescence technique. Mar. Biol. 67: 71-79.
- DALE, T. 1984. Mikrodyreplankton. I: Preliminære resultater fra tokt med F/F "G.O. SARS" i Barentshavet, 28.5.-18.6.1984. Appendix F, 8 p. Havforskningsinstituttet, Bergen, Rapport FO 8409 (in Norwegian).
- DALE, T. 1984. Oljeutslippet på Haltenbanken sommeren 1982: Effekter på ciliater og andre mikroplanktonorganismer. Rapport til "Forskningsprogram om Havforurensing", Institutt for Marinbiologi, 57 p. (in Norwegian).
- DALE, T. and H. BURKILL 1982. "Live counting" - a quick and simple technique for enumerating pelagic ciliates. Ann. Inst. oceanogr. Paris, 58(S): 267-276.
- GIFFORD, D.J. 1985. Laboratory culture of marine planktonic oligotrichs (Ciliophora, Oligotrichida). Mar. Biol. 23: 257-267.

- HEINBOKEL, J.F. and J.R. BEERS 1979. Studies on the functional role of the tintinnids in the southern California Bight. III. Grazing impact of natural assemblages. Mar. Biol. 52: 23-32.
- JOHANSEN, P.J. 1976. A study of tintinnids and other protozoa in eastern Canadian waters with special reference to tintinnid feeding, nitrogen excretion and reproduction rates. Ph.D.-thesis. Dalhousie University, 156 pp.
- LEE, C.C. and T. FENCHEL 1972. Studies on ciliates associated with sea ice from Antarctica. II. Temperature responses and tolerances in ciliates from antarctic, temperate and tropical habitats. Arch. Protistenk. 114: 237-244.
- MARGALEFF, R. 1963. Role des cilies dans le cycle de la vie pelagique en Mediterranee. Rapp. P.-v. Reun. Commn. int. Explor. Scient. Mer. Mediterr. 17: 511-512.
- MEUNIER, A. 1910. Campagne arctique de 1907. Microplankton des Mers de Barents et de Kara. Imprimerie Scientifique, Charles Bulens, Editeur, 75, Rue Terre-neuve, 75, Bruxelles.
- PORTER, K.G., M.L. PACE and J.F. BATTEY 1979. Ciliate protozoans as links in freshwater planktonic food chains. Nature 277: 563-565.
- SLEIGH, M. 1973. The biology of protozoa. 315 pp. Edward Arnold, London.
- SMETACEK, V. 1981. The annual cycle of protozooplankton in the Kiel Bight. Mar. Biol. 63: 1-11.

- SOROKIN, Y.I. 1977. The heterotrophic phase of a plankton succession in the Japan Sea. Mar. Biol. 41: 107-117.
- STOECKER, D., L.H. DAVIS and A. PROVAN 1983. Growth of Favella sp. (Ciliata: Tintinnina) and other microzooplankters in cages incubated in situ and comparison to growth in vitro. Mar. Biol. 75: 293-302.
- TANIGUCHI, A. 1983. Microzooplankton distribution along a transverse section crossing a marked oceanic front. La Mer 21: 95-101.
- TANIGUCHI, A. 1984. Microzooplankton biomass in the arctic and subarctic Pacific ocean in summer. Memoirs of National Institute of Polar Research Special Issue no. 32, Proceedings of the sixth Symposium on Polar biology. pp. 63-76.
- TUMANTSEVA, N.I. 1982. Biomass and productive characteristics of protozoan plankton in subantarctic and antarctic waters of the southwestern Pacific. Oceanology 22: 604-608.
- WULFF, A. Ueber das kleinplankton der Barentssee. Aus dem laboratorium fur internationale Meeresforschung in Kiel. Biologische Abteilung. 28: 97-118.





## SEDIMENTATION OF ORGANIC MATERIAL IN THE BARENTS SEA

By

PAUL WASSMANN

University of Oslo

Biological Institute

Department of Marine Zoology and Marine Chemistry

Post box 1064, Blindern

N-0314 Oslo 3, Norway

### INTRODUCTION

On a previous cruise in 1984 the sedimentation of organic matter was measured during a late spring/early summer situation in the western and central parts of the Barents Sea. The aim of the present investigation is the quantification of suspended biomass loss out of the euphotic zone of the Barents Sea during a summer situation.

An understanding of the loss of suspended biomass from the euphotic zone is an essential part of a system ecological approach such as PRO MARE. At the end of the spring phytoplankton bloom large scale sedimentation of phytoplankton takes place in the Barents Sea (REY et al., in prep.). The deposition rates measured in 1984 were of the same magnitude as in west-Norwegian fjords and other boreal coastal areas. The euphotic zone was thus depleted for food sources and nutrients. The stratified surface water of the Barents Sea prevents during spring and summer major supplies of dissolved nutrients to the euphotic zone. Only along the Polar Front on the eastern part

of the Svalbard Bank upwelling of subsurface water supplies the euphotic zone with dissolved nutrients, resulting in high concentrations of suspended biomass during the whole productive season. It is, therefore, essential for the understanding of the all over function of the planktonic processes of the investigated ecosystem that the loss of energy and matter is also known during the oligotrophic summer period. Sediment traps were only deployed on "heavy" stations, i.e. stations where most of the parameters which could be measured by the team were taken. The significance of sedimentation can thus be evaluated on the background of an as complete set of data as possible.

#### METHODS

Sedimentation was measured with 160 cm high cylindrical double traps especially constructed for the investigations carried out by PRO MARE (Fig. 1). According to results given in the literature these traps have an adequate design for investigations in the open ocean. They are always situated vertically in the water column and the cylinders point against the current. This type of trap was successfully used in the Barents

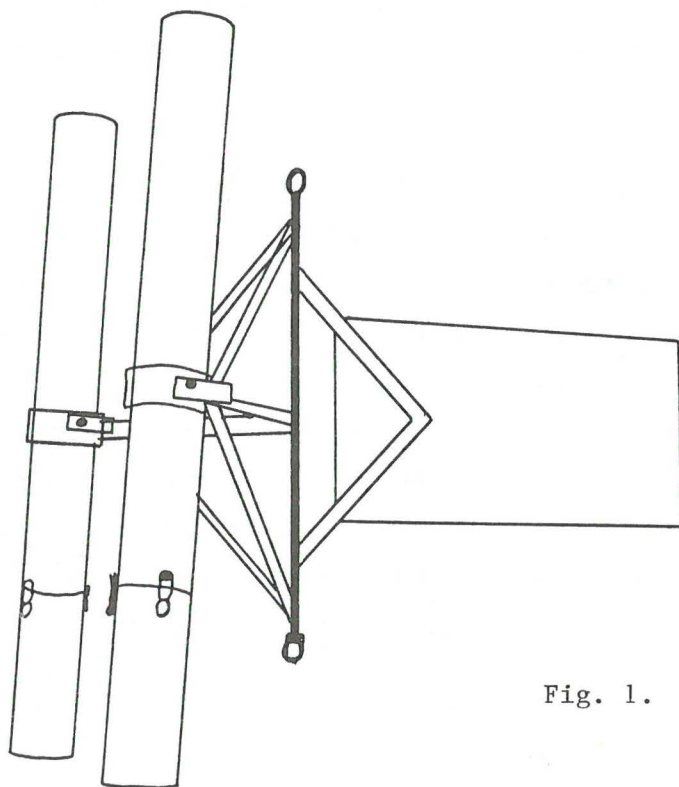


Fig. 1. Schematic drawing of the sediment trap.

Sea in 1984. Only small changes were done to improve the design. One or two traps were deployed well below the euphotic zone and fluorescence maxima at generally 60 and 110 m depth by R/V "G.O. Sars" (Paul Wassmann) at the stations given in Table 1 using 14 mm rope, an anchor (ca. 300 kg), a subsurface float (ca. 180 kg) and a surface buoy equipped with a radar reflector. Most of the traps were picked up by R/V "H. Mosby" (Mona Gilstad), the remaining by "G.O. Sars". No major problems arised in the collaboration between the two research vessels and such combined cruises will hopefully also be done in the future. The amount of results on the sedimentation of suspended biomass were due to this collaboration more than doubled.

Table 1. Station numbers where sedimentation was measured, the depth of the traps and the length of trap exposure.

Station no.	Depth of trap (m)	Length of trap exposure (d)
813	50	4.8
829	60 110	4.1
850	60	7.8
875	60 110	3.8
882	60 110	6.3
885	60 110	5.1
887	50 100	4.7

As in 1984 one of the cylinders was poisoned with 1-2 ml of chloroform while the other one was not. Samples for the analysis of total particulate material (TPM), particulate inorganic material (PIM), particulate organic carbon (POC) and nitrogen (PON), particulate total phosphorus (PTP), particulate silicate (PSi), chlorophyll a and phaeopigment analysis as well as for microscopical examination were taken as described by

WASSMANN (1983) and SKJOLDAL and WASSMANN (1985). Large zooplankton organisms were removed from the filters using a forceps.

#### RESULTS AND DISCUSSION

None of the samples have been analysed until now. A presentation of results and their discussion must therefore be very limited. However, some more general conclusions can be drawn.

The deployment, the retrieval as well as the handling of the traps gave not rise to any larger difficulties. All measurements were successfully. The positioning of the traps were no problem. The design of the traps and the moorings will not be changed on future cruises.

The sedimentation rates obtained during the cruise have generally to be characterised as quite small. Even though differences in sedimentation between the various stations were recorded (based on visual examination), the obtained results apparently support the hypothesis that loss of suspended material is very small during periods when the community of planktonic heterotrophs is well developed.

The interpretation of the data obtained will be difficult due to the presence of large amounts of zooplankton in the poisoned traps. Microbial degradation is known to influence the quantity and quality of organic material caught by traps, especially during long time exposures. This results in apparently lower sedimentation rates and trapping of more degraded organic matter. Chloroform reduces the degradation of organic material inside the traps, however, the poison also attracts and kills vertical migrating net-zooplankton. Since not all zooplankton can be removed prior to analysed, this artifact increases the sedimentation rates, especially those of nitrogen and phosphorus. As long as little is known about what processes take place inside the traps during exposure with and without preservatives, interpretation of sedimented material obtained during periods with a well developed zooplankton community will be difficult. There is, however, hope that some answers might be

given in near future to what extent chloroform influences the organic material obtained from traps based on the research of cand.mag. Kjell Gundersen at the University of Bergen.

## REFERENCES

REY, F., H.R. SKJOLDAL and P. WASSMANN (in prep.). The fate of spring phytoplankton blooms in the Barents Sea.

SKJOLDAL, H.R. and P. WASSMANN 1985. Sedimentation of particulate organic matter and silicium during spring and summer in Lindåspollene, western Norway. (Mar. Biol., in press).

WASSMANN, P. 1983. Sedimentation of organic and inorganic particulate material in Lindåspollene, a stratified, land-locked fjord in western Norway. Mar. Ecol. Prog. Ser. 13: 237-248.

